Eukaryotic Initiation Factor 2 (eIF2): Conformational studies of eIF2β subunit, intersubunit interaction and Met-tRNAi binding

Thesis submitted for the degree of

Doctor of Philosophy

by

KOLA SHOBHA KRUPA RANI

(Enrollment No. 07LBPH15)

Department of Biochemistry
School of Life Sciences
University of Hyderabad
Hyderabad – 500 046
INDIA

July 2014

University of Hyderabad
School of Life Sciences
Department of Biochemistry
HYDERABAD – 500 046, INDIA

CERTIFICATE

This is to certify that this thesis entitled **"Eukaryotic Initiation Factor 2 (eIF2): Conformational studies of eIF2β subunit, intersubunit interaction and Met-tRNAi binding"** submitted to the University of Hyderabad by Ms. KOLA SHOBHA KRUPA RANI for the degree of Doctor of Philosophy is based on the studies carried out by her under my supervision. I declare to the best of my knowledge that this work has not been submitted earlier for the award of degree or diploma from any other University or Institution.

Prof. K. V. A. Ramaiah
(Research Supervisor)

Head
Department of Biochemistry

Dean
School of Life Sciences

University of Hyderabad
School of Life Sciences
Department of Biochemistry
HYDERABAD – 500 046, INDIA

DECLARATION

I hereby declare that the work presented in my thesis is entirely original, plagiarism free and was carried out by me in the Department of Biochemistry, University of Hyderabad, under the supervision of Prof. K. V. A. Ramaiah. I further declare that this work has not been submitted earlier for the award of degree or diploma from any other University or Institution.

K. Shobha Krupa Rani

Prof. K. V. A. Ramaiah
(Research Supervisor)

ACKNOWLEDGEMENTS

I thank Lord, Almighty for His grace and mercy for perseverance to go through the learning phases in my life.

It was a long journey of my dream, that was at last fulfilled and I wish to express my deep sense of gratitude to my supervisor and mentor Prof. K.V.A. Ramaiah Department of Biochemistry for his guidance, constant encouragement, timely suggestions, support and meticulous supervision throughout my doctoral research. I remain forever thankful to him for every help.

I would like to extend my sincere thanks to the former and present Dean, School of Life Sciences, and also former and present Head, Dept. of Biochemistry facilities for allowing me to use the School.

I thank Dr. Lalji Singh, Former Director, CCMB for permitting me to register my doctoral work at University of Hyderabad.

I thank my doctoral committee members Prof. Siva Kumar and Prof. T. Suryanarayana for their suggestions during my work. I thank Prof. Rajagopal and his students for the help in carrying out CD studies.

I take this opportunity to express my heartfelt thanks to Dr. Rajan Sankaranarayanan, Head, Structural Biology, CCMB for valuable suggestions and support which have helped me to gain more knowledge and confidence about the subject.

I wish to thank all my colleagues Ms. Sambhavi, Ms. Rukmini, Dr. Suma, Dr, Biswajit Pal, and Dr. Vijaya for their moral support.

I thank all my present and former labmates of HCU, Dr. Pushpa, Dr. Rajesh, Dr. Aarti, Mr. Jagadish, Ms. Shweta, Mr. Daniel, for their co-operation and help.

I am thankful to my friendly past and present lab members of CCMB Venu, Jisha, Suresh, Sravan, Sadeem, Asfarul, Priyadharshan, Satya, Soundarya, Komal, Santhosh for all their support. My special thanks to Ms. Lalitha and Bhaskar. Thanks are due to all my friends and well wishers.

The help and cooperation of the non-teaching staff in the school and at CIL is deeply acknowledged.

I appreciate my children Bubby, Prashlu and in-laws for their prayer, love and support, without their blessings, It would not have been possible in making this endeavor successful and especially to my mother for being my strength and support.

Above all I have no words to express my indebtedness to my husband, Kiran for his patience, encouragement and for being my strength and support in this endeavor.

I am immensely grateful to all those individuals who have helped me in making this endeavor possible.

Shobha

CONTENTS

List of Figures

List of Tables

Abbreviations

ATP	Adenosine 5′ triphosphate
Bis-acrylamide	N, N'-methylene-bis-acrylamide
BSA	Bovine serum albumin
cDNA	Complementary DNA
Ci	Curie
Cpm	Counts per minute
^{0}C	Degree centigrade
C-terminal	Carboxy terminal
CD	Circular dichroism
dNTPs	Deoxyribonucleoside triphosphates
DNA	Deoxy ribonucleic acid
DTT	Dithiothreitol
EDTA	Ethylene diamine tetraacetic acid
eEF	Eukaryotic elongation factor
eIF2	Eukaryotic initiation factor2
eEFs	Eukaryotic elongation Factors
eIF2α	Alpha subunit of eukaryotic initiation factor 2
eIF4EBP	eIF4E binding protein
eIFs	Eukaryotic Initiation Factors
ER	Endoplasmic reticulum
eRF	Eukaryotic release factor
EtBr	Ethidium bromide
GDP	Guanosine 5′ diphosphate
GTP	Guanosine 5′ triphosphate
HRI	Heme regulated inhibitor
Kbp	Kilo base pairs
KDa	Kilo daltons
K_D	Dissociation constant
LB	Luria- Bertani
L	Litre
Met	Methionine
Mr	Marker

mg	Milligram
min	Minutes
ml	Millilitre
mM	Milli molar
ng	Nano gram
Ni-NTA	Nickel-nitrilotriacetic acid agarose
nm	Nanometer
nM	Nanomolar
N-terminal	Amino terminal
OD	Optical density
PAGE	Polyacrylamide gel electrophoresis
pmol	Pico mole
PMSF	Phenyl methyl sulphonyl fluoride
RFs	Release Factors
RBF	Ribosome release factor
IFs	Prokaryotic initiation factors
EFs	Prokaryotic elongation factors
Met- tRNAi	Initiator tRNA
mRNA	Messenger RNA
tRNA	Transfer RNA
S	Svedberg unit
SDS	Sodium dodecyl sulphate
TEMED	N',N',N',N' tetramethyl ethylene diamine
Tris	Tris (hydroxyl methyl) amino methane
UV	Ultra violet
wt	Wild type
μg	Microgram
μl	Microlitre
μM	Micromolar

Introduction

CHAPTER 1

INTRODUCTION

Protein synthesis is accomplished through a process called translation. During transcription, DNA is transcribed into a messenger RNA (mRNA) molecule and the nucleotide sequence information in the mRNA is decoded to the corresponding amino acid sequences of a protein by special machinery that contains ribosomes, transfer RNAs (tRNAs), enzymes such as aminoacyl-tRNA synthetases, and several other protein factors.

Unlike in prokaryotes where transcription and translation are coupled, protein translation in eukaryotes is uncoupled both temporally and spatially from RNA synthesis that occurs in the nucleus. In eukaryotes, in addition to prokaryotic-like protein synthesis that occurs in the organelles, translation also occurs both in the cytoplasm and also on the surface of endoplasmic reticulum (ER). The primary transcript of eukaryotic mRNA undergoes processing that removes the non-coding introns and also post-transcriptional modifications such as splicing (removal of introns and splicing of exons), 5′ capping (addition of m^7 GTP) and 3′ polyadenylation (addition of polyA tail) before being transported into the cytoplasm and translated thereafter. In contrast, prokaryotic mRNAs are not spliced, do not carry a polyA tail or 5′cap, and are polycistronic coding for multiple proteins. Prokaryotic ribosomes, 70S, consist of a large 50S subunit and a small 30S subunit, whereas eukaryotic ribosomes, 80S, are made up of 60S and 40S subunits. Each subunit exists separately in the cytoplasm, but the two join together on the mRNA molecule.

A single copy of protein is produced if the mRNA is read by a monosome. Multiple copies of proteins are made if mRNAs are read by more than one ribosome. An mRNA with multiple ribosomes is called a polysome. A polysome can be formed because of increased initiation or decreased elongation rates. The ribosomal subunits contain proteins and specialized RNA molecules called ribosomal RNAs (rRNAs). The sequence of amino acids to be incorporated into the protein is specified by the codon information on the mRNA. Amino acids are brought to the template mRNA by tRNAs. The tRNA molecules are adaptor molecule, they have one end that can read the triplet code in the mRNA through complementary base-pairing, and another end that attaches to a specific amino acid (Chapeville *et al.*, 1962; Grunberger *et al.*, 1969). The idea that tRNA was an adaptor molecule was first proposed by Francis Crick. Aminoacyl-tRNA synthetases couple individual amino acids to the corresponding tRNAs in an ATP-dependent manner. mRNA along with tRNA and ribosomes work together to produce proteins during protein translation.

Protein synthesis is a complex and dynamic process that can be divided into four different phases: initiation, elongation, termination and ribosome recycling (**Figure. 1.0**). The various events in initiation, elongation and the release of nascent polypeptide are aided by specific protein factors called initiation, elongation, termination or release and ribosome recycling factors respectively. The nomenclature of these factors in prokaryotes and eukaryotes is somewhat different. Translation factors play a role both in the synthesis of proteins and also their regulation. To determine the *in vivo* protein synthesis,

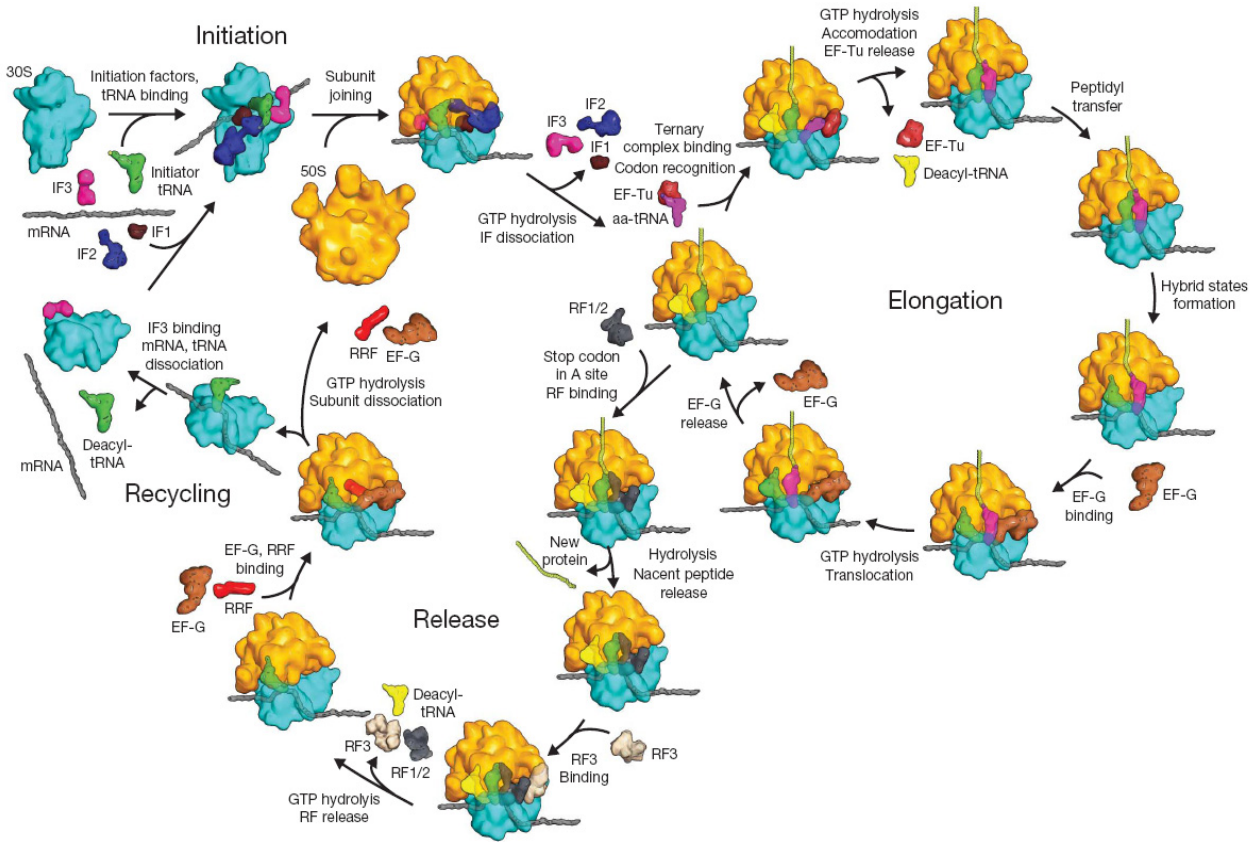

(Courtesy: Schmeing T M and Ramakrishnan V, 2009)

Figure 1.0. Steps in Translation: The various steps in translation are a) initiation b) elongation c) termination and d) ribosome recycling. All these steps are found both in prokaryotes and in eukaryotes. However, the figure depicts the steps in bacterial translation. Each step is functional by its respective protein factors called initiation, elongation, termination and release factors.

cells are incubated in a culture with a radio labelled amino acids like [S^{35}] methionine, [^{14}C] leucine etc. The incorporation of label into the acid precipitable protein is taken as a measure of protein synthesis. Similarly protein synthesis *in vitro* can be measured using cell extracts that are devoid of their nuclei. These extracts contain the necessary translational apparatus. Such cell extracts are supplemented with the necessary amino acids, energy generating compounds like ATP and GTP with salts such as Mg^{2+} and K^{+}. Translation of specific exogenous mRNA requires the removal of endogenous mRNAs by nuclease treatment and inactivating it prior to the addition of any mRNA of our choice. This type of cell free translational systems have helped to decipher the genetic code, understand the basic steps in protein synthesis and also uncovered various regulatory mechanisms involved in translation and the mechanism of action of antibiotics.

The initiation of protein synthesis is clearly a crucial process for the cell. There are significant differences between how this process is accomplished in eukaryotes and in bacteria. Each step is performed by their respective factors. Bacteria rely on the Shine–Dalgarno sequence of the mRNA to locate the 'start' codon (AUG that codes for a methionine) and require just three initiation factors (IFs). In contrast, eukaryotic translation initiation relies on a scanning mechanism to locate the 'start' codon and involves 13 core initiation factors, called eIFs, some of which are large and multimeric complexes. Initiation step in protein synthesis is marked by the formation of translation-competent 80S ribosomes with initiator Met-tRNAi base-paired to the mRNA- AUG start codon at the ribosomal P-site.

During elongation, aminoacylated tRNAs are delivered to the A-site of 80S ribosomes by elongation factors like EF.Tu., EF.Ts and EF.G (in prokaryotes) or eEF1α, β and γ or eEF2 (in eukaryotes) in a GTP dependent manner. Initially, the aminoacylated tRNAs are delivered to the A-site in ribosome and subsequently they move through the peptidyl- (P-) and exit- (E-) sites. These binding sites are located at the interface of the 30S and 50S subunits. Adjacent amino acids in the mRNA are linked by a peptide bond which is catalyzed by the peptidyl transferase centre present in the large subunit of ribosome (50S/60S). Peptidyl transferase center has mostly 23S (in prokaryotes) or 28S rRNA (in eukaryotes) that catalyzes the peptide bond formation, leaving a deacylated tRNA in the ribosomal P-site and the newly formed peptidyl tRNA in the A-site. This pre-translocational state of the ribosome is the substrate of the GTPase eEF2 (eukaryotic elongation factor 2), or EF-G (prokaryotes), which catalyses the coordinated movement of the two tRNA molecules and the mRNA in addition to causing conformational changes in the ribosome through its GTP hydrolysis**.** The consequence of this movement is that the mRNA moves by three bases (one codon) and the deacylated tRNA moves from P-site to E-site. So that aminoacylated tRNA carrying the polypeptide would move to the P-site leaving the A-site available for the incoming aminoacylated tRNA.

Termination of the protein synthesis occurs when the elongating ribosome reaches any of the three stop codons: UAA, UAG, UGA. Unlike the sense codons, stop codons are not recognized by aminoacylated tRNAs but are

recognized by proteins which are called release factors (RFs). Release factors are broadly classified as class 1 and class 2 release factors. Class 1 RFs have two functions: recognize stop codon and release the newly made polypeptide chain by hydrolysing the ester bond linking the polypeptide chain with the P-site tRNA from ribosomes. Prokaryotes have two class 1 release factors. These are called RF1 and RF2. While RF1 recognizes UAG, RF2 recognizes UGA stop codon. The third stop codon is recognized however by both by RF1 and RF2. In contrast, eukaryotes and archea have only one class1 release factor called as eRF1 or aRF1 that recognizes all the three stop codons. Class-2 release factors (RF3 in prokaryotes and eRF3 in eukaryotes) are required to release class-1 factors from ribosomes.

Class-1 release factors, based on their function, have four distinct sites: 1. A ribosome binding site (RBS), 2. Termination codon recognition site (TCRS), 3. A peptidyl-tRNA interaction site (PRIS), 4. A binding site for class 2 release factors like RF3. For bacterial class 1 RFs two tripeptides Pro-Ala-Thr in RF1 and Ser-Pro-Phe in RF2, determine their stop codon identity (Ito et al., 2000; Nakamura and Ito, 2002). The eukaryotic class 1 release factor, eRF1, on its N-terminus, has two highly conserved domains containing amino acids YxCxxxF between 125-131 residues and NIKS at 61-64 positions which play a role in the recognition of stop codons. All Class- 1 factors, irrespective of their origin and codon specificity share a common GGQ (Gly-Gly-Gln) motif (Frolova et al., 1999, 2000). The sensing of stop codons causes a complex cascade of conformational changes in the ribosome and associated proteins. GGQ motif triggers the release of nascent polypeptide when RF1/RF2 bind

the stop codon. GTP hydrolysis by RF3 (class 2 release factor) promotes the dissociation of RFs from ribosomes (reviewed in Kisselev et al., 2003; Song et al., 2000; Frolova et al., 1999; reviewed in Nurenberg and Tampe, 2012).

Ribosome recycling is the fourth step in translation and follows after termination of protein synthesis. The ribosome, after termination of protein synthesis, is bound by mRNA and deacylated tRNAs in the P and E sites. The dissociation or splitting of ribosomes into subunits, the removal deacylated tRNAs and mRNA is aided by ribosome recycling factor (RRF) in prokaryotes and ABC-type ATPase, ABCE-1 (previously named as RNAse L inhibitor (Rli) or host protein (HP) 68). In bacteria, RRF is recruited after the release of RFs. In bacteria, it is suggested that RRF and EF-G catalyze the release of tRNA and mRNA. Alternatively, IF3 promotes spontaneous dissociation of mRNA after it detaches tRNA. RRF involved in prokaryotic ribosome subunit dissociation is delivered to the A-site of ribosome by EF-G (GTPase) (Rao and Varshney, 2002; Singh et al., 2005; Seshadri et al., 2010; reviewed in Nurenberg and Tampe, 2012).

Ribosome recycling in eukaryotes can occur passively by initiation factors, eIF3, eIF1 and eIF1A can occur in the absence of expenditure energy at low Mg^{2+} concentrations (Pisarev et al., 2007). However in the presence of wide range of Mg^{2+} concentrations, ABCE1, one of the members of ATP-binding cassette family of proteins, promotes dissociation of post-termination complexes into free 60S ribosome subunits, 40S bound tRNA and mRNA. ABCE1 has nucleotide triphosphate hydrolase activity which is stimulated by

the post-termination complexes (Pisarev et al., 2009). Unlike in bacteria, post-termination complexes bound by eRF1/eRF3 are dissociated by ABCE1. In addition to ABCE1, members of ABC proteins like ABC50, GCN20 and eEF3, are involved in translation and stimulate eIF2.GTP.Met-tRNAi complexes, activation of GCN2, eIF2α kinase in the presence of GCN1, and in the release of deacylated tRNA in fungus from the E-site of ribosome etc., respectively (Paytubi et al., 2009, Marton et al., 1997; Anderson et al., 2006). ABCE1 factor is also shown to interact with several initiation factors like eIF1, 1A and eIF3. Ribosome recycling connects termination on one side and initiation step of protein synthesis on the other side. It is important that ribosomes separated into subunits have to remain separated by anti-association factors that presumably interact with the RRFs.

1.1. Pathway of Eurkaryotic Translation Initiation

Translation is a cyclical process and translation initiation requires a pool of separated ribosomal subunits. At the end of initiation, mRNA is bound to 80S or 70S ribosome with the initiator tRNA carrying methionine that is positioned in the P-site of ribosome. The mechanism of eukaryotic translation initiation (**Figure 1.1**) can be divided into four sub-steps:

1. Ternary complex formation and assembling of Pre-initiation complex (PIC).
2. PIC recruitment to mRNA.
3. PIC scans mRNA and recognizes initiation codon.
4. Ribosomal subunit joining and 80S initiation complex formation.

Figure 1.1. The canonical pathway of eukaryotic translation initiation

Eukaryotic translation initiation results in the formation of an 80S ribosomal initiation complex. The stages are (1) eukaryotic initiation factor2 (eIF2).GTP.Met-tRNAi^{Met} ternary complex formation. (2) Formation of a 43S preinitiation complex comprising a 40S subunit, eIF1, eIF5, eIF1A, eIF3, eIF2–GTP–Met-tRNAi^{Met}. (3) mRNA activation, during which the mRNA cap-proximal region is unwound by eIF4F with eIF4B. (4) attachment of the 43S complex to mRNA region. (5) Scanning of the 5′ UTR in a 5′ to 3′ direction by 43S complexes. (6) Recognition of the initiation codon and 48S initiation complex formation, which switches the scanning complex to a 'closed' conformation. (7) Joining of 60S subunits to 48S complexes and concomitant displacement of eIF2–GDP and other factors (eIF1, eIF3, eIF4B, eIF4F and eIF5) mediated by eIF5B. (8) GTP hydrolysis by eIF5B and release of eIF1A and GDP-bound eIF5B from assembled elongation-competent 80S ribosomes.

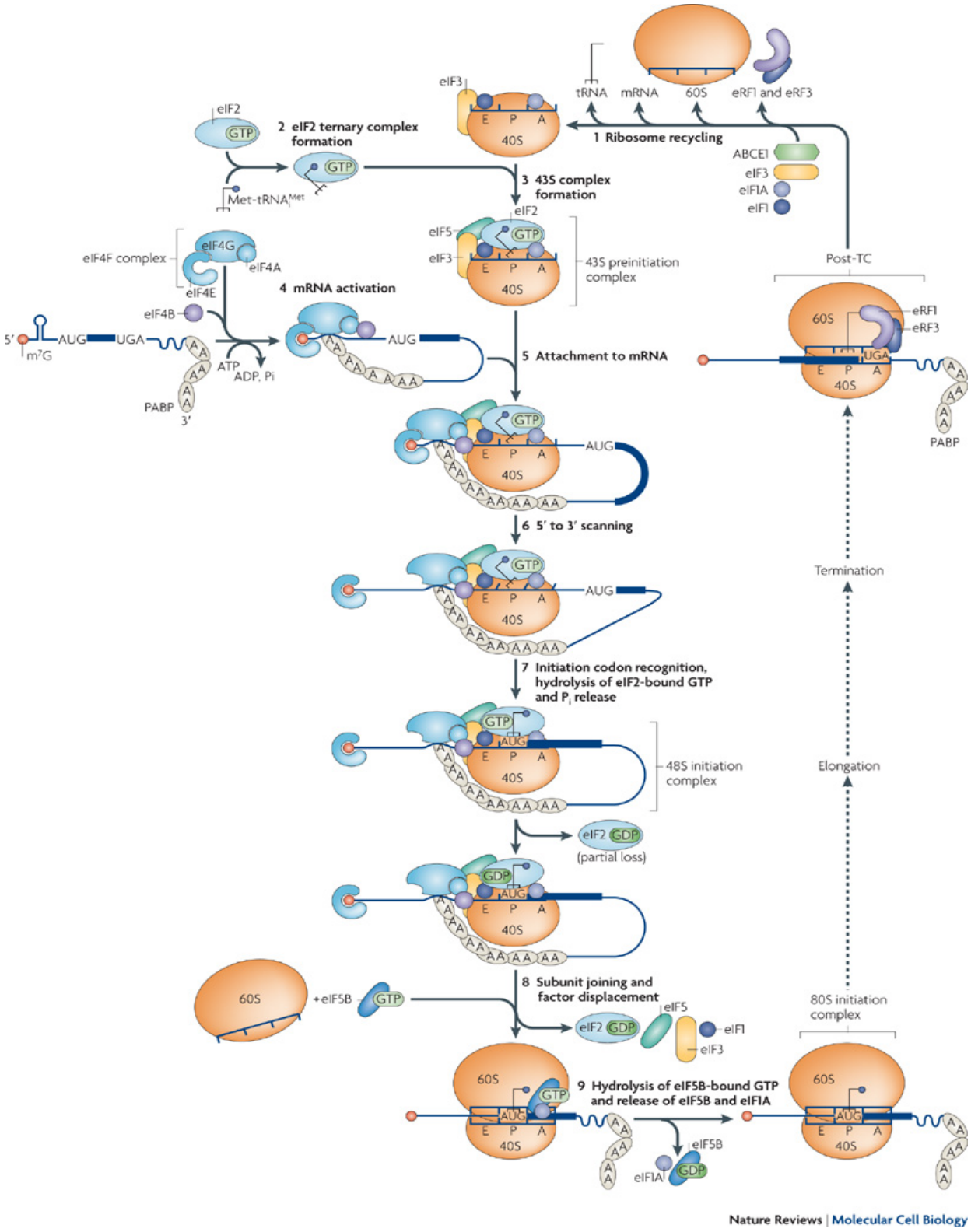

Figure 1.1. The canonical pathway of eukaryotic translation initiation

(Courtesy: Jackson R.J, Hellen C.U.T and Pestova T.V, 2010)

1.1.1. Ternary complex formation and assembling of pre-initiation complex (PIC)

At the end of termination, 80S ribosomes are dissociated into their individual subunits (40S and 60S) and are bound by anti-association factors to prevent their reassociation. The first step in initiation is formation of a ternary complex, eIF2.GTP.Met-tRNAi, which is delivered to 40S ribosomal subunits which is bound by other factors like eIF3, eIF5, eIF1A, and eIF1. The 40S subunits without mRNA but with the ternary complex and various factors as mentioned above constitutes 43S preinitiation complex (PIC). The formation of 43S PIC occurs probably in one of the two ways. In one case, the ternary complex and eIF5 join the 40S-eIF1-eIF1A-eIF3 that is formed at the end of termination. Alternatively, if the factors are dissociated from 40S subunits at the end of termination, then the ternary complex joins the multifactor complex (MFC) consisting of eIF1, 5, 3, 1A to 40S subunit simultaneously to form PIC (Valásek, 2012). The functional importance of various factors are as follows: eIF2, a heterotrimer composed of peripheral α and β-subunits bound to a central γ–subunit, recognizes unique structural features of the initiator tRNA. It delivers initiator tRNA to 40S subunit. Met-tRNAi binds eIF2•GTP with higher affinity than eIF2•GDP. Ternary complex binds to 40S subunit with the aid of eIF1, eIF1A, and the multi-subunit factor eIF3, the latter acts as a central hub for various interactions. The main function of eIF3 seems to prevent the 60S subunit from joining the 43S PIC. eIF3a-CTD and eIF3c-NTD are involved in the interaction with the multifactor complex (MFC). eIF3 binds to the solvent face of the 40S subunit and coordinates with every component of the PIC

(40S, eIFs1, 1A, 2, 5) to assemble it. eIF1 is the smallest of the initiation factors (12.7 and 12.3 kDa in human and yeast respectively) and prevents eIF5B-catalyzed 60S subunit joining in the absence of mRNA (Trachsel et al., 1977), implying a role in coordinating mRNA and tRNA binding to initiation complex. In concert with eIF1A, eIF1 promotes 48S complex formation with the ribosome positioned at the initiator AUG codon (Pestova et al., 1998). eIF1A is also a small, stable protein of 17-22 kDa (Wei et al., 1995) and is one of the most highly conserved initiation factors. Depletion of eIF1A in yeast cells results in polysome runoff and thus an inhibition of translation initiation (Kainuma and Hershey, 2001). The role of eIF1A in initiation is pleiotropic, as has been implicated in ribosome dissociation, ternary complex binding and mRNA binding to the ribosome (Wei et al., 1995). The carboxyl terminal domain (CTD) of eIF1A interacts with the CTD of eIF5B, a homologue of bacterial IF2 (Choi et al., 2000), and the amino-terminal domain (NTD) of eIF1A binds to eIF2 and eIF3 (Olsen et al., 2003). eIF5 is a GTPase activating protein (GAP) that stimulates the intrinsic GTPase activity of eIF2 complex (Das et al., 2001) and its C-terminus interacts with eIF2β and also associates with the p93 (Nip1) subunit of eIF3. In yeast, a multifactor complex (MFC) consisting of eIF1, eIF2, eIF3, eIF5, and Met-tRNAi assembles independently of the ribosome and its integrity depends on the AA-box at the C-terminal of eIF5 (Asano et al., 2000). Another factor, eIF6 has been shown to bind the 60S subunit to prevent its association with the 40S ribosomal subunit (Russell and Spremuli, 1979; Raychaudhuri et al., 1984).

Initiator tRNA carrying methionine is required in the initiation step of protein synthesis. The sequence divergence between the initiator and elongator forms of Met-tRNAs is critical for the initiation function and is universally conserved amongst cytoplasmic eukaryotic initiator tRNAs and not in elongator tRNAs. A1:U72 base pair is a key feature of human initiator tRNA that discriminates against its activity in elongation, both *in vitro and in vivo* (Drabkin et al.,1998), in addition to promoting initiator function. Also, human Met-tRNAi contains A60 in place of pyrimidine 60, and A54 instead of T54 present in the TψC sequence found in elongator tRNAs. Finally, the Met-tRNAi contains three consecutive G:C base pairs (G29:C41, G30:C40, G31:C39) in the anticodon stem (**Figure 1.2**). GTP bound form of eIF2 binds the Met-tRNAi more tightly, recognizing determinants from both the tRNA and the methionine moiety (reviewed in Hinnebusch, 2000; Farruggio et al., 1996).

1.1.2. PIC recruitment to mRNA

Eukaryotic mRNAs, unlike their prokaryotic counterparts, have m^7Gppp a 5′ cap (m^7G) and 3′ polyA tail. They do not carry a Shine-Dalgarno sequence to identify the ‘start codon’ as in prokaryotic mRNA. The binding of eIF1 and 1A promote conformational changes in the 40S ribosome that opens the mRNA binding channel for loading mRNA and eIF1 is translocated at this time to the P-site of ribosome. The 5′cap of eukaryotic mRNA is bound by eIF4F complex that consists of 4E (cap binding protein), 4A (DEAD-box RNA helicase), and 4G (a scaffold protein). In addition, cofactors of eIF4A helicase (eIF4B or 4H in mammals) also join the mRNA. The factor, eIF4G, serves as a scaffolding

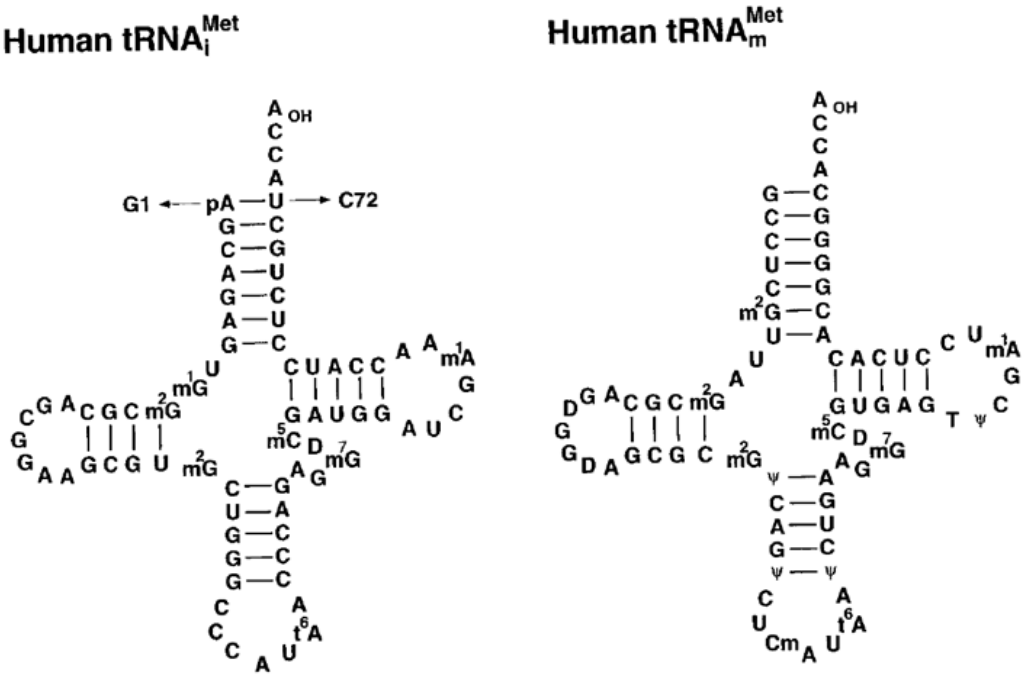

(Courtesy: Farruggio et al., 1996)

Figure 1.2 Cloverleaf structures of human initiator and human elongator methionine tRNAs. The first base pair A1.U72 at acceptor end is conserved, 3 consecutive G.C pairs at anticodon region are specific to initiator tRNA. The first basepair is G1.C72 base pair found at the corresponding position of the human elongator tRNA. Arrows indicate the sequence changes in human initiator tRNA gene.

protein mainly to bring together other components of the initiation pathway. Human eIF4G may be divided into three distinct domains of roughly similar size. The central domain of eIF4G (residues 635-1039) binds eIF3 and eIF4A (Imataka and Sonenberg, 1997) and possesses an RNA binding site (Pestova et al., 1996). The carboxyl-terminal domain contains a second eIF4A binding site and binds Mnk1, a kinase. eIF4B (~69 kDa) is an RNA binding protein that promotes the recruitment of ribosomes to mRNA and stimulates the RNA helicase activity of eIF4A. The eIF4E factor is clamped to the m^7G cap. eIF4E has a concave side that provides a small hydrophobic slot for insertion of the cap structure and a contiguous region for mRNA binding. The opposite convex face of the protein is the contact region with eIF4G. Its primary function in translation is to enhance the binding of the eIF4F complex to the 5' end of the mRNA. Phosphorylation of eIF4E is correlated to increased translation rates and growth status of the cell (Kleijn et al*.,* 1998), but it is still not clear whether phosphorylation increases (Minich et al., 1994) or decreases (Scheper et al., 2002) its cap binding affinity. The association of eIF4E with eIF4G and subsequent assembly of eIF4F complex are prevented by the binding of 4E binding proteins (BPs) to eIF4E. In turn, phosphorylation of 4E-BPs modulates their affinity for eIF4E; hypophosphorylated 4E-BPs bind efficiently to eIF4E, hyperphosphorylation abrogates their interaction with eIF4E (Lin et al., 1994; Pause et al*.,* 1994; Fadden et al*.,* 1997).

The polyA tail of 3′ end of mRNA is bound by polyA binding protein (PABP). The amino terminal (residues 1-634) region of eIF4G binds the polyA binding

protein (PABP) and eIF4E is required for cap-dependent translation (Lamphear et al., 1995; Mader et al., 1995; Imataka et al., 1998). The interaction between eIF4G and PABP facilitates pseudo-circularization of the mRNA and may facilitate reinitiation (reviewed in Presis and Hentze 2003; reviewed in Sonenberg and Hinnebusch, 2009; Sachs and Varani, 2000).

The mRNA complex bound by eIF4F complex and PABP is delivered to 43S PIC to form 48S PIC. The interaction between small ribosome subunit in 43S PIC and mRNA complex is mediated by eIF3 of 43S PIC and eIF4G of mRNA complex. The ribosome then scans the mRNA to identify the 'start codon'. During scanning, the secondary structures in mRNA that impede the movement of ribosome are melted out with the help of helicase activity associated with eIF4A and its cofactors (eIF4B or 4H) and at the expense of ATP. The topology of eIF4A–eIF4G–eIF4H complex indicates that eIF4H binds the single-stranded mRNA behind eIF4A, suggesting that eIF4H (or eIF4B) could activate eIF4A's helicase activity by promoting processive unidirectional eIF4A movement and thus preventing mRNA re-annealing (Marintchev, A. et al*.,* 2009).

1.1.3. PIC scans mRNA and recognizes initiation codon

Eukaryotic mRNAs have a 5′ cap and a 3′ PolyA tail. The mature mRNA has typically three regions: 5′ untranslated region (5′ UTR), 3′ untranslated region and ORF (openreading frame). While 5′ and 3′ UTRs contain signals to bind to regulatory proteins and other *cis* regulatory elements, the nucleotides of ORF contain the necessary information for the protein to be synthesized. The

ribosome seeks the initiation codon after the binding of 43S complex to the m^7G cap at the proximal 5′ end of the mRNA. To identify the 'start' codon in mRNA, the 48S PIC and its associated factors scan along the mRNA from the 5′ terminus in an energy dependent manner. The fidelity of initiation depends on the scanning complexes and they must have a discriminatory mechanism that prevents partial base pairing of triplets in the 5′ UTR with the Met-tRNAi anticodon. The first AUG triplet in an optimum context- GCC(A/G)CCAUGG, with a purine at the -3 and a G at the +4 positions (relative to the A of the AUG codon, which is designated +1) is required for efficient recognition of the 5′ proximal AUG triplet (Kozak, 1991). This mechanism which involves the location of the start AUG codon by the ribosome is called as scanning model. The presence of any RNA secondary structures in the 5′ UTR blocks scanning and prevents the 43S subunit from binding at the AUG. The intricate molecular mechanism to communicate start codon recognition occurs by a network of components that have been identified through yeast genetics. Mutations in factors involved in start codon recognition can either decrease (Sui- phenotype) or increase (Ssu- phenotype) the fidelity of the process. Initiation factors such as eIF1, eIF2 and eIF5 also play an important role in AUG recognition. Biochemical characterization of these mutants has shed further light on the roles of the individual components during start codon recognition. The open conformation of ribosome induced by eIF1 and 1A is required for scanning. At this time the anticodon of Met-tRNAi is not fully engaged in the P-site of ribosome in order to avoid recognition of putative start codons. The partial hydrolysis of eIF2.GTP by the GTPase accelerating

factor, eIF5, and the inability of the release of the resultant phosphate ion by eIF1 produce two states of the factor: GTP and GDP-Pi bound that are possibly in equilibrium. Identification of start codon induces a structural change in the 48S PIC to the closed or scanning arrested form that is stabilized by an interaction between eIF1A and 5 with initiator tRNA completely accommodated in the P-site. This is apparently an irreversible reaction that can stall the protein synthesis machinery at the AUG codon and triggers the dissociation of eIF1 and release of free Pi (reviewed in Valasek, 2012).

1.1.4. Ribosomal subunit joining and 80S initiation complex formation:

The joining of 60S subunit to the scanning- arrested 48S PIC in eukaryotes is regulated by the recently discovered factor, that is, GTP-bound eIF5B. This factor promotes a second round of GTP hydrolysis at the end of the initiation pathway (Pestova et al., 2007). Most of the eIFs, with the exception of eIF1A, bound to 48S PIC are released in response to the conformational changes induced by the first hydrolysis of GTP bound to eIF2 that is mediated by eIF5. The newly discovered factor eIF5B interacts with the extreme C-terminus region in eIF1A. This interaction facilitates the recruitment of eIF5B.GTP to 48S PIC, joining of 60S subunit, activation of the GTPase center of the 60S subunit to induce hydrolysis of GTP bound to eIF5B, and eviction of eIF1A and eIF5B. The 80S ribosome complex with the initiator tRNA positioned on the start AUG in the P site of ribosome is now poised for elongation (**Figure 1.1**).

Keeping in view of the studies presented here in this thesis, the available information on the importance of eukaryotic initiation factor 2 (eIF2) in the mechanism of initiation step of protein synthesis, its subunit structure, function, intersubunit and interprotein interactions, and regulation are briefly mentioned here.

1.2. Structure and function of eIF2

The eIF2 complex is a heterotrimer with three subunits: α-, β- and γ- subunits in the order of increasing molecular mass. Human eIF2α has 315 amino acids, eIF2β has 333 and eIF2γ has 472 amino acids. The molecular mass of human eIF2α-, β-, and γ-subunits are 36, 38 and 52 kDa respectively as calculated from their cDNA constructs (Ernst et al., 1987; Pathak et al., 1988; Gaspar et al., 1994). The trimeric native eIF2 results from 1:1:1 association of the three subunits (Pathak et al., 1988; Schmitt et al., 2002). However, β- and γ- subunits migrate close to each other on 10% SDS-PAGE. The apparent higher molecular mass of β- subunit on SDS-PAGE may be due to the presence of large blocks of lysine residues (Pathak et al., 1988). The human eIF2α, eIF2β, and eIF2γ sequences are respectively, 58%, 47%, and 72% identical to the corresponding subunits from yeast. The functions of eIF2 include binding of GDP/GTP, Met-tRNAi and mRNA. In addition, eIF2 has GTPase activity, promotes start codon recognition and interacts with other initiation factors. The γ- subunit of eIF2 is implicated mainly in the function of eIF2 which include GDP/GTP and Met-tRNAi binding and the ability to hydrolyze GTP which is stimulated by eIF5 (GTPase activating protein).

Identification of the start codon by initiator tRNA and positioning of its anticodon on the start AUG codon of mRNA in the P-site of ribosome triggers hydrolysis of GTP bound to eIF2 by eIF5, a protein that activates the GTPase activity of the γ- subunit of eIF2. The native protein eIF2 has ~100-fold higher affinity for GDP than for GTP (reviewed in Kapp and Lorsch 2004) and hence the rate constant for GDP release is slow. An eIF2.GDP binary complex, which is formed at the end of initiation step is inactive and cannot join the initiation cycle unless the GDP is exchanged for GTP (**Figure 1.1**). eIF2.GTP state has 10 fold higher affinity for Met-tRNAi than the eIF2.GDP state (Erickson and Hanning, 1996; reviewed in Kapp and Lorsch, 2004). Loss of methionine moiety or GTP hydrolysis weakens the interaction between eIF2.GTP and Met-tRNAi. The GDP off rate is very slow (0.2 min^{-1}). Hence, the recycling of eIF2.GDP to eIF2.GTP is catalyzed by a rate-limiting heteropentameric protein called eIF2B (Fabian et al., 1997; Sudhakar et al., 2000; Ramaiah et al., 1994; Krishnamoorthy et al., 2001; Pavitt et al., 1998). In archaea, GTP hydrolysis on aIF2 occurs without GAP (GTPase- activating protein) like eIF5 and also the GTP/GDP exchange occurs more spontaneously than mediated by an eIF2B like factor (reviewed in Hinnebusch, 2000, 2005; Webb and Proud, 1997; Pavitt, 2005).

The GTPase activity associated with eIF2 is very weak but it is enhanced when it joins GTP and Met-tRNAi, and subsequently becomes part of 43S PIC suggesting that structural features of eIF2 and its interaction with the 40S subunit may regulate its GTPase activity (Algire et al., 2005). A1: U72 base

pair in the initiator tRNA is the main determinant that interacts with eIF2.GTP stably and specifically, and orients the charged methionine into its binding pocket on the γ-subunit (Erickson and Hannig, 1996). In yeast, it has been shown that A928 nucleotide of 18S rRNA located in the P-site is required for delivering the ternary complex (eIF2.GTP.Met-tRNAi) to the 40S subunit and also probably for making a direct contact with Met-tRNAi (Dong et al., 2008). Also eIF2 interacts with eIF1, 1A and eIF3 which might be stabilizing eIF2 interaction with the 40S ribosomal subunit (reviewed in Hinnebusch et al., 2007). As of now none of the eIF2 subunits in its complex form has been structurally solved. However, the structures from human and yeast are available for α-subunit, but not β- and γ-subunits, the subunits of archeal IF2 and the trimeric form without Met-tRNAi have been solved (reviewed in Schmitt et al., 2010). These structural studies suggest that α- and β-subunits are flexible and are stabilized by their binding to the 40S ribosome subunit.

Very early studies had purified dimeric eIF2 from reticulocyte lysates consisting of α- and γ- subunits without β-subunit. Such preparations devoid of β-subunit or removal of β-subunit by proteolysis from native trimeric eIF2 has very little effect on the ability of eIF2α and eIF2γ subunits binding to guanine nucleotides and initiator tRNA (Mitsui et al., 1981), But subsequent experiments with yeast strains carrying mutations in β-subunit or removal of the eIF2α subunit suggested that β-subunit plays an important role in binding to the initiator tRNA and in the GDP/GTP exchange catalysed by eIF2B (Donahue et al., 1988; Nika et al., 2001). The results obtained however with

the archaeal IF2 (aIF2) are different. The C-terminal domain of aIF2α is sufficient to confer on γ-subunit its full tRNA-binding activity and is not affected by its β-subunit (reviewed in Schmitt et al., 2010; Marintchev and Wagner, 2004). These findings therefore suggest that the archaeal IF2 behaves somewhat differently from typical eukaryotic IF2. The eukaryotic eIF2β subunit, but not the eIF2α subunit, enhances the ability of eIF2γ subunit to bind Met-tRNAi (Nika, et al., 2001).

1.3. eIF2γ subunit

The gamma (γ) subunit is the biggest and homologous to EF1A, eEF1A and SelB/eEFSec (Leibundgut et al., 2005). The N-terminus region of γ-subunit of eIF2 contains all the three conserved consensus guanine nucleotide binding domains (GXXXXGK, DXXG, NKXD) and separated by 40-80 residues as reported in other GTP-binding proteins suggesting that it is mainly involved in binding GTP directly. Mutations in the NKXD consensus elements found in both the subunits (β and γ) indicate that GTP binds to the γ-subunit of eIF2 (Naranda et al., 1995). While the γ-subunit binds Met-tRNAi, eEF1 binds elongator tRNAs. Although the structure of eukaryotic γ- subunit of eIF2 is not available, the archaeal γ-subunit has considerable structural similarity with the prokaryotic elongation factor EF-Tu that delivers amino acylated tRNAs to the A site of 70S ribosome. The γ-subunit of aIF2 and EF-Tu has three domains: N-terminal GTP- binding domain and beta-barrel domains II and III. Keeping in view of this difference, it is likely that these proteins may have different

docking arrangements on the A- versus P-sites of the ribosome. γ-subunit of eIF2 is found in contact with the acceptor stem of initiator tRNA and has also binding interface between 18S rRNA and domain III of γ-subunit as revealed by hydroxyl radical probing experiments (Shin et al., 2004). These results are consistent with the biochemical analyses which demonstrated that domain III of eIF2γ is important for ribosomal binding but not for initiator tRNA binding. Mutations in domain I (or G domain) and II of eIF2γ altered the fidelity of AUG recognition probably by affecting the conformation of initiator Met-tRNAi (Alone et al., 2006 and 2008).

1.4. eIF2β subunit

The β-subunit of eIF2 has two domains conserved in all eukaryotes. These are the N-terminal and zinc-binding domains (ZBD). In the amino-terminal half of the protein there are three runs of seven lysine residues which are conserved in yeast, human and *Drosophila* (Donahue et al., 1988; Pathak et al., 1988; Ye et al., 1994) but not in archaea. The C-terminal moiety of the β-subunit, where there is a C2-C2 motif reminiscent of a potential zinc finger structure, is common to both eukaryotes and archaea. However, no zinc could be detected on purified eIF2 and zinc is not required for the GTP-dependent initiator Met-tRNAi binding activity of eIF2. It may be important for the structural stability. The N-terminal part of eIF2β is specific to eukaryotes and is involved in the binding of the C-terminal domains of eIF5 (GTPase-activating protein) and eIF2B (GDP/GTP exchange factor). This interaction of β-subunit plays a crucial role in the fidelity of initiation codon selection and

regulation of GTPase activity of the γ-subunit of eIF2. The three lysine boxes in the N-terminal part of the β-subunit also do not influence the GTP-dependent initiator Met-tRNAi binding by the eIF2 complex. It is not clear how the β-subunit influences the tRNA binding activity. A recent study suggests that the tRNA binding site on the core γ-subunit may be stabilized by the peripheral β- and α-subunits through their interaction with the γ- subunit (Naveau et al., 2010). The ability of eIF2 to bind mRNA is dependent on both the amino and carboxyl domains of the β- subunit, involving the lysine repeats and the C2-C2 domains (Laurino et al., 1999). The β-subunit is also a hub for protein-protein interactions. It interacts with initiation factors such as eIF5, eIF2B, and indirectly with eIF3a and c (Das et al., 1997; Kimball et al., 1998; Singh et al., 2004). Also, the lysine-rich region in the N-terminus of β- subunit interacts with eIF5 and the ε-subunit of eIF2B (Asano et al. 1999). The β-subunit of mammalian eIF2 also interacts with other proteins such as PP1, a type 1 protein phosphatase, Nck1, a tyrosine kinase adaptor protein, and also with casein kinase II (CKII) (Wakula et al., 2006; Kebache et al., 2002; Llorens et al., 2006). The N-terminal and the zinc-binding domain of β-subunit does not contact directly each other but are linked by a flexible helical linker. The importance of ZBD of β- subunit in 'start codon' AUG recognition is shown through mutational analyses of the conserved residues in ZBD that promote initiation events at UUG codons and allow eIF5-independent GTP hydrolysis and dissociation of initiator tRNA from eIF2.GTP *in vitro*. These findings thus suggest ZBD of β-subunit inhibits GTP hydrolysis by eIF2γ. The ZBD domain

is shown to contact the G- domain of eIF2γ based on the crystal structure of archaeal heterotrimeric IF2. Structural studies on archaeal β-subunit reveal similarity between eIF2β ZBD and GTPase-activating protein, eIF5. Keeping in view of this similarity, eIF2β ZBD may be displaced from eIF2γ- G or domain I by a similar ZBD of eIF5 NTD to stimulate GTP hydrolysis (Alone et al., 2006). In addition to β- and γ- subunits, eIF2α is also involved in the AUG recognition and has been substantiated by demonstrating that the heterodimer lacking α-subunit reduces the efficiency of AUG recognition (Pisarev et al., 2001).

1.5. eIF2α subunit

eIF2α is the smallest subunit (36 kDa) and the eIF2α-CTD is structurally homologous to the CTD of eEF1Bα (eEF1Bα-CTD) (Ito et al., 2004) a GTP/GDP exchange factor of eEF1A that delivers elongator tRNAs to the A-site of 80S ribosome. However, eIF2α does not have the GEF activity as in archaea. During evolution, eIF2α has lost its GEF activity to eIF2B, a heteropentameric protein that catalyzes GTP/GDP exchange on eIF2 (Marintchev and Wagner, 2004). Interestingly, eEF1A is structurally and functionally homologous to the γ-subunit of eIF2 that binds to GDP/GTP and initiator tRNA. So far no structural details are available on the organization of human eIF2 heterotrimer complex with Met-tRNAi. Structural organization of archeael heterotrimeric complex is well characterized and it reveals that the γ-subunit is the central core in the structure of eIF2 complex interacting with α

and β-subunits on eitherside and the direct interaction between α- and β-subunits was not observed (reviewed in Marintchev and Wagner, 2004; Yatime et al., 2007). Earlier studies from this laboratory have suggested that unlike in archaea and yeast, the α- and β-subunits of human eIF2 interact with each other and β-subunit of eIF2 binds to eIF2B complex but not to the α-subunit (Rajesh et al., 2008; Suragani et al., 2005).

1.6. eIF2 Regulation

eIF2 is a phosphoprotein and all subunits are shown to be phosphorylated *in vitro* by different kinases. The serine 51 residue of human eIF2α is phosphorylated by many stress- activated eIF2 α kinases like heme-regulated inhibitor (HRI), double stranded RNA-induced inhibitor (dsI) or RNA-dependent protein kinase (PKR), general control nonderepressible kinase (GCN2) and endoplasmic reticulum (ER)-resident kinase called PERK (reviewed in Baird and Wek, 2012). While all eIF2α kinases are able to phosphorylate the same Ser^{51} residue in the α-subunit, regulation and activation of these kinases however are different. HRI regulation is dependent on heme availability, PKR is regulated by double stranded RNA or virus infection, GCN 2 is activated by uncharged tRNA, where as PERK regulation or activation is mediated by unfolded proteins. Phosphorylation of eIF2α inhibits general protein synthesis and upregulates translation of gene-specific mRNAs such as GCN4 or ATF4 that code for transcriptional factors which in turn facilitate transcription of many of those genes involved in amino acid and redox metabolism (reviewed in Hinnebusch 2005; Vattem and Wek, 2004).

Phosphorylation of eIF2α is a stress, survival and suicidal signal (Aarti et al., 2010). Abrogation of eIF2α phosphorylation leads to transformation of cells in culture, and promotes hypoglycemia and hypoinsulnemia in homozygous mice. A heterozygous mouse of eIF2$\alpha^{ser51ala/+}$ harboring one copy of nonphosphorylatable form of eIF2α becomes obese on high fat diet and it performed better in several behavioral tasks and exhibited a facilitated long-lasting LTP (long-term potentiation), a cellular model for the changes in synaptic strength that occur during learning and memory (Scheuner et al., 2001; Scheuner and Kaufman, 2008). Thus phosphorylation of eIF2α couples protein synthesis with glucose sensing, glucose metabolism, insulin production and also memory. A small portion of phosphorylation of eIF2α (30% of total eIF2) is sufficient to inhibit general protein synthesis. This is because it sequesters the rate- limiting heteropentameric GDP/GTP exchange factor called eIF2B whose concentration is 20-30% of total eIF2 and inhibits the ability of eIF2 to recycle eIF2.GDP to eIF2.GTP. While unphosphorylated eIF2α does not interact with eIF2B, phosphorylated yeast eIF2α has been shown to interact with the β-subunit of the regulatory subcomplex in eIF2B comprising α-, β- and δ– subunits (Pavitt et al., 1998, Krishnamoorthy et al., 2001). However, the interaction between human or mammalian eIF2 and eIF2B is mediated by the β-subunit of eIF2 (Suragani et al., 2006; Rajesh et al., 2008).

The recent studies suggest that β- and γ- subunits of human eIF2 can also be phosphorylated by various kinases (Welsh et al., 1994; Rajesh et al., 2008;

Andaya et al., 2011). The mammalian β-subunit of eIF2 is found to interact with DNA- dependent protein kinase (DNA-PK), a nuclear enzyme and also serves as a substrate for DNA-PK which raises questions regarding its role, if any, in DNA repair (Ting et al., 1998). Unlike its yeast or archaeal counterpart, the human eIF2β subunit is phosphorylated by CKII (Ser-2 and Ser-67 residues), PKC (Ser-13) and PKA (Ser-218) (Welsh et al., 1994) Phosphorylation of the β-subunit by CKII appears to be constitutive in HeLa cells and mutations at these sites alter the functions of the β-subunit (Llorens et al., 2006). Phosphorylation of the β-subunit shows minimal physiological impact as compared to that of the α-subunit. The physiological significance of the β-subunit phosphorylation is not substantiated. Recent studies have shown that capable of phosphorylating Thr-66 of eIF2γ *in vitro* (Andaya et al., 2011). Structural mapping of the phosphorylation sites revealed Thr-66 mapping to the nucleotide- binding pocket of the γ-subunit. Like β-subunit, the physiological significance of phosphorylation of the γ-subunit of eIF2 is not understood.

Objectives

OBJECTIVES

Much of the work dealing with eIF2 heterotrimeric complex was carried out on γ- and α-subunits. The role of β-subunit is not well explored. While γ-subunit is implicated in the various functions of eIF2 such as GDP/GTP binding, Met-tRNAi binding and in GTP hydrolysis, phosphorylation of the α-subunit is implicated in the regulation of protein synthesis. Very early studies from Dr Maitra's laboratory (Stringer et al., 1980) showed that the eIF2 purified from rabbit reticulocyte lysates consisted of two subunits: α- and γ- but without the β-subunit. Subsequently, Ochoa's laboratory (Mitsui et al., 1981) found that the β-subunit was susceptible to protease digestion. The protease treated eIF2 consisting of α- and γ- subunits was found to retain the same activity as the native factor in promoting ternary complex, eIF2.GTP.Met-tRNAi or 43S complex consisting of 40S ribosomes with the ternary complex. This αγ complex was able to restore translation in heme-deficient reticulocyte lysates suggesting that the β-subunit of eIF2 has no role in the joining of Met-tRNAi. In contrast, cross-linking studies have implicated the mammalian β-subunit of eIF2 in nucleotide- and Met-tRNAi^{Met} binding (Gaspar et al., 1994; Bommer et al.,1991, Anthony et al., 1990; Dholakia et al., 1989) suggesting the interaction of β-subunit with γ-subunit. Subsequent studies by Flynn et al., 1993 have shown that purified reticulocyte eIF2 preparations devoid of β-subunit had little or no effect on the binding of guanine nucleotides. However such preparations significantly reduced Met-tRNAi binding suggesting that the β-subunit perhaps plays an important role in Met-tRNAi binding. The eIF2B

catalyzed guanine nucleotide exchange on eIF2 is also reduced *in vitro* in eIF2 preparations lacking the β-subunit, suggesting that the β-subunit also plays a role in eIF2B catalyzed guanine nucleotide exchange of eIF2.

Subsequently most studies were performed in archael and yeast eIF2. Purified yeast eIF2βγ complex, from a yeast strain lacking α-subunit, has shown that β- and γ-subunits, but not the α-subunit, are important for tRNA binding. However eIF2α is required for structural interactions. The rate of nucleotide exchange between eIF2 and eIF2B is promoted better in the presence of eIF2α (Nika et al., 2000). Consistent with these studies, phosphorylated yeast eIF2α, but not unphosphorylated subunit is shown to interact with eIF2B (Krishnamoorthy et al*.,* 2001). Interestingly, studies from archaeal aIF2 are found at variance with many of the results obtained from mammalian or yeast eIF2. The archaeal α-subunit of IF2 is shown to contribute to the tRNA binding affinity for the full aIF2 heterotrimer where as β-subunit contributes slightly to tRNA binding (Pedulla et al., 2005; Yatime et al., 2004 and 2006). These findings raise the possibility that archeal IF2 behaves somewhat differently from yeast or eukaryotic IF2.

Most of the structures of archaeal individual subunits of α, β and γ or the heterotrimeric complex of aIF2 with and without GDP, Met-tRNAi were solved. Crystal structures of yeast and mammalian eIF2α are available. However the structures of eukaryotic β- and γ-subunits from eukaryotes are not available. The crystal structures of N-terminal domain of α-subunit from yeast and mammals and NMR structure of wt eIF2α were solved (Dhaliwal and Hoffman, 2003; Ito et al., 2004). Much of the studies in eukaryotes are based on

genetics and biochemical studies. Subunit interactions among the trimeric eIF2 complex are well studied in archaea by structural studies and in yeast by biochemical studies. These studies have shown that α- and β-subunits do not interact with each other but interacts with γ-subunit and is proposed to be the centre of the complex. Being the center of the complex γ-subunit interacts with Met-tRNAi with less efficiently compared to the heterotrimeric complex (reviewed in Schmitt et al., 2010; Hashimoto et al., 2002 and Thompson et al., 2000).

In archaea, however, GTP hydrolysis on aIF2 occurs without GAP (GTPase activating protein) like eIF5 and also the GTP/GDP exchange occurs more spontaneously than mediated by an eIF2B like factor (reviewed in Hinnebusch, 2000, 2005; Webb and Proud, 1997; Pavitt 2005). In yeast and mammals, phosphorylation of the α-subunit is shown to promote a 15S complex formation between trimeric eIF2 and pentameric eIF2B proteins and inhibit the guanine nucleotide exchange activity of eIF2B and recycling of eIF2.GDP to eIF2.GTP (Ramaiah et al., 1994; Sudhakar et al., 2000, Krishnamoorthy et al., 2001). Based on these studies, it is thought that the α-subunit mediates the interaction between eIF2 and eIF2B. In contrast to such a belief, Kimball et al., 1998 demonstrated interaction between the C-terminus of eIF2β and the δ– and ε-subunits of mammalian eIF2B, where as the interaction between the N-terminus of eIF2β and the ε–subunit of yeast eIF2B were demonstrated by Asano et al*.,* 1999. Based on their observations, Kimball et al., 1998 suggested that α-subunit interacts with the β-subunit of eIF2 and predicted that phosphorylation of eIF2α induces a conformational change in the β-subunit of protein to enable it to interact tightly with eIF2B.

Consistent with such a notion, recent studies from this laboratory have shown that:

a) recombinant α- subunit of human eIF2 interacts with eIF2B complex,

b) α- and β- subunits of eIF2 interact with each other and

c) phosphorylation of the α-subunit enhances the interaction between α and β subunits and subsequently with eIF2B (Rajesh et al., 2008).

Keeping in view of these previous studies, the present thesis work is taken up to further determine the interaction between α- and β-subunits of human eIF2, their importance in Met-tRNAi binding and to understand the structural dynamics of the β-subunit of eIF2.

The major objectives are:

I. Characterization of the interaction between eIF2α and eIF2β subunits of human eIF2.

a. Expression of recombinant wt eIF2α and β and their N-terminal and C-terminal domains.
b. To identify broadly the regions in the subunits necessary for their interaction.
c. Interaction of eIF2α and β-subunits by biophysical studies.

II. Biophysical characterization of eIF2β subunit.

III. To determine the importance of eIF2α and eIF2β subunits on Met-tRNAi binding.

Materials and Methods

CHAPTER 2
MATERIALS AND METHODS

2.0. Materials:

Tryptone, yeast extract, peptone and agar powder for preparation of culture media were obtained from HiMedia, India. Agarose, ethidium bromide, isopropyl-beta-D-thiogalactopyranoside (IPTG), acrylamide, bis-acrylamide, ammonium per sulphate (APS), sodium dodecyl sulphate (SDS), N, N, N', N'-tetramethylethylenediamine (TEMED), were obtained from sigma, India. The two component systems of chemiluminescent substrates for horseradish peroxidase (HRP) are two-component systems consisting of a stable peroxide solution and an enhanced luminol solution, was purchased from Pierce. Nitrocellulose Hybond-N^+, Hybond C-extra and PVDF membranes were purchased from Amersham-Pharmacia. All restriction endonuclease enzymes, T4 DNA ligase, DNA molecular weight standards were purchased from New England Biolabs (NEB), USA. Taq DNA polymerase, protein molecular weight markers, horse radish peroxidase conjugated secondary antibodies were purchased from Bangalore Genei, India. Gel extraction kit, PCR purification kit, midi and mega plasmid preparation kits were obtained from MN (Hilden, Germany). Oligonucleotides were synthesized from Bioserve India biotechnology Pvt Ltd. Bradford's reagent was purchased from Bio-Rad, USA. Monoclonal anti-eIF2β, polyclonal antibodies against eIF2α, were obtained from Santacruz, USA. Secondary antibodies conjugated with horseradish peroxidase were obtained from Promega, USA. Radiolabelled nucleotides were purchased from Jonaki (Hyderabad, India). MEGAshortscript^{TM} *in vitro* transcription kit was obtained from Ambion Inc. Complete protease inhibitor was obtained from

Sigma. All other chemicals were purchased from local manufacturers (Qualigen, E-Merck, SDS-Fine biochemicals. etc.,) and chemicals were of a reagent grade. eIF2γ subunit purified protein was obtained from Abnova company (Size-100 µg).

2.1. Cloning, expression and characterization of human eIF2 subunits.

2.1.1. Selection of subdomains

Based on the domain organization of aIF2α and structure based sequence alignment of aIF2β and sequences of eIF2, mutants or the truncated domains of eIF2α and β comprising their N and C- terminal domains were constructed respectively.

2.1.2. PCR amplification and cloning of sub-domains into pET vector

The N-terminal sub-domain of eIF2α comprising of nucleotides 1- 450 bp and the C-terminal sub-domain comprising of nucleotides 451-945 bp were amplified from the parent vector pET32a harboring the recombinant full length gene. In human eIF2β subunit, the N-terminal sub-domain comprises of nucleotides from 1- 510 bp and the C-terminal domain comprises of nucleotides 511-1000 bp were amplified using the designed primers with the restriction sites at the 5′ and 3′ ends. The oligonucleotides used to amplify the sub-domains of α and β are given in **TABLE 1.** Eppendorf PCR machine was used for amplification studies. The procedure used for PCR has basically three steps: denaturation, annealing and extension. The strand separation of template strand DNA was carried out at 95^0C for 2 min in the first step. Annealing of short oligos (primer DNA) to its complementary region on template DNA was performed at 55^0C for 30 sec in the second step. In the third step,

S. No.	Target gene	Tm	Primer Sequence 5' ⟶ 3'	Restriction Site	Name of the clone	Gene Size (kbp)	Molecular mass of protein (kDa)
1.	eIF2α NTD	64	CCG GAG TGG GGC CGCTATCGATCATCGTCAG	*NdeI*	pET21b- α NTD	0.549	20.5 kDa
		64	CCA GGC GCC GTA GAA GTC GTCAGCTTAGCAGC	*XhoI*			
2.	eIF2α CTD	74	CAT AAC CAT GGT GGC CAG CTG TGC CGG CGT G	*NdeI*	pET21b- α CTD	0.450	18 kDa
		75	ATC CGC TCG AGC TTC AGG CCA TCA CTG ACCGCC	*XhoI*			
3.	eIF2β NTD	75	CAT AACCAT GGT GGC GCC CGC GCA GCC ACC GATC	*NdeI*	pET21b- β NTD	0.510	19.5 kDa
		75	ATC CGC TCG AGA TCG CCG ATG CGC GCC TTC TG	*XhoI*			
4.	eIF2β CTD	75	CAT AAC CAT GGT GGC CGA CCC CAC GCC CGC CAC	*NdeI*	pET21b- β CTD	0.495	18 kDa
		75	CCC AAGCTT TTT CCCCA GGG TCA CCTCA TCC	*XhoI*			
5.	MetRS	75	CAT AAC CAT GGT GCA CGG CAC CAT GAC CACGCC G	*NdeI*	pET22- MetRS	1.2	66 kDa
		77	ATC CGC TCG AGG TAC GCG ATC CAC GCA TCG CGC C	*XhoI*			
6.	MettRNA	75	CGC GGA TTC GCC GAG GTG GAC CGC CGG ATT	*EcoR1*	pMet		-
		71	CCG GAA TCC TCA TTC CGA GTC CAC CTT CGC	*PstI*			
7.	MettRNA T7 promoter	71	AATTTAATACGACTCACTATAAGCAAGAGTGGCGCAGCGG	*BamHI*	-		-
		75	TGGTAGCAGAGGATGGTTTTCGA	*EcoRI*			

Table 1.0 Details of eIF2, MetRS and Met-tRNAi genes cloning

primer DNAs were extended at 72^0C for 90 sec in the presence of proof reading thermostable phusion DNA polymerase and nucleotides as described by Sambrook et al., (1989). These steps were repeated for 30-35 cycles to obtain desired amplified PCR product. The amplified PCR products were analyzed by 1% agarose gel electrophoresis and the inserts were purified by PCR purification kit. Restriction digestion reaction was set up overnight using restriction enzymes *NdeI* and *XhoI*. The digested products were gel purified. The host pET21b vector plasmid was isolated from DH5α. The purified plasmid DNA was digested with respective enzymes used for insert digestion and the digested vector was gel purified. Afterwards, the insert DNA was ligated to the plasmid vector. 50-100 ng of restriction digested vector DNA was mixed with a 3-fold molar excess of the insert DNA with compatible ends, in 1X ligase buffer (50 mM Tris.HCl, pH 7.5, 10 mM $MgCl_2$, 10 mM DTT, 1 mM ATP and 25 mg/ml BSA). 200 units of T4 DNA ligase was generally used for ligation reaction, which was carried out at 16^0C for 16 hrs. The volume of the ligation reaction was usually 10-20μl. The ligation mixtures were then transformed into competent *E. coli.* DH5α strain cells prepared by using Innoue Method as described (Sambrook et al., 1989). Recombinant clones were screened to identify the positive clones either by colony PCR or by restriction digestion using respective enzymes. The confirmed clones were further sequenced using DNA sequencing facility.

2.1.3. Over expression

The recombinant plasmid was transformed and over expressed in *E.coli* Rossetta BL21 (DE3). Cells were grown in Luria-Bertani medium with 100 µg ml^{-1}ampicillin and 34 µg ml^{-1} chloramphenicol at 37^0C until OD_{600} reached to 0.6

absorbance units. The cells were induced for expression of recombinant proteins by the addition of 0.5 mM IPTG at 18^0C and the growth was continued for 16 hrs.

2.2 Protein purification strategies

2.2.1. Ni-NTA agarose chromatography:

All recombinant proteins in this study were expressed in three litre cultures with hexa-histidine tag forms and were purified by nickel-nitrilotriacetic acid (Ni-NTA) metal-affinity chromatography following the manufacturer's protocol (Qiagen). The column was equilibrated with lysis buffer (50 mM Tris pH 7.5/300 mM NaCl/10 mM imidazole). Cell lysate prepared in lysis buffer was then passed through the column to allow binding of hexa-histidine tag proteins to Ni-NTA agarose beads. Column was then washed with 10 volumes of wash buffer (same composition as lysis buffer except with 50 mM imidazole). Bound proteins were eluted by 5 column volumes of elution buffer containing 250 mM imidazole but having the same composition as lysis buffer.

2.2.2. Size-exclusion column chromatography:

The exclusion limit of the column was 3-3000 kDa. The column containing superdex 75 with a bed volume of 120 ml was fitted to FPLC (Biorad). For 120ml bed volume, 1ml/min flow rate was used for 2 hr. The column was first equilibrated with 2-bed volume of gel filtration buffer (25 mM Tris-HCl pH7.5, 100 mM NaCl). 1 ml of concentrated protein solution obtained from Ni-NTA was injected into the superdex column and allowed the proteins to pass through the column at a flow rate of 1ml/min. Optical density at 280 nm was recorded for the eluted protein fractions in a recorder which was connected to a UV spectrophotometer. Eluted proteins were collected in 3 ml fractions. The protein

fractions were analyzed by 12% SDS-PAGE following staining of the proteins with coomassie brilliant blue. The pooled fractions were concentrated for further studies.

2.2.3. SDS-Polyacrylamide gel electrophoresis:

SDS-PAGE was carried to analyze the protein samples. A stock solution containing 30% acrylamide (w/v) and 0.8% N, N'-methylene bisacrylamide (w/v) was used. Acrylamide and TEMED stock solutions were stored in the cold in dark bottles. Proteins were separated by 10-12% resolving gels that contain 4-5% stacking gels of the above acrylamide-bis acrylamide solution. The gels were polymerised by adding TEMED and freshly prepared ammonium persulphate (0.1%, final concentration). The gels were casted in a vertical gel electrophoresis apparatus (BioRad). Prior to electrophoresis, the protein samples were mixed with equal volume of 2X SDS-loading buffer (50 mM Tris-HCl, pH 6.8, 2% SDS, 10% glycerol, 0.01% bromophenol blue and 5% β-mercaptoethanol) and heated in a boiling water bath for 3-5 min and centrifuged at 12000 rpm for 10 minutes at room temperature. Proteins were resolved at a constant current of 20 mA until the dye front reached the bottom of the gel. The gels were generally stained with coomassie blue. However the gel bands of purified proteins transferred to nylon membrane were detected by ponceau stain.

2.2.4. Estimation of protein concentration:

Bradford's reagent was used to estimate the quantity of protein. Different concentration of bovine serum albumin (BSA) was used to plot a standard protein curve. Protein in the purified form or in the cell lysate was mixed with the dye in Bradford's reagent, obtained from Biorad and the change in OD of

the solution was measured at 595 nm. In a typical estimation, 3-4 ml of 20% bradford reagent is supplemented with 4-5 µl of protein solution and the change in colour is measured at 595nm by a spectrophotometer. Purified protein was also quantified when required, by measuring the optical density at 280 nm and calculated with the help of following formula: $C = A/\varepsilon l$

Where A represents the absorbance of protein solution at 280 nm, C is concentration of the protein per ml in solution and ε is the extinction coefficient.

2.2.5. Western analysis:

Western blot analysis was carried out after resolving the proteins on SDS-PAGE. Proteins were transferred to a Hybond-C Extra using Bio-Rad semi-dry transfer apparatus by applying current of 0.8 mA per cm^2 area of the membrane for 1 hour. The transfer buffer (100 ml) contained 0.293 g glycine, 0.58 g Tris, 0.037 g SDS and 20 ml methanol. After the transfer, the membrane was stained with Ponceau S dye to check for the transfer of the proteins. The membrane was then washed thoroughly with TBS-T, pH 7.6 (20 mM Tris, 137 mM NaCl and 0.1% polysorbate20 (Tween20) to remove the Ponceau stain. The blot was then incubated in a blocking solution containing 5% skimmed milk powder in TBS-T for 1 h in shaking at room temperature. The membrane was then incubated with the primary antibody solution made in TBS-T for 1 h in a shaking orbiter at room temperature. At the end of incubation, the membrane was rinsed with TBS-T thrice for 10 minutes each. The membrane was incubated with appropriate secondary antibody horse radish peroxidase labeled made in TBS-T containing 1% milk powder, for 1 hour shaking orbiter followed by washing thrice for 10 min each with TBS-T. The blot was developed using chemiluminescent substrates which consists of two-component systems, a

stable peroxide solution and an enhanced luminol solution. The luminescence was captured by an X-ray film.

2.3. Biophysical Characterization of the sub units

2.3.1. Steady state fluorescence spectroscopy

The intrinsic fluorescence spectra measurements were recorded using F-4500 Fluorescence spectrofluorimeter (Hitachi Inc., Japan) that is equipped with a thermostatically controlled sample holder at 25^0C. The protein concentration in the fluorescence measurements were in the range of 0.03-0.05 mg/ml. The protein solution was excited at 295 nm and the emission was recorded in the range of wavelengths, 300–400 nm. Both the excitation and emission spectra were obtained by setting the slit width at 5 nm, and scan speed at 100 nm min^{-1} in a correct spectrum mode. Baseline corrections were carried out by using appropriate reaction mixtures (i.e) either buffer or buffer with denaturant.

2.3.2. Equilibrium unfolding studies

Equilibrium unfolding of heIF2β was studied using guanidinium chloride (Gdn-HCl) in the range of 0–6 M concentration with an interval of 0.1 M Gdn-HCl (total of 60 data points for each unfolding transition states). Protein samples prepared in increasing concentrations of Gdn-HCl (0 to 6 M) in 50 mM Tris buffer, pH 7.5, containing 100 mM NaCl at room temperature. Tryptophan fluorescence emission spectra were recorded by exciting the samples at 295 nm and unfolding was monitored by following the changes in intrinsic Trp emission fluorescence.

The ratios of fluorescence intensity (at 360/320 nm) was plotted as a function of Gdn-HCl concentration and the data were fitted to the following equation, which

relates fluorescence intensity to the extent of unfolding. The free energy of unfolding (ΔG_D) was determined from the ratio of native to denatured protein at each Gdn-HCl concentration, and plotted against the respective Gdn-HCl concentration.

Equation used for two-state model:

$$Yobs = \frac{\{ Y_N + Y_U \exp(-(\Delta G^0_u - m1]D) / RT) \}}{\{1 + \exp(-(\Delta G^0_u - [m1]D) / RT)\}}$$

Where Y_N is signal of the folded protein, Yu is signal of the unfolded forms, m is denaturant dependence of the free energy change in units of kcal mol^{-1} M^{-1}, R is the universal gas constant (1.987 cal mol^{-1} K^{-1}) and T is the absolute temperature.

2.3.3. Hydrophobic dye binding studies

8-Anilino-1-naphthalene sulfonic acid (ANS) emission spectra were recorded in the range of 430–550 nm with an excitation at 375 nm using slit widths of 7 nm for emission and excitation in a steady-state spectrofluorimeter. The protein samples (0.01 mg/ml) at room temperature were incubated for 4 h at pH 7.4 and pH 10.0 and the fluorescence spectra were recorded. The protein concentration of the samples kept at pH 2.0 was 0.005 mg/ml instead of 0.01 mg as the fluorescence intensity was very high at 0.01 mg/ml for low pH. The final spectrum was obtained by subtracting the results of the spectrum of ANS in respective buffers at different pH from the protein-ANS spectrum.

2.3.4. Circular dichroism (CD) measurements

CD measurements were performed in a Jasco 815-150S (Jasco, Tokyo, Japan) spectropolarimeter connected to a Peltier Type CD/FL Cell circulating water bath (Jasco,Tokyo, Japan). Far-UV CD measurements were recorded using 0.1 mg/ml protein with a 1 mm path length cell. Near-UV measurements were made at 1.0 mg/ml protein concentration with a 10 mm path length cell. Each spectrum was the average of three scans. The CD spectral studies were carried out to characterize the subunits and also for studying the interaction between subunits.

The effect of low pH on the secondary structure was studied by incubating the protein samples in HCL- KCl buffer. The buffer consists of 10.6 mM HCL and 50 mM KCL that gives pH 2.0. The protein was also incubated at high pH in Glycine-NaOH buffer for pH 10.0, the buffer consists of 50 mM glycine and 32 mM NaOH. All incubations were done for 4 h at room temperature. In addition, the effect of temperature on the protein was studied by two methods. In one method, the protein samples were incubated at different temperatures ranging from 25 to 85^0C and each scan was independently recorded. In the other method, the temperature of the protein samples was increased at the rate of 2^0C/min for the temperature ranging from 25 to 85^0C and the ellipticity was recorded at 208 nm. The Tm of the protein sample was determined based on the changes in the ellipticity as recorded above. All data were collected by subtracting the respective buffer base line.

2.3.5 Dynamic light scattering measurement

DLS experiment was performed using a DLS instrument (Nanobiotek) of purified eIF2β protein operating at wavelength 830 nm. The measurement

was done in 20 µl quartz cuvettes (Hellma Analytics) of 2 mg/ml concentration of the protein. Prior to analysis, protein samples were filtered through 0.22 µm pore size membrane filter. Data was collected at 25^0C with duration of 20 s. The resulting autocorrelation function was fitted using OmniSize3.0 software (Malvern Instruments). Hydrodynamic radius (R_h) was estimated from the results.

2.4. Subunit interaction by Immunoprecipitation

Co- Immunoprecipitation (Co-IP) assay

The Interaction between recombinant eIF2α and recombinant eIF2β was analyzed by immunoprecipitation. The protein G agarose beads were used for incubation with eIF2β mouse monoclonal antibodies. These beads were initially washed with RIPA buffer to remove ethanol. The assay involves the following steps

Pre-incubation

Specific antibodies (20µg) were pre- incubated with protein G-agarose beads of 20 µl in PBS buffer (10mM sodium phosphate buffer, pH 7.2, 100 mM NaCl containing 0.1% Triton X-100 at 4^0C for 1 hr. Pure protein of eIF2β (20-30 ug) specific to anti bodies was incubated at 4^0C with gentle mixing on a rotortorque.

Immunoprecipitation

The protein antibody-agarose bead complex was then incubated with the interacting protein or the cell lysate expressing the protein of interest for 5 hrs or overnight at 4^0C with gentle mixing on a rortorque. The protein antibody-agarose beads and the interacting protein complex were spun down at 100g

for 3 min at 4^0C. The protein bound to antibodies is considered to be the IP and the interacting protein as Co-IP. As a negative control, BSA was bound to the protein antibody-agarose bead complex.

Washing

To remove the components that non-specifically bind to agarose beads The immunoprecipitate was then washed 5-6 times with five volumes of PBS containing 0.1% Triton X-100, by removing the supernatant after every spin at 100g for 3 min at 4^0C. The washed immunoprecipitate was boiled in SDS-sample buffer and processed for gel electrophoresis.

Analysis of immunoprecipitates

The immunoprecipitates were separated by SDS-PAGE, following which the gel was equilibrated for 10 min in transfer buffer (39 mM glycine, 48 mM Tris base, 0.0375% SDS and 20% methanol) and electroblotted on to a Hybond-P PVDF membrane by semi-dry method using a Nova Blot apparatus (Pharmacia Biotech, Sweden). The PVDF membrane was pre-wetted in methanol, rinsed in distilled water and equilibrated in transfer buffer. The gel was placed in contact with membrane and sandwiched between 3 pieces of Whatman No.3 paper on each side. The sandwich was then placed between graphite plate electrodes with the membrane facing the anode. The proteins were transferred for 1.5 hr using a current of 0.8 mA/ cm^2 blot. After transfer, the proteins were visualised by staining with Ponceau-S dye (0.2% Ponceau-S dissolved in 3% trichloroacetic acid and 3% sulfosalicylic acid, fixed with methanol and washed in deionised water. A pre-stained protein weight marker was used to identify the positions of the proteins.

Immunodetection by chemiluminescence reaction

The PVDF membrane containing electroblotted proteins was blocked with 5% blotto in TBS containing 0.1% Tween-20 for 1hr at room temperature. The blot was incubated in the primary antibody diluted in TBST containing 0.5% Blotto for 1-2 Hr at room temperature and washed 3 times for 5-10 min each with TBST. The blot was then incubated with HRP-conjugated anti-IgG antibody diluted in TBST for 30 min and washed extensively as described above. Immunoreactivity was determined using luminol as substrate and detected by chemiluminiscence using an ECL detection kit by chemiluminiscence imager.

2.4.1. Circular dichroism

CD measurements were performed in a Jasco 815-150S (Jasco, Tokyo, Japan) spectropolarimeter connected to a Peltier Type CD/FL Cell circulating water bath (Jasco,Tokyo, Japan). Far-UV CD measurements at 200-250 nm were recorded using 0.1 mg/ml protein with a 1 mm path length cell. Each spectrum was the average of three scans. Measurements were recorded for eIF2α and eIF2β separately, an also for the complex of eIF2α:eIF2β and eIF2αCTD: eIF2β was measured.

2.4.2. Isothermal titration calorimetry (ITC)

ITC measurements were performed at 30^0C in an ITC-200 calorimeter (MicroCal, Inc). The titrations were carried out in 50 mM Tris-HCl buffer (pH 7.8) containing 50 mM NaCl. 10 µM of the reactant protein (eIF2α) was placed in the 200 µl sample cell. The injection syringe contains eIF2β protein of 300 µM concentration. The eIF2β protein was injected into eIF2α solution in the

cell. The volume of each injection was 2 µl except the first injection was 0.5 µl. The titration experiment consisted of 25 consecutive injections of four seconds duration with 120 seconds interval between injections. Control experiments were performed under identical conditions to determine the heat signals that arise from the addition of the protein into the buffer. The data was fitted with the single site binding model using the Origin software package (MicroCal, Inc).

2.5. Binding kinetics

2.5.1. In vitro transcription and preparation of [^{32}P] labeled RNA substrates

Plasmid, ptRNA^{met} harbouring mammalian initiator tRNA gene, has been constructed in the following manner. The two self-complementary synthetic DNA oligomers encoding appropriate tRNA sequence with *EcoRI/PstI* overhang were denatured at 94^{0}C for 2 min and annealed at 55^{0}C for 5 min. The 5′ terminus was phosphorylated by poly nucleotide kinase (PNK) and ligated at EcoRI/PstI sites of pBS vector. Template for *in vitro* transcription was prepared by PCR using a forward primer containing the T7 promoter sequence upstream of tRNA sequence and a tRNA complementary reverse sequence. The PCR product concentration was quantified before proceeding to *in vitro* transcription. *In vitro* T7 RNA polymerase runoff transcription was performed using Megashort Script kit (Ambion). The transcript was phenol-extracted and passed through a G-25 spin column (GE Healthcare).

Radiolabelling of the 3′ terminus of tRNA is performed utilizing the natural function of tRNA nucleotidyl transferase to exchange the endogenous A76 of tRNA with [α-^{32}P] ATP. Nucleotidyl transferase enzyme is responsible for the

addition of the universally conserved 3′ terminal CCA sequence to tRNAs (Schurer H, et al., 2001). The enzyme has been used here to exchange radiolabelled A to unlabelled A in CCA. The protocol is divided into two steps: first one favours the removal of the unlabeled endogenous adenosine and the second to favour the addition of [α-^{32}P] ATP. The first step involves adding pyrophosphate to a reaction containing a tRNA and tRNA nucleotidyltransferase enzyme to stimulate the removal of A76 to form ATP. The equilibrium is then shifted in the opposite direction by adding pyrophosphatase to degrade the free pyrophosphate and stimulate the nucleotidyltransferase catalyzed addition of [α-^{32}P] ATP to the tRNA. A typical 50 µl reaction consists of 1 µM tRNA, 50 µM sodium pyrophosphate, 0.2 µM tRNA nucleotidyltransferase, 0.3 µM (α-^{32}P ATP) (specific activity 3000Ci/m mole), 10 mM $MgCl_2$, and 50 mM glycine pH 9.0. The reaction is incubated at 37^0C for 5 minutes in order to complete the removal of the endogenous A76 residue. It is crucial that the reaction time remains short to minimize the subsequent removal of C74 and C75 of the tRNA. In the second step of the reaction, 1 µM CTP and 10 u/mL baker's yeast inorganic pyrophosphatase is added and the reaction is incubated at 37^0C for an additional 5 minutes. The pyrophosphatase is added to degrade the pyrophosphate added in the first step. The CTP is added to ensure that those tRNAs missing C74 or C75 are properly repaired. While extracting the tRNA, care has to be taken to avoid proteins and unreacted [α-^{32}P] ATP that contributes a high background signal in the product analysis. Hence the aqueous phenol layer was passed through consecutive Microspin P-6 columns (Biorad) and was eluted by low

concentration of 10 mM Tris buffer and the sample was ethanol precipitated and re-suspended in water (Ledoux & Uhlenbeck, 2008).

2.5.2. Purification of methionyl-tRNA synthetase (MetRS)

Purification of MetRS his-tag protein was performed by affinity chromatography (Ni-NTA). Cells were centrifuged at 4K for 5 min and resuspended in ice-cold lysis buffer containing 50 mM Tris-HCl buffer pH 8.0, 150 mM NaCl, and 10 mM Imidazole. Cells were lysed by sonication on ice. The crude cell extract was subjected to nucleic acid precipitation with 1% of streptomycin sulphate for 30 min at 4^0C with constant stirring. The precipitate was then centrifuged at 40,000x g for 45 min at 4^0C. The supernatant was loaded on Ni-NTA affinity column (Qiagen) previously equilibrated with lysis buffer. Protein was eluted with buffer containing 250 mM imidazole. Concentrated protein was further purified on a Superdex-200 gel filtration column in 50 mM Tris-HCl pH 8.0, 150 mM NaCl. The concentrated protein was buffer exchanged with 20 mM Tris-HCl pH 8.0, 150 mM NaCl and 5 mM BME. The pure protein was 25 mg/ml of concentration. Purified MetRS has the concentration of 256 µM and is stored in aliquots at -70^0C.

2.5.3. Aminoacylation of [^{32}P] 3′tRNA

Aminoacylation was carried out in the buffer containing 20 mM Tris (pH 7.6), 150 mM KCl, 7 mM $MgCl_2$ in the presence of 10 mM DTT, 2 mM ATP, 2 µM (α-^{32}P) 3′ tRNA as described earlier Met-tRNA, 1 µM MetRS and 1 mM methionine. Reactions were incubated for 30 min at 37^0C, phenol extracted, ethanol precipitated and resuspended in 20 mM sodium acetate (pH 4.6), 100 mM KCl and 0.1 mM EDTA. Analysis of aminoacylated [3′-^{32}P] tRNAs was

done by acid urea PAGE containing 10X buffer of 10.66g of Na acetate (Calbiochem) in 130 ml H_2O and the pH was adjusted to 5.5 using acetic acid (Varshney et al., 1991).

2.5.4. RNA binding assays

Hybond-C and Hybond-N^+ membranes were purchased from Amersham Biosciences. Hybond-C membrane was presoaked in 0.5 M NaOH for 10 min and rinsed in H_2O until the pH was neutral. Hybond-N^+ membrane was washed once in 0.1 M EDTA (pH 8.8) and three times in 1M KCl for 10 min each, followed by rinsing with 0.5 M NaOH and washing with H_2O until the pH became neutral. Hybond-C and Hybond-N^+ membranes were equilibrated in binding buffer (40 mM Tris-HCl, pH 7.5, 2 mM DTT, 2 mM $MgCl_2$, 10% glycerol) for at least 1 h prior to use. A 96-well dot-blot apparatus was assembled so that the Hybond-N^+ membrane were placed underneath the Hybond-C membrane. Reaction mixtures (20 μl) containing 40 mM Tris-HCl, pH 7.5, 2 mM DTT, 2 mM $MgCl_2$, ^{32}P-labeled tRNA, and varying amounts of protein (eIF2α,β,γ) were incubated on ice for 30 min. Each well was washed with binding buffer (200 μl) just prior to loading the sample. Samples were loaded and vacuum was applied, and the wells were again washed twice with 100 μl of binding buffer. The apparatus was disassembled, the two filters were air-dried, and then visualized and analyzed using a Phosphorimager (Fuji). Quantification was carried out by ImageJ and the fraction of RNA bound was determined from (% Bound RNA signal/ %Bound RNA signal + Unbound RNA signal). The fraction of RNA bound was plotted against the total protein concentration and the K_D value was determined by non-linear regression analysis using a one-site binding hyperbola using GraphPad Prism Software.

2.6. Bioinformatic methods

2.6.1. Softwares used for analyzing DNA and protein sequences:

The following softwares were used for analyzing DNA and protein sequencing

1. Homology searches of the sequences were done using BLAST program available at www.ncbi.nlm.nih.gov
2. Multiple alignments of protein sequences was done using CLUSTALW program available at www.ebi.ac.uk
3. Expasy (www.expasy.org) was used to analyze protein sequence. Calculation of extinction coefficient of a given protein sequence was also performed using Expasy.
4. Chromas Software was used for DNA sequence analysis of the chromatograms obtained from the gene sequencer (ABI Prism 3700).
5. NEB cutter was used for restriction digestion analysis of the given DNA sequence.
6. GraphPad Prism ver 6.0 was used for generating graphs and analyzing the enzymatic reactions.
7. Origin was used for CD and fluorescence data analysis.

2.6.2. Modeling of eIF2β and eIF2γ protein:

A structural model of human eIF2β and human eIF2γ was build using MODELLER Release 9v7version MODELLER **(**Sali & Blundell, 1993). This is most frequently used for homology or comparative protein structure modeling. The user provides an alignment of a sequence to be modeled with known related structures and MODELLER will automatically calculate a model with all non-hydrogen atoms. The eIF2β sequence and eIF2γ sequence were aligned with archaeal aIF2β (PDB, 1NEE) and archaeal aIF2γ (PDB, 1SOU3). Then 3D

model of the eIF2β and eIF2γ was generated using MODELLER (Release 9v7, r6923). The models were viewed and checked using the program O (Jones et al., 1991) and was compared with that of the template and related structures. For a comparison of the models, the structures were superimposed manually, using the program O and/or PyMOL (Schrodinger, 2010) with that of the aIF2β and aIF2γ (PDB, 1NEE and 1SOU3).

Results

CHAPTER 3

RESULTS

3.1. Designing the mutants of human eIF2α and β-subunits based on structure based sequence alignment and domain organization

To construct the mutants of eIF2α and β-subunits of human eIF2, the available eukaryotic sequences were aligned with the known archaeal structures, PDB ID - 1NXU and 1NEE, using the structure-based sequence alignment program MAFFT as shown in **Figure 2.1.** The domain organization of human β-subunit is derived from the above sequence alignment between archaea and humans as shown in **Figure 2.2**. This alignment has shown that only the C-terminal domain of eIF2β from 170 to 333 residues has 30% sequence identity with archaeal aIF2β subunit. Further, the N-terminal domain which is lysine-rich, is specific to eukaryotes. Keeping in view of these differences/similarities, two mutants of human eIF2β subunit carrying the N and C-terminal domains were constructed. The first one harbors 1-168 amino acid residues and the second one has 169-333 amino acids.

The selection of sub-domains for human eIF2α was based on the recently published structures of eIF2α (Ito et al., 2004) as shown in **Figure 2.3.** Two mutants of eIF2α were generated consisting of 1-183 residues and 186-315 residues. The N-terminal mutant containing 1-183 residues has been shown to possess two sub-domains: S1 sub-domain (residues 15-85) and α-helical sub-domain (91-183) and the C-terminal domain that includes a C-terminal tail (275-315 residues) is specific to eukaryotes as shown in **Figure 2.4**.

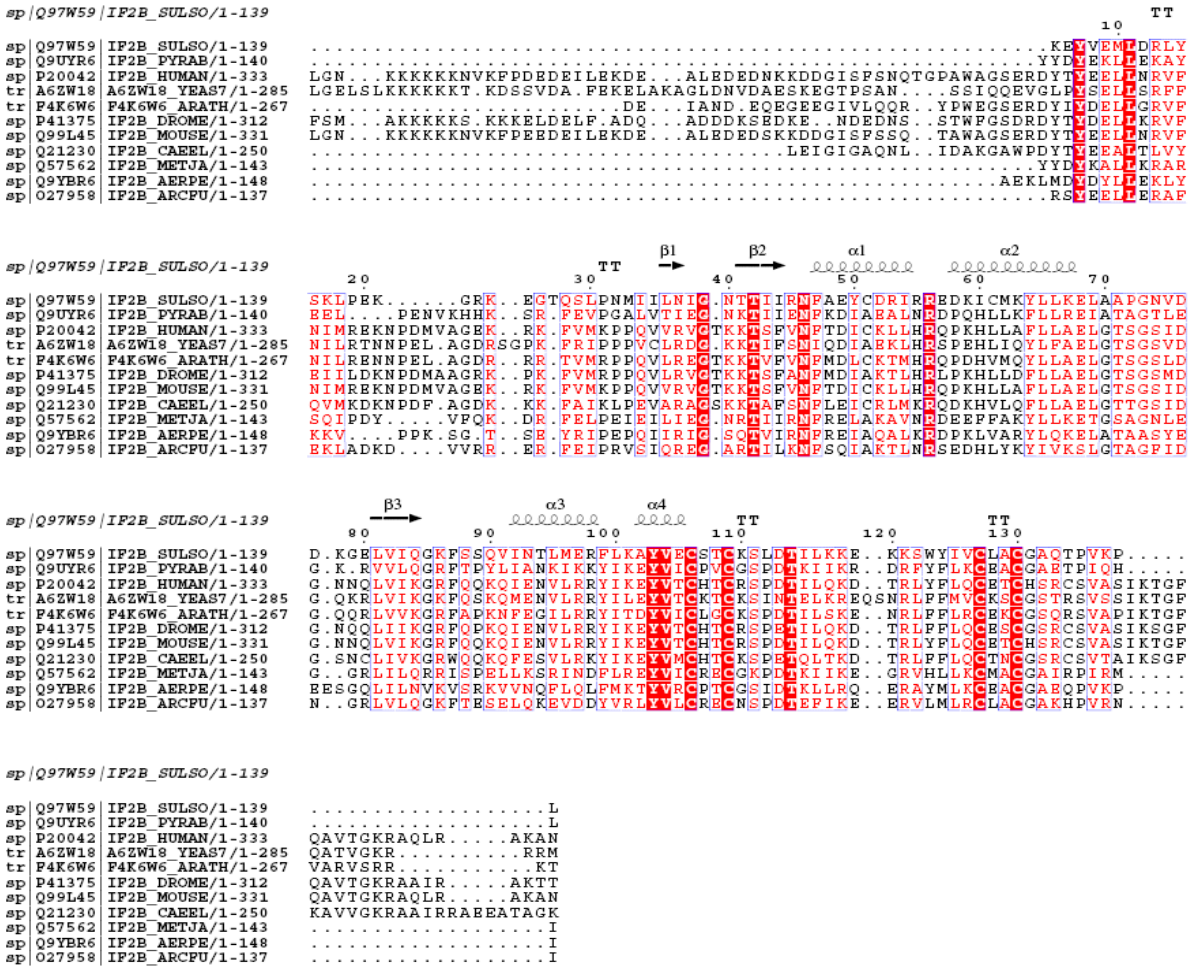

Figure 2.1. Structure-based sequence alignment of eIF2β homologues sequences from selective species of archaea and eukaryotes.

Sequence numbering corresponds to *Sulfolobus solfataricus* eIF2β (NCBI ID: Q97W59). Secondary structural elements are denoted as follows: α-3_{10}-helices are represented as springs; β-strands as arrows and random coil as lines. The four cysteines involved in zinc ion binding are conserved. ESPript sequence similarity is color coded using a gradient from white (<40% identity) to dark red (100% identity).

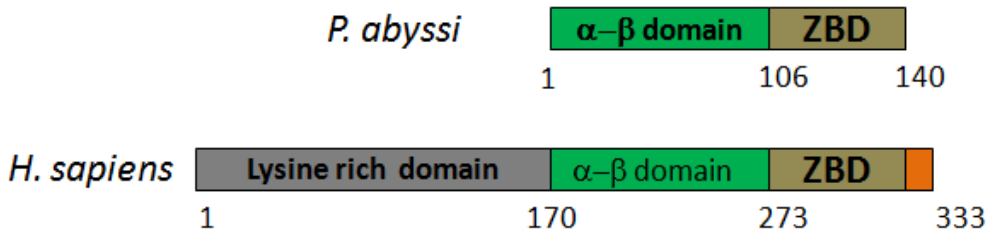

Figure 2.2. Schematic structural organizations of eIF2β/aIF2β.

Eukaryotic and archaeal initiation factors were aligned based on the structural similarity. The structural organization of eIF2β subunit from *Homo sapiens* was compared to that of corresponding factor from *Pyrococuss abyssi*. The colored boxes indicate regions of significant sequence similarity between the proteins. 140 e/aIF2β sequences were aligned; the N-terminal extension attached to the core domain of e/aIF2β is shown as a grey box, and the C-terminal extension is shown as an orange box.

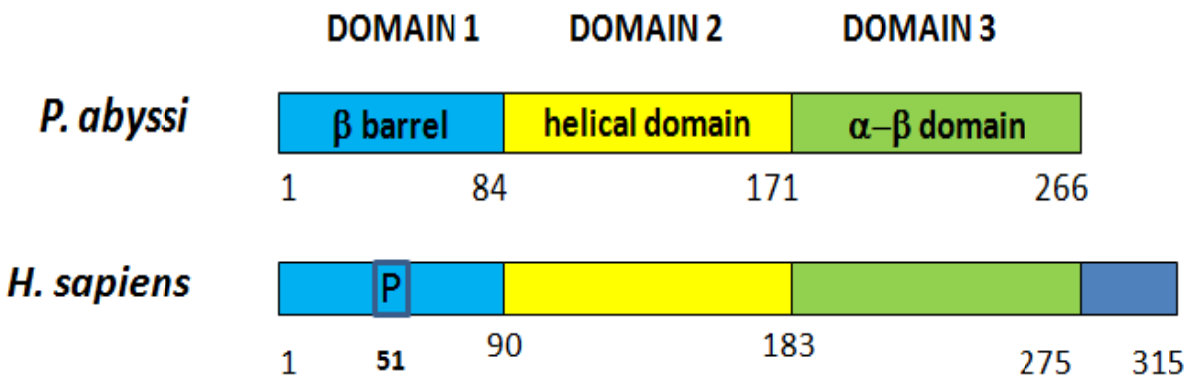

Figure 2.3. Schematic structural organizations of aIF2α/eIF2α.

The structural organization of the eIF2α from *H. sapiens* was compared to *P.abyssi*. The colored boxes indicate regions of significant sequence similarity between the proteins. The numbering refers to the limits of characterized structural domains in each species. 120 e/aIF2α sequences were aligned; the C-terminal extension to the core domain of e/aIF2α is shown as a blue box.

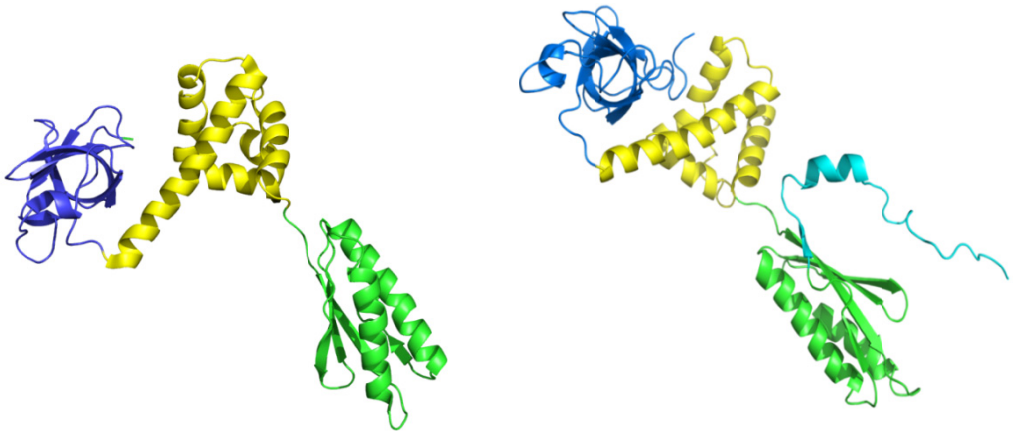

Figure 2.4. Structure of human eIF2α and archaeal aIF2α.

The three structural domains are coloured as follows in aIF2α (*P.abyssi* PDB ID 1YZ6): domain 1 (residues 1-84, aIF2α *P.abyssi* numbering) in blue, domain 2 (residues 85-171) in yellow, and domain 3 (residues 172-266) in green. Same organization is observed in *H. sapiens* eIF2α PDB ID 1Q8K except the C-terminal extension seen as cyan in colour.

3.1.1. Characterization of recombinant bacterial clones harboring wild type and mutants of eIF2α and eIF2β

The recombinant clones representing the subunits of human eIF2α, and eIF2 β, were cloned in bacterial expression vector pET32a (Rajesh et al., 2008). The wild type constructs of the subunits were used as templates for generation of separate N- and C-terminal domains of α- and β-subunits. The mutants N-terminal and C-terminal domains of α- and β-subunits were generated based on the domain organization of eIF2 with respect to other eukaryotes and well-studied archaeal system as mentioned above in **Figures 2.1-2.3.** Plasmids harboring eIF2α and eIF2β cDNAs were isolated from transformants of *E. coli* DH5α. The isolated plasmid DNA was used as a template for amplification. The restriction sites used for cloning were *NdeI* and *XhoI*. The excised PCR product was then ligated into the pET21b vector with hexa-histidine tag at its C-terminal end that was digested by the restriction endonucleases as mentioned in Materials and Methods. The recombinant clones of pET-21b vector harboring mutants of human eIF2α–CTD, α–NTD, β–NTD and β–CTD were confirmed by restriction digestion analysis as shown in **Figure 2.5.** The positive clones were also confirmed by colony PCR and their ORF were been confirmed by sequencing. The insert DNA sequences have the following sizes: α–CTD 450bp; α–NTD 549bp; β–NTD 510bp; and β–CTD 495bp respectively**.**

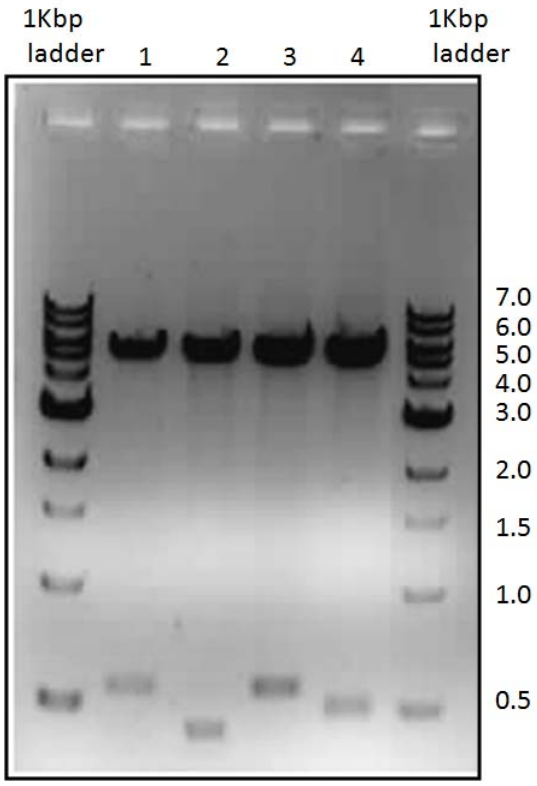

Figure 2.5. Restriction analysis of recombinant clones harboring N- and C-terminal domains of eIF2α and β.

The amplified products of mutants of eIF2α- and β-, were ligated into pET21b vector and the ligation mixture was transformed into *E. coli* DH5α cells. Antibiotic resistant colonies were selected and recombinant plasmids were isolated as described in Materials and Methods. The plasmids were subjected to restriction digestion with *NdeI* and *XhoI* for recombinant pET21b vector harboring wt and mutants of human eIF2α and β- subunits, for confirmation of the recombinant clones. The samples were analyzed by 1% agarose gel electrophoresis. The lanes are as follows 1 Kbp ladder; lane-1 αNTD, 549bp; lane-2 αCTD, 450bp; lane-3 βNTD, 510bp; lane-4 βCTD, 495bp; and 1 Kbp ladder as marker as mentioned in the figure.

3.1.2. Overexpression, purification and identification of wild type and mutant proteins of eIF2α and eIF2β

The recombinant plasmids were transformed and overexpressed in *E. coli* Rosetta BL21 (DE3) under the control of T7 promoter. Cells were grown at 37°C, 210 rpm until OD_{600} reached to 0.6 – 0.7. The medium containing cells was supplemented with IPTG to a final concentration of 0.5 mM for the expression of recombinant proteins. Incubation was continued for another 12 hrs until OD_{600} reached 2.0-2.5. Cells were then harvested, lysed and centrifuged briefly to obtain supernatant and pellet fraction. Expression of the recombinant proteins was analyzed by 15% SDS-PAGE as shown in **Figure 2.6**.

3.1.3. Purification of wild type and mutant proteins of eIF2α

Purification of recombinant wt, N- and C- terminal domains of eIF2α was carried out by Ni-NTA affinity chromatography. The columns were washed with low concentrations (30 and 50 mM) of imidazole and the proteins bound to the matrix were then eluted by 250 mM imidazole as described in Materials and Methods. Concentrated protein was further purified on a Superdex-75 and Superdex-200 gel filtration column in 50 mM Tris-HCl pH 8.0, 150 mM NaCl and 5 mM βME. The purification profile of the recombinant subunits was analyzed by coomassie-blue stained gels. The wild type (wt) eIF2α was soluble and the final yield was 2 mg. The truncated N-terminal domain comprising 183 amino acids was insoluble and could not be purified. The C-terminal domain of eIF2α was present in the supernatant and was purified by Ni-NTA affinity chromatography. The protein yield was 5 mg. The protein was

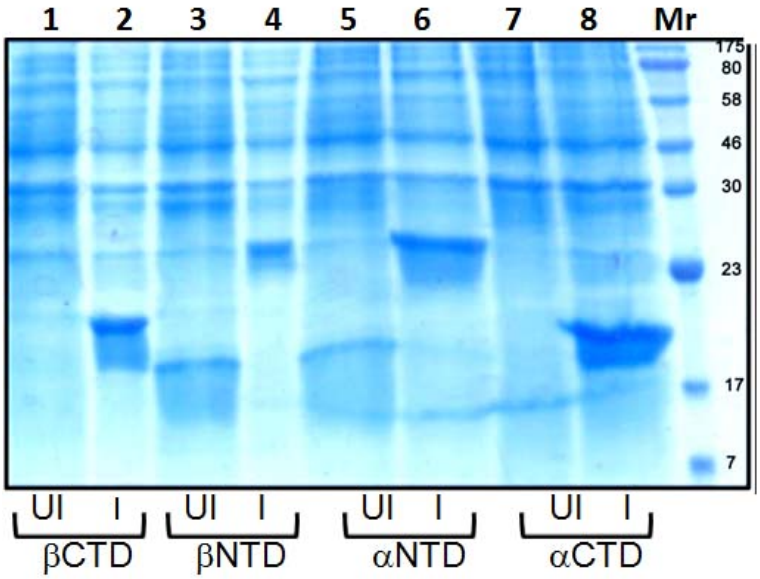

Figure 2.6. Expression of N-terminal and C-terminal domains of eIF2 subunits in bacterial cell extracts.

The N- and C- terminal domains of eIF2α and β– subunits were expressed in *E. coli* cells with hexa histidine tag. Cells were boiled in SDS sample buffer and the proteins were separated by 15% SDS-PAGE. The figure represents coommasie blue-stained gel. Different lanes are as follows: lanes 1 and 2 uninduced and induced cell extracts of eIF2β C-terminal domain, lane 3 and 4, uninduced and induced cell extracts of eIF2β N-terminal domain, lanes 5 and 6, uninduced and induced cell extracts of eIF2α N-terminal domain and lanes 7 and 8 uninduced and induced cell extracts of eIF2α C-terminal domain lane M, pre-stained molecular weight markers.

95% pure as judged by SDS–PAGE analysis (**Figure 3.0**)**.** The purified eIF2α wt, N-terminal and C-terminal domains of eIF2α were identified by using a polyclonal anti-eIF2α antibody. The antibody recognizes both the wt and mutants as shown in **Figure 3.1**.

3.1.4. Purification of wild type and mutant proteins of eIF2β

The wt and mutants of eIF2β proteins were purified by Ni-NTA affinity chromatography. The wild type protein purified by Ni-NTA had some contaminants, as the protein was eluted in low imidazole concentration. Hence the column was washed with high salt concentration of 500 mM NaCl to remove contaminants. The protein fractions eluted by 250 mM imidazole were pooled and further purified by Superdex-200 gel filtration column. The purification profile of the recombinant subunits was analyzed by Coomassie-blue stained acrylamide gels. The wt eIF2β was soluble and the protein yield was 2 mg (**Figure 3.3 Panel A**)**.** The N-terminal region of the protein has high lysine- rich region. The presence of these basic residues in the protein makes its migration anomalous and moves to a higher molecular weight on SDS-PAGE. The N-terminal domain of eIF2β consisting of residues from 1-169 was soluble and could be purified by Ni-NTA. The protein yield was 3 mg as shown in **Figure 3.2 Panel A.**

The truncated C-terminal domain consisting of residues from 170-333 were overexpressed and the cell lysate was loaded on Ni-NTA column. It was observed that protein did not elute in the presence of high imidazole concentration and the overexpressed protein was found in the pellet fraction as shown in the purification profile of **Figure 3.2 Panel B**. The purified wt

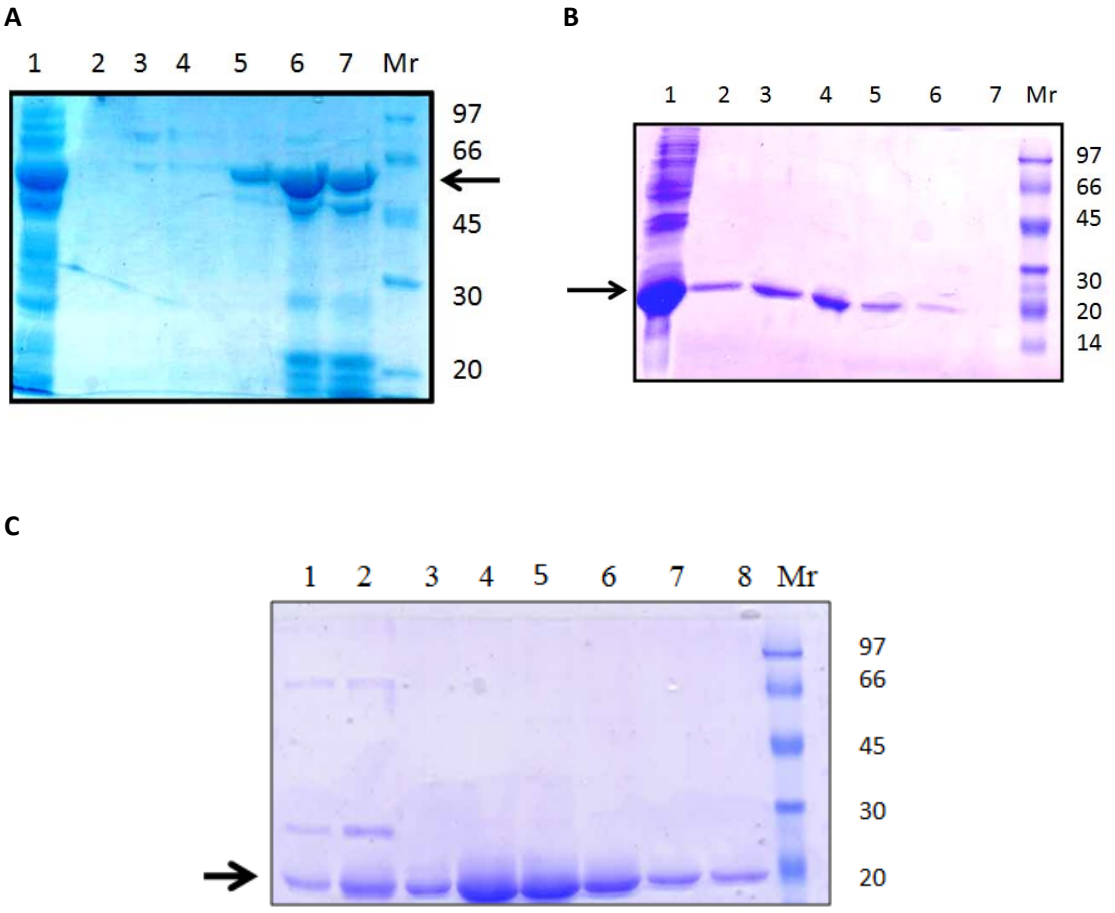

Figure 3.0 Purification of recombinant wild type and, N- and C- terminal domains of eIF2α.

Bacterial cultures expressing recombinant his-tagged human eIF2α wt, N- and C-terminal domains were harvested and the cell pellet was processed as described in Materials and Methods. All proteins were purified by using Ni-NTA chromatography. Proteins purified were separated by 12% SDS-PAGE. The figures represent coommasie blue stained gels.

Panel A represents purification of wt eIF2α. Various lanes are as follows: Lane 1, supernatant, lanes 2-4, wash fractions; lanes 5-7, fractions eluted with 250 mM imidazole. Mr represents molecular weight marker.

Panel B represents purification profile of eIF2α N-terminal domain. Various lanes are as follows: Lane 1, pellet; lanes 2-4, wash fractions; lanes 5-7 fractions eluted with 250 mM imidazole. Mr represents molecular weight marker

Panel C represents purification profile of eIF2α C-terminal domain. Various lanes are as follows: Lane 1, flow through or unbound fraction; lanes 2-3 wash fractions; lanes 4-8, represent the fractions eluted with 250 mM imidazole.

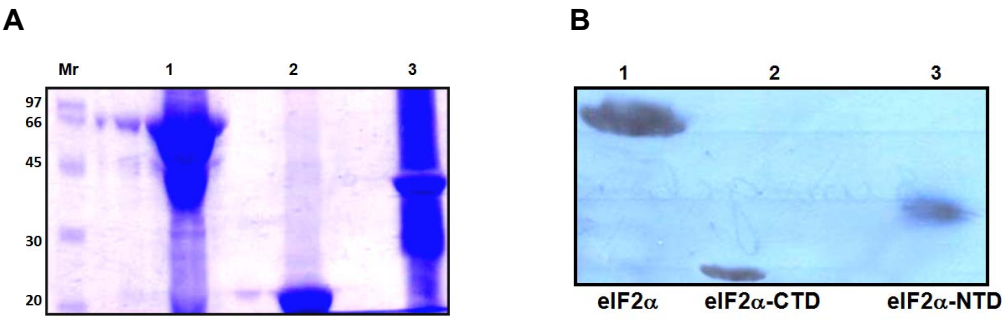

Figure 3.1. Analysis of eIF2α wild type, N- and C- terminal domains by SDS-PAGE and Western blot.

Panel A represents wt and mutants of eIF2α that are separated on 12% SDS-PAGE and stained by coommasie blue. The various lanes are as follows; Mr, Molecular weight marker; lane 1- eIF2α wt, lane 2- eIF2α–CTD and lane 3- eIF2α–NTD. N-terminal domain of eIF2α is found in pellet fraction of the cell extract.

Panel B represents the western blot of recombinant wt eIF2α, eIF2α–CTD and eIF2α–NTD. The blot is probed by polyclonal anti- eIF2α antibody.

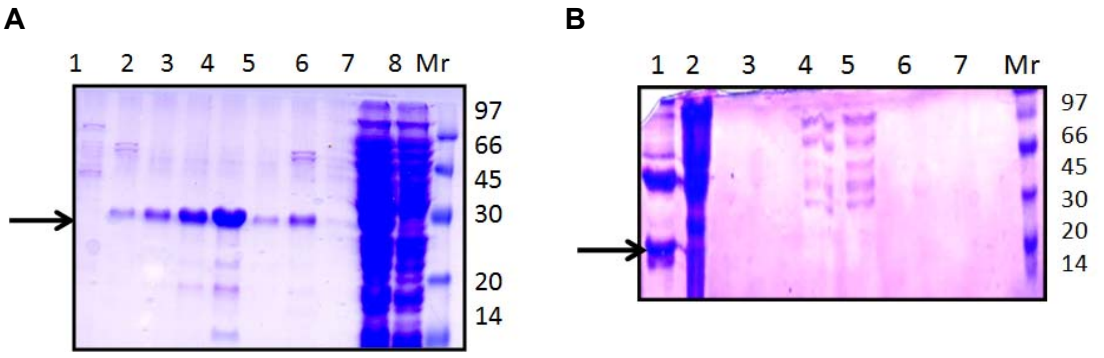

Figure 3.2 Purification of recombinant eIF2β N- and C-terminal domains.

Bacterial culture expressing recombinant eIF2β subunit was harvested and the pellet was processed to purify his- tagged protein as described in 'Materials and Methods'.

Panel A: **Purification profile of recombinant NTD of eIF2β by Ni-NTA chromatography.** Various lanes are as follows: lanes 1-3, fractions eluted by 250 mM imidazole; lanes 4-6, wash fractions; lanes 7 and 8, represent pellet and supernatant. Mr depicts the molecular weight marker.

Panel B: **Purification profile of recombinant CTD of eIF2β.** Lane1, represents protein in pellet, lane 2 represents supernatant, lanes 3-7 represent wash and elution fractions.

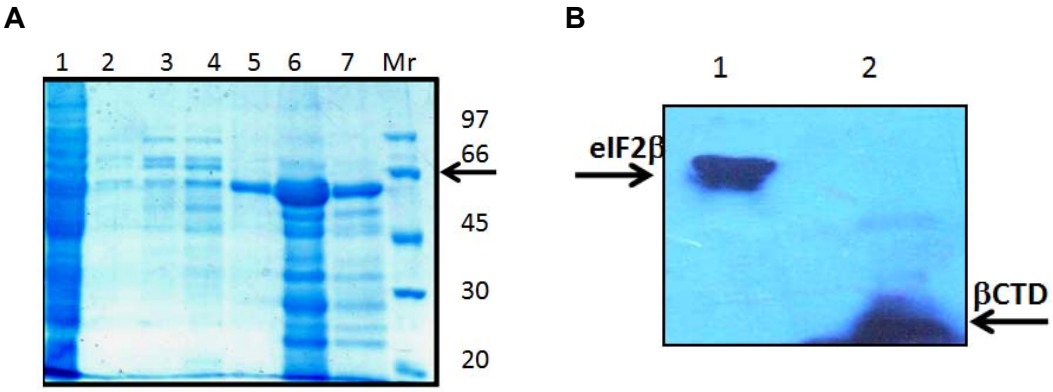

Figure 3.3 Purification of wt human eIF2β subunit and Western analysis

Panel A: Purification profile of recombinant wt eIF2β. Various lanes are as follows: Lane 1, supernatant of cell extract; lanes 2-5, wash fractions; lanes 5-7, fractions eluted with 250 mM imidazole, Mr depicts the molecular weight marker.

Panel B: Purified recombinant wt eIF2β wt and β–CTD were separated by 12% SDS-PAGE. Proteins were transferred to nitrocellulose membrane. The membrane was probed by a monoclonal anti- eIF2β antibody.

eIF2β protein and the C-terminal domain of eIF2β protein which was present in the pellet fraction were probed by a monoclonal anti-eIF2β antibody. The antibody identifies both the C-terminal domain and the wt protein, but the N-terminal domain was not recognized by the antibody **(Figure 3.3 Panel B).**

3.2. Characterization of the subunits

3.2.1. Intersubunit interactions of α- and β-subunits of human eIF2

Earlier experiments in the lab have shown that baculovirus-expressed human eIF2 subunits interact with each other in ELISA and dot blot assays. Bacterially expressed subunits of eIF2 were also found to interact with each other to form αβ, βγ and αγ complexes both in far-western analysis and in pull down experiments (Rajesh et al., 2008). To further determine the domains involved in the interaction between α- and β-subunits of eIF2, we studied here initially the interaction between wt α- and β-subunits of eIF2 by co-immunoprecipitation assay**.** In this assay, agarose G beads were incubated with a monoclonal anti-eIF2β antibody. Purified eIF2β protein immunoprecipitated with specific antibody is considered as IP. eIF2α protein and a negative control protein BSA were co-immunoprecipitated with antibody-protein complex. The immunoprecipitated samples were washed with 1x PBST for at least 5 times and the washed immunoprecipitate was boiled in SDS sample buffer and was processed for gel electrophoresis. The unbound samples were loaded in lanes1-3, wash fractions in lane 4 and the negative control BSA in lane 5 and the last lane 6 contains the IP and Co-IP samples resuspended in SDS sample buffer. The gels were transferred to PVDF and the western blots were probed by authentic polyclonal anti-eIF2α antibody and monoclonal anti-eIF2β antibody for the recognition of α– and β–

proteins respectively as shown **in Figure 4.0 Panel A and B.** In another experiment, the interaction was studied for C-terminal domain of eIF2α with wt eIF2β protein. The eIF2α C-terminal domain was immunoprecipitated with eIF2β protein and was probed by an anti eIF2α antibody as mentioned earlier. The antibody recognizes eIF2α C-terminal domain suggesting that the recombinant eIF2α and eIF2β subunits interact with each other, consistent with the previous findings. However, the observations point out that the carboxy terminal domain of eIF2α only is important for this interaction as shown in **Figure 4.1 Panel A and B**.

3.2.2. Biophysical techniques to demonstrate intersubunit interactions

Circular Dichroism (CD) spectroscopy was used to quantitatively analyze the conformational changes that can occur upon interaction between α and β–subunits of eIF2. CD measurements were carried out separately for both the proteins: eIF2α and eIF2β. The spectral measurements as shown in **Figure 5.0 Panel A** indicate that eIF2α subunit has a negative peak at 208 nm and 222 nm suggesting that it has a typical helical structure. The CD spectrum of eIF2β exhibits a negative band in the UV region at 208 nm that is characteristic for a helix structure (**Figure 5.0 Panel B**)**.** However the CD programme analysis by CD Pro indicates that β–subunit has higher amount of random coil compared to α–subunit as shown in **Table 2.0**.

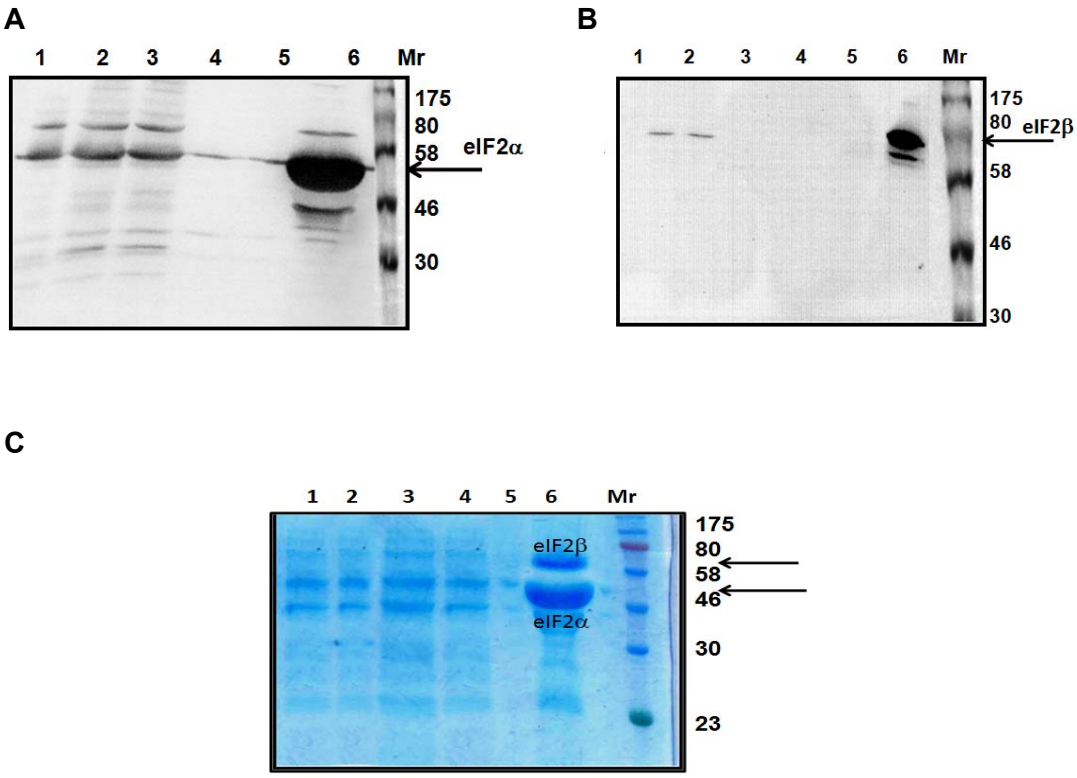

Figure 4.0 Interaction between wt eIF2α– and β–subunits by Co-Immunoprecipitation

Purified recombinant wt eIF2β subunit was incubated with a monoclonal anti- eIF2β antibody complexed with agarose G beads as described in Materials and Methods. The samples were separated by 12% SDS-PAGE gel and then transferred to a PVDF membrane. The amount of bound protein was analyzed by chemiluminiscence imager.

Panel A and B represent the corresponding western blot probed by respective antibodies. In Panel A, the membrane was probed by a polyclonal anti-eIF2α antibody and in Panel B, the membrane was probed by a monoclonal anti-eIF2β antibody. **Panel C** represents the SDS-PAGE corresponding to the western blots of panel A and B.

Panel A: Lanes 1-3, unbound fraction of wt eIF2α; lane 4, wash fraction; lane 5, negative control protein (BSA); lane 6, eIF2α protein as Co-IP.

Panel B: Lanes 1-3, unbound fraction of wt eIF2β; lane 4, wash fraction; lane 5, negative control protein (BSA); lane 6, eIF2β protein as IP.

Panel C: Lanes 1-3, unbound fractions; lane 4, wash fraction; lane 5, negative control protein (BSA); lane 6, bound fractions of eIF2α and eIF2β complex to the beads.

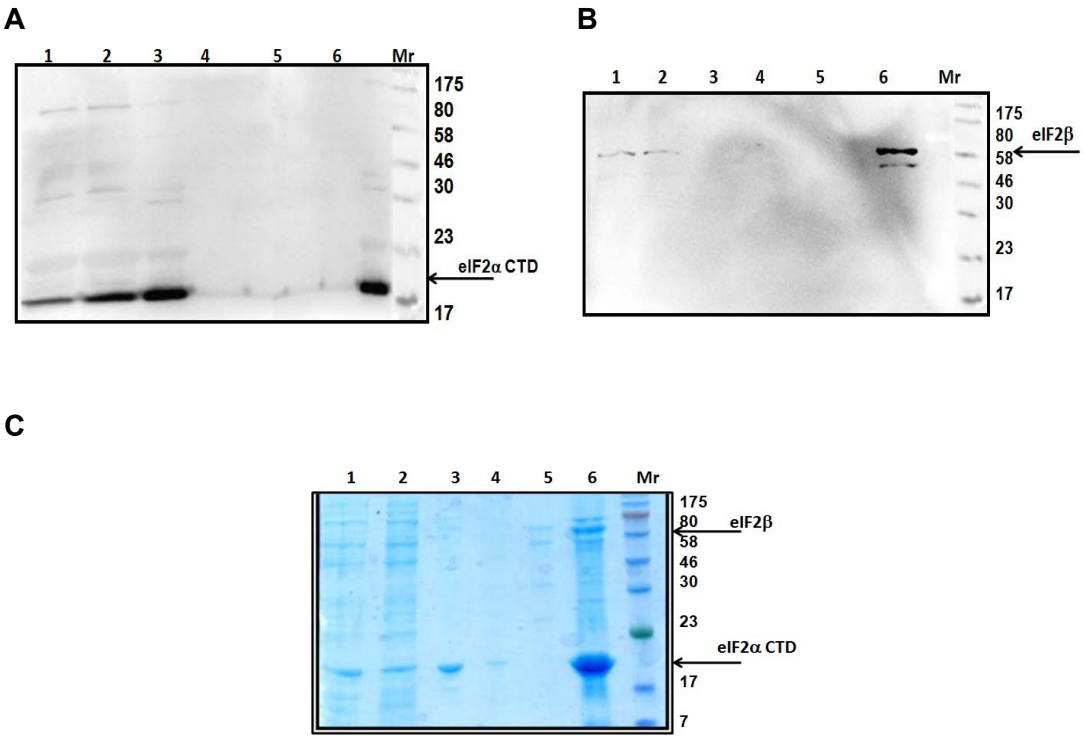

Figure 4.1 Interaction between eIF2α C-terminal domain and wt eIF2β subunit by Co-Immunoprecipitation

Purified recombinant wt eIF2β subunit was incubated with a monoclonal anti-eIF2β antibody that is complexed with agarose G beads. The interacting protein, CTD of eIF2α was incubated with the complex as described in Materials and Methods. The precipitated samples were separated by 12% SDS-PAGE and then transferred to a PVDF membrane. The amount of bound protein to the complex was analyzed by chemiluminiscence imager. **Panel A and B** represents the corresponding western blots probed by respective antibodies. In Panel A, the membrane was probed by a polyclonal anti-eIF2α antibody and in Panel B, the membrane was probed by a monoclonal anti-eIF2β antibody. Panel C represents the SDS-PAGE corresponding to the western blots of panel A and B.

Panel A: Lanes 1-3, unbound fraction of CTD of eIF2α; lane 4, wash fraction; lane 5, negative control protein (BSA); lane 6, eIF2α CTD as Co-IP.

Panel B: Lanes 1-3, unbound fraction of wt eIF2β; lane 4, wash fraction; lane 5, negative control protein (BSA); lane 6, eIF2β protein as IP.

Panel C: Lanes 1-3, unbound fractions; lane 4, wash fraction; lane 5, negative control protein (BSA); lane 6, eIF2α CTD and wt eIF2β complex and lane 7, pre-stained protein molecular weight marker.

Environment	Helix	Sheet	Turns	Random Coil
Native heIF2β	30.1	25	18.4	26.50
pH 2.0	37	17.6	15	30.4
pH 10.0	27	18.5	17.5	35
Temp 45 ^{0}C	27. 80	28.10	15.8	30
Temp 85 ^{0}C	20.5	21.2	16.3	42
Native eIF2αCTD	75.4	20.2	4.2	0.2
Native eIF2α and eIF2β	35	28.4	22.6	14
Native eIF2αCTD and eIF2β	35.2	24.6	28	12.2

Table 2.0 Secondary structure elements of eIF2β and its complex.

The far-UV CD spectra of the eIF2β under different pH conditions and temperatures were analyzed. The far UV CD spectra of the complex eIF2α:eIF2β and eIF2α-CTD:eIF2β were analyzed by CD programme available online.

3.2.3. Interaction between eIF2α and eIF2β subunits by CD studies

To obtain an insight into the structural changes that occur in eIF2α and β– subunits because of their interaction, we performed far-UV CD separately for eIF2α and β–subunits and also for the complex containing both the proteins. The interaction between eIF2α and β-subunits resulted in a change in the ellipticity, indicating that the interaction between the subunits has induced conformational changes in the β protein as shown in the **Figure 5.1**. Interestingly, the secondary structure content analysis mainly shows that the interaction between subunits also decreases the random coilness in the β-subunit as calculated by the CD programme. The cumulative CD spectrum of α and β–subunits do not overlap with the spectrum of the α–β complex suggesting that the α and β– interact with each other.

3.2.4. Interaction between eIF2α C-terminal domain and eIF2β protein by CD studies

The CD spectrum of eIF2α CTD protein has a negative peak at 208 nm suggesting a typical helical structure as has been shown in **Figure 5.2**, P**anel A.** The complex of wt eIF2β and eIF2α CTD shows a change in the ellipiticity compared to the eIF2β as shown in **Figure 5.2, Panel B** suggesting that the interaction promotes secondary structural changes in eIF2β. Overall the CD studies suggest that α- and β-subunits of human eIF2 interact with each other and it is the C-terminal domain of eIF2α that interacts with the eIF2β subunit and these findings are consistent with the co-Immunoprecipitation assays performed here (**Figure 4.1, Panels A and B**).

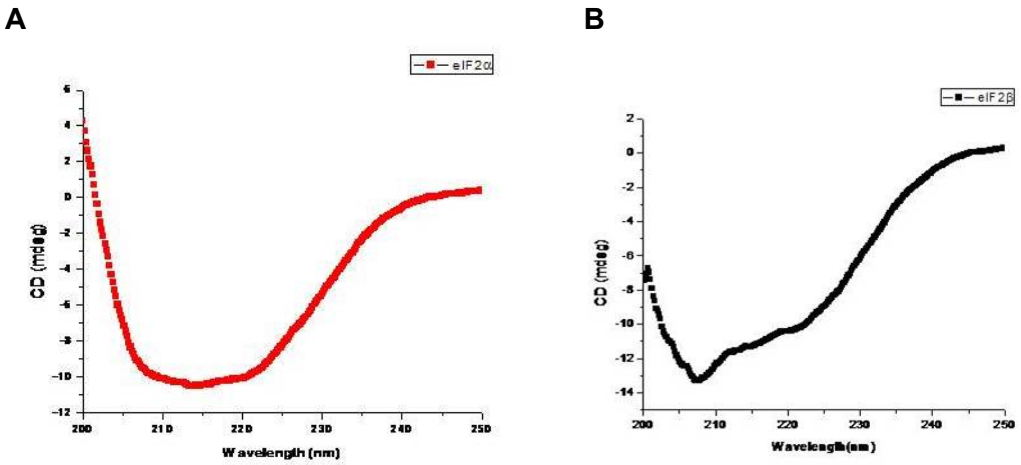

Figure 5.0 Far UV CD spectra of wt eIF2α and eIF2β.

The protein concentrations for all CD measurements were kept at 0.1mg/ml in 20 mM Tris-HCl buffer at pH 7.5. Data were collected in cells with 1 mm path lengths for both panel A and panel B and recorded as described in Methods. **Panel A** shows the far UV CD spectra of eIF2α and **Panel B** shows the far UV CD spectra of eIF2β.

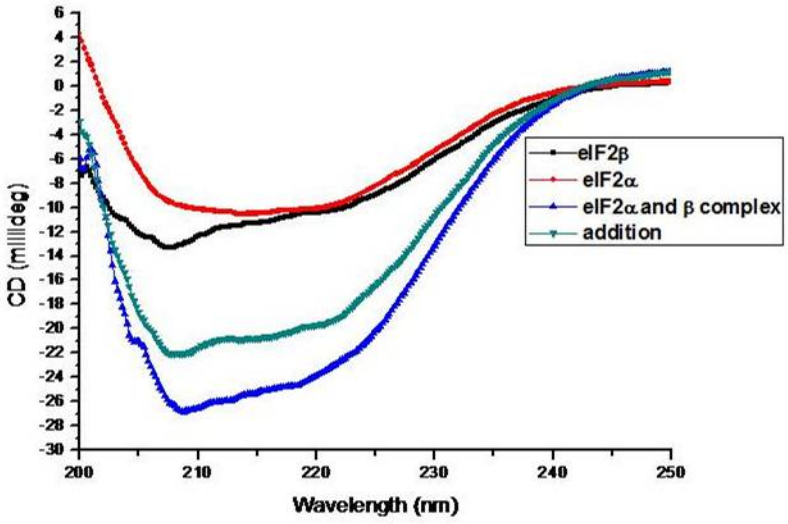

Figure 5.1. Interaction of eIF2α and eIF2β by CD.

The CD spectra of recombinant wt eIF2α (red), eIF2β (black) subunits and also the complex of these subunits were recorded to determine changes in the secondary structure of eIF2β upon interaction with eIF2α. The eIF2α:eIF2β complex in blue colour spectra shows a rearrangement of secondary structure. The cumulative spectrum of the α– and β–subunit (green) was plotted together with the spectra obtained for α-β complex (blue) for comparison.

A

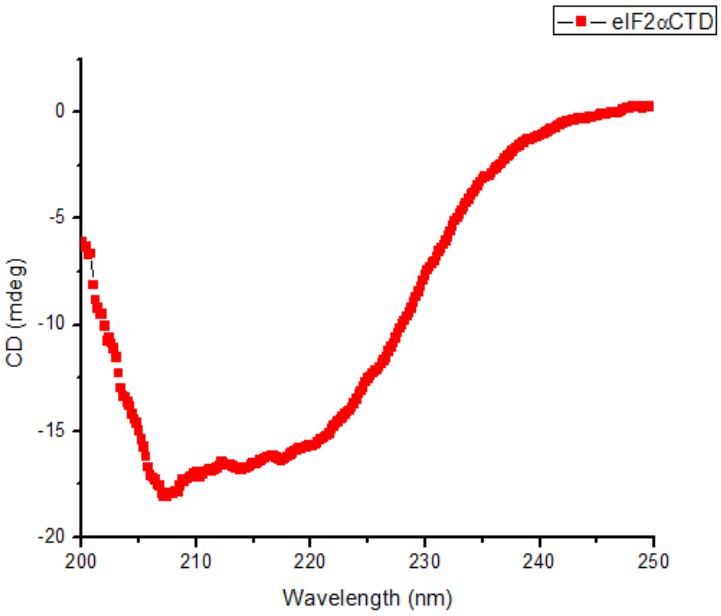

B

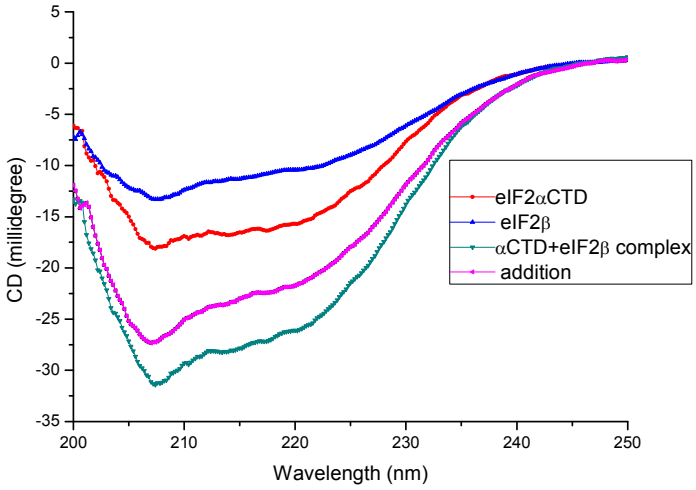

Figure 5.2. Far UV CD spectra of eIF2α C-terminal domain and wt eIF2β complex.

Panel A represents far UV-CD spectra of eIF2α CTD only.

Panel B represents far UV-CD spectra of eIF2α CTD (red), wt eIF2β (blue), complex of wt eIF2β and and eIF2α CTD (green). The cumulative CD spectra of eIF2α CTD and wt eIF2β in pink colour does not overlap with the CD spectra obtained for the complex. Data were collected in cells with 1 mm path lengths for both panel A and panel B and the protein concentration was 0.1 mg/ml in buffer containing 20 mM Tris-HCl, pH 7.5.

3.2.5. Isothermal titration calorimetry (ITC) to determine intersubunit interaction

To further quantify the binding affinity between α– and β–subunits of eIF2, isothermal titration calorimetry studies were undertaken. 25 injections of 300 μM solution of β–subunit were delivered into the cell containing 20 μM eIF2α subunit at 30^0C. In other words, the binding is followed by titrating eIF2β on eIF2α that is kept constant. Changes in the heat energy have been used to monitor the binding affinity. The binding promoted exothermic heat changes as shown in the thermogram with increase in the concentration of the β–subunit protein. The binding stoichiometry was calculated by the Origin software supplied with the MicroCal machine and the K_D is found to be 8 μM as shown in **Figure 6.0.** These results support the interaction between α– and β– subunits, which is consistent with immunoprecipitation studies. However, ITC studies indicate a weak interaction between α– and β–subunits.

3.3. Biophysical characterization of eIF2β

3.3.1. Steady state fluorescence spectroscopy

Fluorescence of tryptophan residues in a protein are used to determine the relative position of each Trp residue, whether they are in hydrophobic or hydrophilic environment. If the Trp residues are in the hydrophobic environment exclusively, the λ_{max} of intrinsic fluorescence will be at 332 nm. β-subunit of human eIF2 has a single Trp residue at position 169 (NCBI ID: P20042). Steady state fluorescence of the native protein gives a λ_{max} at 338 nm as shown in **Figure 7.0** suggesting that the tryptophan residue is not completely present in a hydrophobic environment. Addition of guanidinium

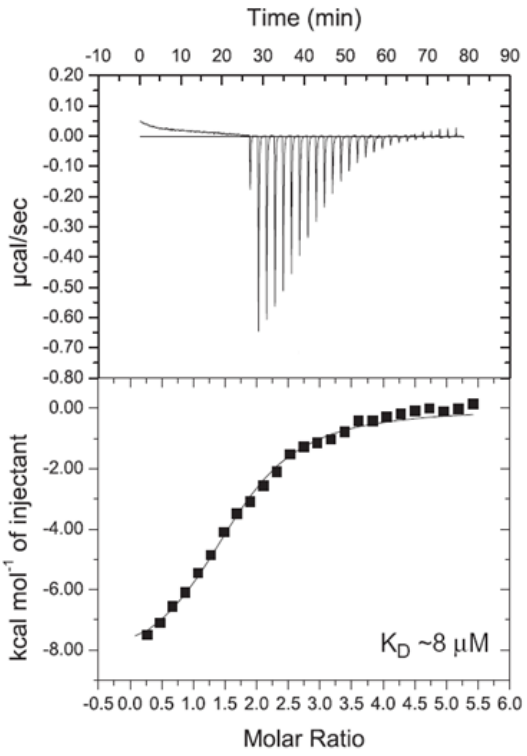

Figure 6.0. Interaction of eIF2α and eIF2β by ITC

Titration of wt eIF2α with eIF2β was performed in a buffer containing 50 mM Tris-HCl (pH 7.0) and 100 mM KCl at 30^0C. The concentrations of the protein used in ITC experiments were 300 µM in syringe and 20 µM in cell respectively. The protein eIF2α present in the sample cell was titrated with eIF2β which was loaded in a syringe with 25 injections. The buffer controls were performed and the values were subtracted in the final plot.

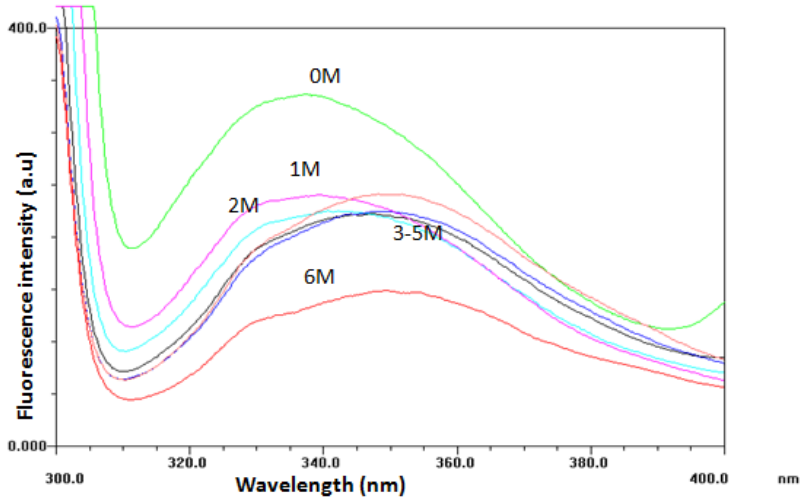

Figure 7.0. Fluorescence Emission Spectra of eIF2β in the presence of different concentrations of Gdn-HCl.

Purified eIF2β protein of (0.2mg/ml) was incubated in the presence and absence of different concentrations of guanidium hydrochloride (Gdn-HCl) for four hours at room temperature in a total volume of 500 µl of 20 mM Tris buffer, pH 7.5. Fluorescence spectra were recorded for each sample using an excitation wavelength of 295 nm. Emission spectra were monitored at wavelengths (330-400 nm). Relative fluorescence intensity is plotted against the wavelength. The numbers on the spectra indicate the respective molarity of Gdn-HCl.

hydrochloride (Gdn-HCl) with increasing concentration of Gdn-HCl from 1-6 M, reduces the fluorescence intensity and shifts the λ_{max} to 357 nm, suggesting that the protein is unfolded in the presence of denaturant and the tryptophan is quenched.

3.3.2. Equilibrium unfolding studies

To determine the thermodynamic stability of the protein and the presence of transition state, equilibrium unfolding studies were performed. Purified β–subunit is subjected to sixty concentrations of Gdn-HCl from 0.1 M to 6 M. The λ_{max} was measured between 300-400 nm range. There was a gradual red shift in the λ_{max} of the fluorescence intensity of the protein in the presence of increasing concentration of Gdn-HCl. The values are plotted as shown in **Figure 7.1.** The conformation of protein in equilibrium experiments was monitored by tryptophan fluorescence. The ratio of unfolding was calculated by the values at 360/320 nm as shown P**anel A**. The residual values of different molar concentration of Gdn-HCl are within the calculated range **Panel B**. The $C_{1/2}$ value indicates the amount of Gdn-HCl required for complete unfolding and is the transition between folded and unfolded state as shown in **Figure 7.1, Panel C.** The changes in the λ_{max} with increasing Gdn-HCl concentration are plotted in **Panel D.** These results indicate that the equilibrium unfolding/refolding transition of eIF2β was best fitted to two-state model with no detectable equilibrium intermediates along the pathway. The fluorescence intensity was reduced drastically for the denatured protein due to the exposure of the side chain of tryptophan to solvent and quenching of fluorescence. The $C_{1/2}$ value is 2.6 M Gdn-HCl suggesting that this

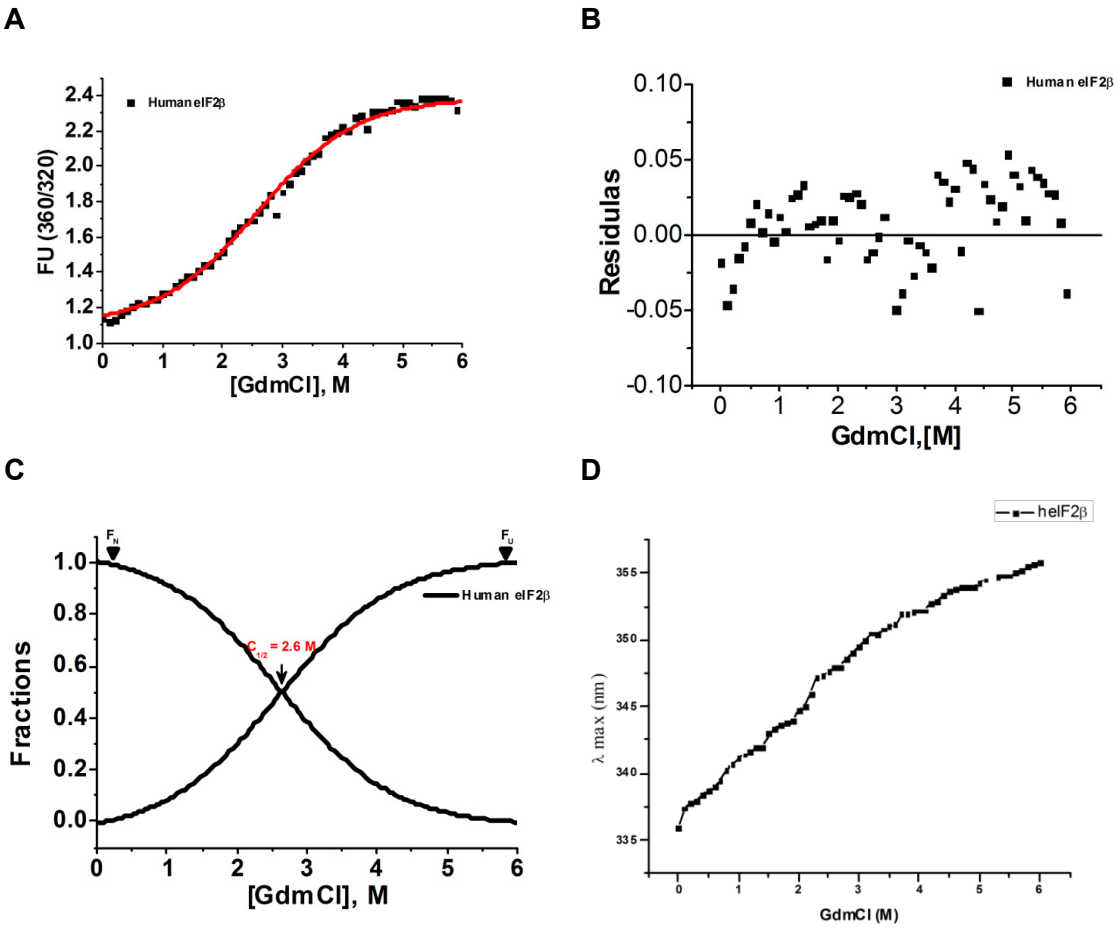

Figure 7.1. Gdn-HCl induced equilibrium unfolding of eIF2β.

Panel A: Fluorescence intensity at 360/320nm was used in order to simultaneously monitor changes in the unfolding and native maxima.

Panel B shows the residuals suggesting that the data are within the range.

Panel C indicates best fit in the two-state unfolding process with Gdn-HCl. F_N and F_U represents the fractions at native and unfolded states respectively. The $C_{1/2}$ value observed is 2.6 M.

Panel D represents changes in λ_{max} upon increase in Gdn-HCl concentration.

concentration is sufficient for completely unfolding of the protein as analyzed by using the ratio of fluorescence intensity at 360/320 nm.

3.3.3. Hydrophobic dye binding studies

To determine different states of folding of a protein or to identify an intermediate or partially folded state of a protein, the human eIF2β subunit is subjected to different pH conditions that would unfold the protein. Unfolding of the protein is followed by the binding of the dye 8-ANS to the exposed hydrophobic regions in the protein resulting in an increase in fluorescence intensity with blue shift in the λ_{max}. The native protein binds to ANS at pH 7.5 and gives an emission of λ_{max} at 458 nm. The intensity of fluorescence increases upon unfolding and binding of ANS to hydrophobic regions. The results suggest that the native protein does bind ANS at pH 7.5 indicating that it has fewer exposed hydrophobic regions. At low pH 2.0, the increased fluorescence intensity of the β–subunit suggests a significant binding of ANS to the protein. In contrast, at higher pH 10.0, the fluorescence intensity was very low, indicating a minimal binding of ANS to the β-subunit as shown in **Figure 7.2, Panel A.**

3.3.4. Circular dichroism (CD) measurements

The far-UV CD measurements for the native eIF2β between 200 and 250 nm was recorded using 0.1 mg/ml protein with a 1 mm path length cell. The spectrum of the native eIF2β was analyzed between 200 and 250 nm by CD Pro programme that is available online. The spectrum shows maximum negative ellipticity at 208 nm indicating predominant α-helix content, as shown in **Figure 5.0 Panel B**. The values obtained for different secondary structure

A B

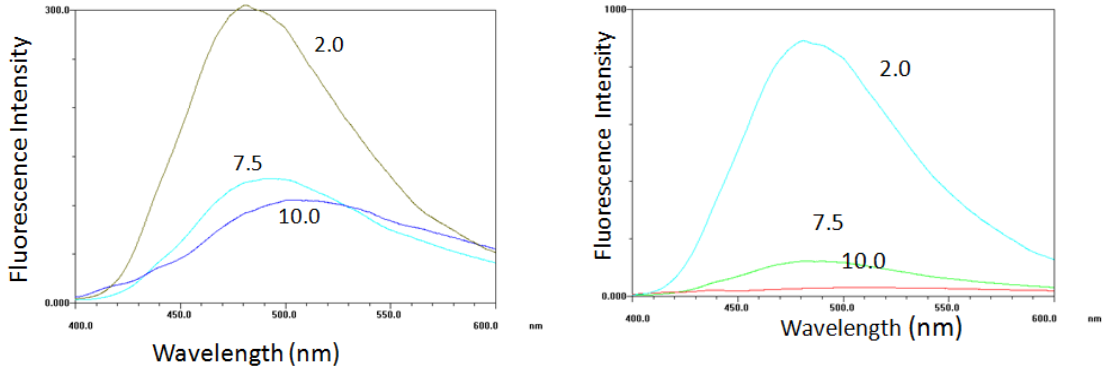

Figure 7.2. ANS fluorescence emission spectra of wt eIF2α and eIF2β.

Protein samples were excited at 375 nm and the emission was recorded from 400-550 nm. Both spectra were carried out at different pH, KCl-HCl buffer for pH 2.0, glycine-NaOH buffer for pH 10.0, Tris-HCl buffer for 7.5. Protein concentration however for spectra recorded at 7.5 and 10.0 was kept at 0.05 mg/ml. The protein concentration was kept at 0.01mg/ml for pH 2.0 in order to keep the fluorescence within the measurable range.

Panel A represents ANS fluorescence emission spectra of human eIF2β.

Panel B represents ANS fluorescence emission spectra of human eIF2α.

elements are: α-helix-30.1%, β–sheet-25%, β–turns-18.4% and unordered structures-26.5%.

The far-UV CD scans of eIF2β incubated at pH 2.0, 7.0 and 10.0 are shown in **Figure 7.4.** The far-UV CD spectra showed an acid-denatured structure with loss of α-helix structure at pH 2.0 (**Table 2**). At pH 10.0 major rearrangement of the secondary structure was observed. The near-UV CD spectra for a protein in the 250–300 nm range provide information on the tertiary structure of the protein. The signals obtained between 250-300 nm are due to the absorption of the environment around aromatic amino acids and also disulphide bridges. Our results on the near-UV CD spectra at neutral pH 7.0 do not show any negative ellipticity, but show maximum peak at the range of 260 to 270 nm suggesting that the protein has different vibrational levels in the excited state (**Figure 7.3)**. The protein when incubated at low pH, also showed a similar spectra, with only slight decrease in intensity, suggesting some unordered tertiary structure.

To determine the T_m value of wt eIF2β, the protein was also incubated at different temperatures ranging from 25°C to 85°C. Upon increasing the temperature, the negative ellipticity observed around 208 nm in the CD spectra reduced gradually. The T_m of the protein calculated was found to be 45°C as shown in **Figure 7.5.** Loss of α-helix structure was observed in the protein at 65°C indicating that the protein is not very stable.

3.3.5 Dynamic light scattering measurement

In order to crystallize eIF2β subunit, the purified protein was analyzed for its homogeneity. The recombinant protein had only a single peak indicating it to

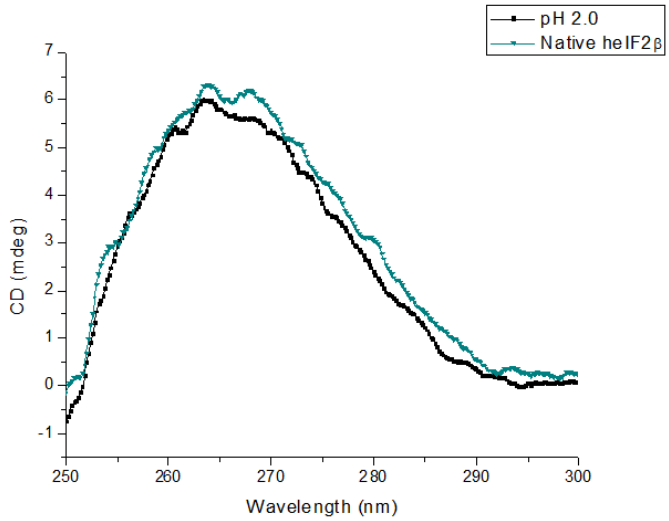

Figure 7.3. Near UV CD spectra of eIF2β.

Near UV CD spectra was performed for eIF2β in Tris-HCl buffer, pH7.5 and in KCl-HCl buffer for pH 2.0 and glycine-NaOH buffer for pH10.0. The buffers were prepared as described in Materials and Methods. The concentration of the protein was 1 mg/ml and the spectra was collected with 10 mm path length and recorded at wavelengths 250-300 nm.

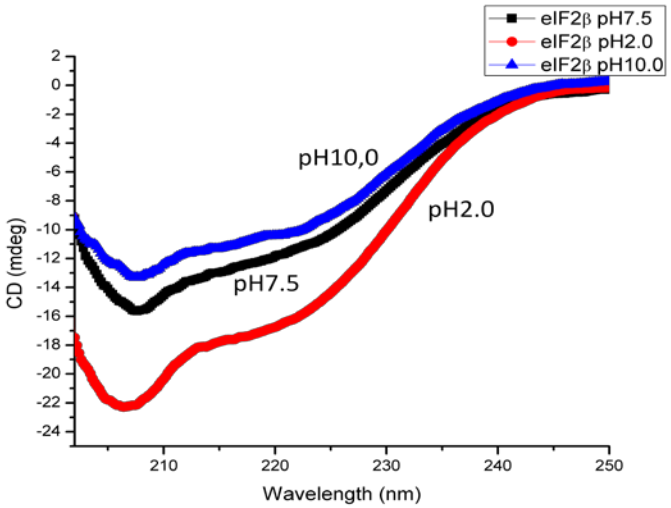

Figure 7.4. CD spectra of eIF2β at different pH.

Far-UV CD spectra of wt eIF2β (0.1 mg/ml) was carried out at different pH: 7.5, 2.0 and 10.0. Concentration of protein was 0.1 mg/ml. Spectra were recorded from 200-250 nm wavelengths. Buffers were prepared as described in Materials and Methods

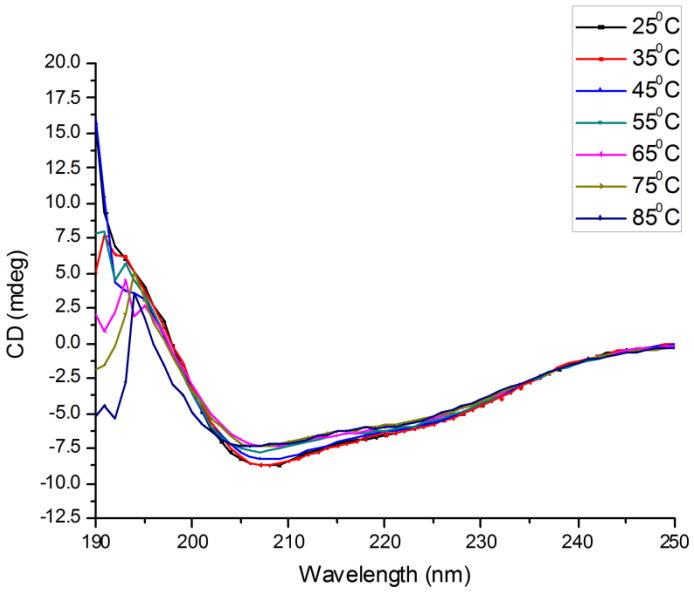

Figure 7.5. Thermal denaturation of eIF2β.

Recombinant human eIF2β protein, 0.1mg/ml, was incubated at different temperatures starting from 25 to 85^{0}C with an interval of 10^{0}C for 10 min time period at each temperature and the far UV-CD spectra was recorded as described in Materials and Methods. The CD signal was monitored at 208 nm.

be homogenous and monodispersed as shown in **Figure 6.1.** The pure monodispersed protein was screened for different crystallization conditions but did not yield any crystals.

3.4. Ternary complex, eIF2.GTP.Met-tRNAi^{Met}, formation

The complex eIF2 obtained from purification studies was shown to interact with charged methionyl initiator tRNA in a GTP-dependent manner forming a stable ternary complex (eIF2**.**GTP**.**Met-tRNAi^{Met}) which is delivered then to 40S ribosomal subunits to form 43S complex in the initiation step of protein synthesis. Biochemical, mutational and structural studies of yeast suggest that eIF2γ subunit is primarily involved in Met-tRNAi and GTP binding (Erickson and Hannig, 1996).

A number of earlier studies as cited in Flynn et al., 1993 found purified eIF2 heterotrimer preparations lacking β-subunit were unable to bind guanine nucleotides or involved in the binding Met-tRNAi. This may be an artifact as subsequent studies have pointed out that such preparations were analyzed by immuneblots, were found to contain fragments of β-subunit resulted due to proteolysis. Subsequent studies with purified $\alpha\gamma$ heterodimers of mammalian eIF2 without β-subunit or its traces was purified on ionexchange and hydrophobic chromatography from rabbit reticulocyte lysates have shown that β-subunit plays a role in Met-tRNAi binding as $\alpha\gamma$ that lacks completely eIF2α helped in purification of eIF2$\beta\gamma$ heterodimer. Using such purified preparations, Nika et al., 2001, have shown that the contribution of α-subunit binding to Met-tRNAi is very minimal compared to the β-subunit. These findings also

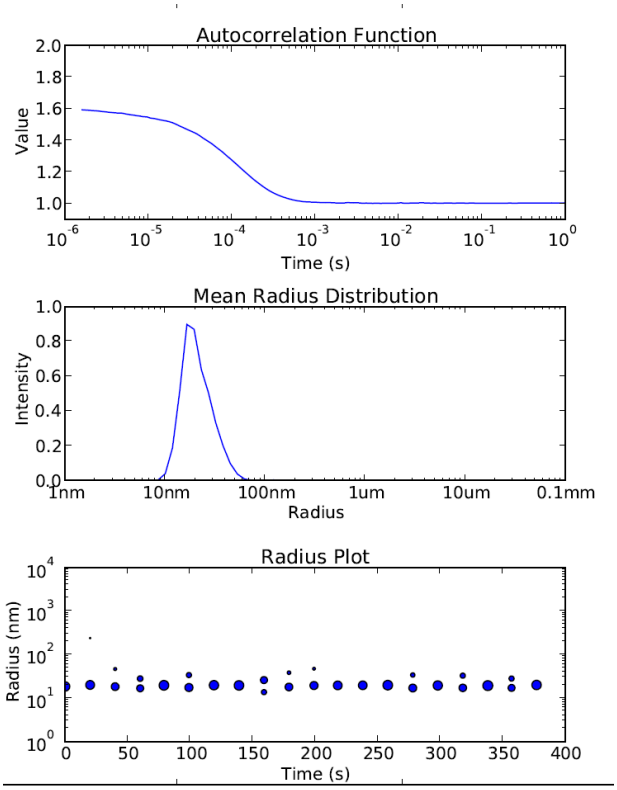

Figure 6.1. Dynamic Light Scattering profile of eIF2β.

Dynamic Light Scattering as described in Materials and Methods was carried out on purified wt eIF2β to assess its homogeneity and suitability for crystallization experiments.

suggested that γ-subunit is essential for initiator tRNA binding whereas β-subunit aids the γ-subunit.

In order to identify the subunits of human eIF2 that is involved in interaction with Met-tRNAi^{Met}, purified recombinant individual subunits were incubated with labeled acylated 3′ Met- tRNAi. The 3′ tRNA was labeled with [α^{32}P ATP] as described in Materials and Methods. The labeled tRNA was acylated with methionine using purified methionyl-tRNA synthetase (MetRS) from *E.coli* as described in Materials and Methods. Purification profile of recombinant MetRS from *E. coli* is shown in **Figure 8.0.** Approximately, 6.5 mg of protein was obtained. Aminoacylation was performed using *in vitro* transcribed tRNA without any modification on the tRNA by *E. coli* MetRS which was shown to acylate human initiator tRNA previously (Pestova and Hellen, 2001). Different concentrations were used as part of standardization, 50 nM MetRS is found to be efficient to achieve 80% of acylation as shown in **Figure 8.1**. All further experiments were carried out with a concentration of 50 nM MetRS for acylation.

3.4.1. Binding kinetics of Met-tRNAi^{Met} of eIF2 subunits

At the end of initiation of protein synthesis, eIF2 is released as eIF2.GDP binary complex. Purified native eIF2 from rabbit reticulocyte lysates is bound by GDP, such preparations can bind Met-tRNAi in the presence of Mg^{+2} and high concentrations of GTP. In physiological conditions in the presence Mg^{+2}, eIF2 has a higher affinity for GDP than for GTP. Since GDP inhibits joining of Met-tRNAi, the GDP bound by eIF2 has to be exchanged for GTP. The GDP to GTP exchange is catalyzed by eIF2B, a heteropentameric protein.

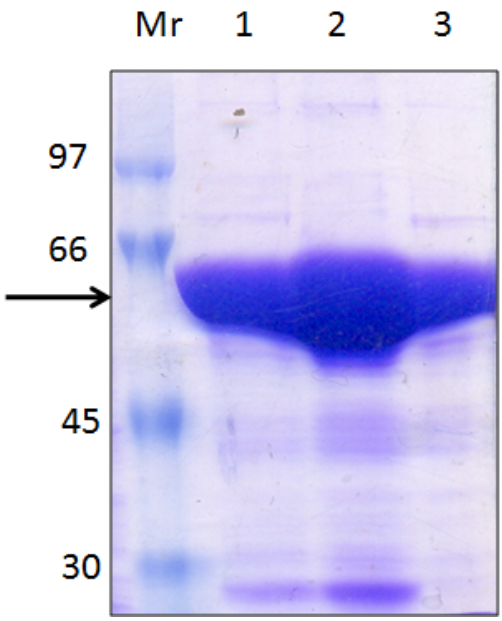

Figure 8.0. Purification of recombinant methionyl-tRNA synthetase from *E. coli.*

The recombinant methionyl-tRNA synthetase with hexa-histidine tag was harvested and the cell pellet was processed as described in Materials and Methods. Purification profile of methionyl-tRNA synthetase by Ni-NTA chromatography: The figure represents a coomassie stained gel. Various lanes are as follows: lanes 1-3, represent the elution fractions and Mr depicts the molecular weight marker.

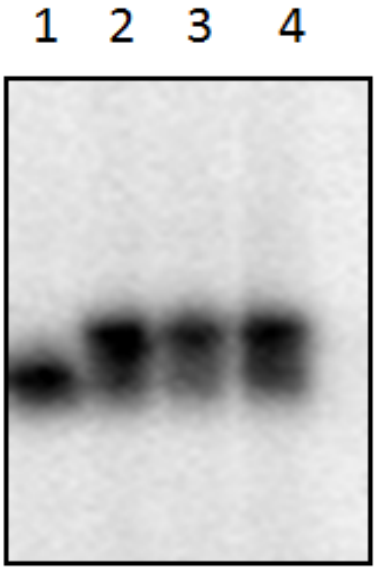

1. **Unacylated Met_i^{tRNA}**
2. **Aminoacylated Met_i^{tRNA} 50 nM MetRS Conc**
3. **Aminoacylated Met_i^{tRNA} 100 nM MetRS Conc**
4. **Aminoacylated Met_i^{tRNA} 150 nM MetRS Conc**

Figure 8.1. Acid-urea PAGE analysis for aminoacylation of Met-tRNAi^{Met}

The *in vitro* transcribed tRNAi was 3′end labeled and charged with L-methionine in the presence of *E. coli* methionyl-tRNA synthetase as described in 'Materials and Methods'. The acylation of Met-tRNAi was analyzed by incubating the reaction mixture with different concentrations of the protein. The reaction mixture was separated on 6% acid-urea PAGE. Various lanes are as follows: Lane 1 represents without enzyme, lanes 2 -4 represent protein concentrations as mentioned above.

However, higher concentrations of GTP can promote purified eIF2 binding *in vitro*. The GDP bound to eIF2 is exchanged for GTP by mass exchange reaction without having eIF2B like protein in the reaction mixtures. Recombinant subunits of eIF2 however may not bind to GDP as they are expressed in bacteria and do not enter the protein synthesis step.

Hence addition of high concentration of GTP may promote recombinant eIF2 binding to Met-tRNAi directly without the presence of eIF2B in partial reactions. In our preliminary studies, to determine the role of each of these subunits to bind initiator tRNA, we carried out double filter binding assays in the presence of free subunits or their combinations with [^{32}P] labeled Met-tRNAi, 500 µM GTP and 2 mM Mg^{+2} in 40 mM Tris-HCl, pH 7.5 buffer that is incubated for 30 min at 37°C as described in Materials and Methods. The bound and unbound tRNAs were captured by filtering the reaction mixtures through two successive membranes: Hybond C and Hybond N^{+}. The protein bound tRNA was retained on Hybond C while the unbound RNA was captured on Hybond N^{+} membrane. The fraction of RNA bound was calculated from the ratio of signals on Hybond C/Total signals of bound and unbound on the two membrane filters as shown in **Figure 8.2** and **Figure 8.3.** The results from the filter binding assays indicate that the intensity of the labeled tRNA band enhances with an increase in the concentration of the γ-subunit. Concomitantly the labeled unbound tRNA intensity is reduced. Interestingly, addition of α– and β–subunits to the γ–subunit enhanced the intensity of the labeled bound tRNA to the membrane suggesting that the heterotrimeric complex joins Met-tRNAi efficiently. The signal intensity of tRNA in the

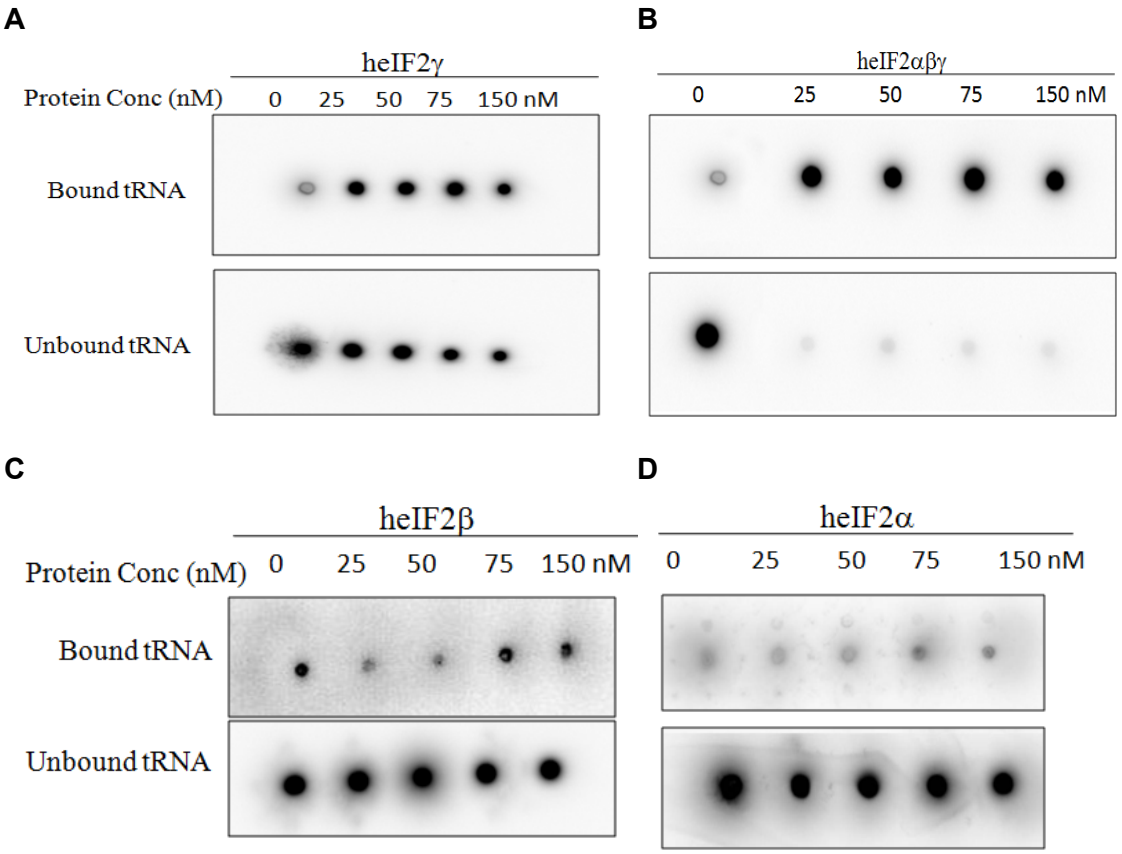

Figure 8.2. Filter binding assay for Met-tRNAi^{Met} binding activities of eIF2γ, eIF2αβγ heterotrimer, eIF2β and eIF2α.

3′ end radiolabeled tRNA substrates were incubated with indicated concentrations of proteins and analyzed as described by Methods in chapter 2. Various panels represent the binding of Met-tRNAi^{Met} to the different subunits of eIF2 or the trimeric eIF2 in the presence of different protein concentrations The protein-bound tRNAs are detected on top-filters Hybond C. The unbound tRNA signals are detected on the bottom-filters of Hybond N^{+}. The radioactive signals were visualized by phosphorimager (Fuji) and intensity of the signals was quantified by imageguage software (Fuji).

Panel A is human eIF2γ, **Panel B** is human eIF2αβγ heterotrimer, **Panel C and D** are human eIF2β and human eIF2α respectively.

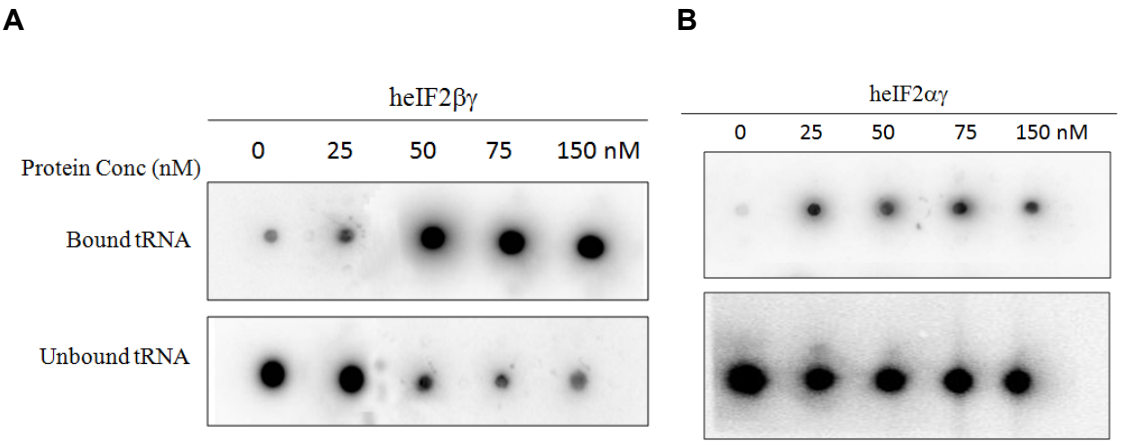

Figure 8.3 Filter binding assay for Met-tRNAi^{Met} binding activities of eIF2αγ, and eIF2βγ

3′ end radiolabeled tRNA substrates were incubated with different concentrations of proteins as indicated above and analyzed as described in the legend to **Fig 8.2**. In each panel, the top filter consists of protein-bound signals of Met-tRNAi^{Met}, whereas the bottom filter consists of unbound signals of Met-tRNAi^{Met}. **Panel A** is human eIF2βγ and **Panel B** is human eIF2αγ.

presence of β–subunit is slightly higher compared to the α–subunit. However γ– subunit compared to α– or β–subunits, showed a better binding.

To further understand the contribution of β– and α–subunits to Met-tRNAi binding, studies were carried out with the single subunits, α and β, and also with the heterodimeric complex, αγ and βγ. The results suggest that the individual α– and β–subunits do not bind Met-tRNAi well compared to the γ-subunit (**Figure 8.4 and Figure 8.5**).

To compare the binding activities of the individual domains and their heterodimeric and heterotrimeric complexes, the dissociation constant (K_D) of acylated Met-tRNAi^{Met} was calculated for each of the above proteins. For this, the fraction of tRNAs bound to the protein was plotted against the protein concentration and K_D values were determined by non-linear regression analysis using a one-site binding hyperbola in GraphPad Prism software. The K_D values for the eIF2α, eIF2β and eIF2γ, their heterodimers eIF2αγ and eIF2βγ, heterotrimeric complex are listed in **Table 3.0**.

3.5. Bioinformatic and structural analysis of eIF2β

As the crystallization of human eIF2β was not successful in our hands, we analyzed the available sequence information of β-subunit in archaea and in higher eukaryotes to obtain some insights into the possible structure of the β-subunit of eIF2 that can explain a) the ability of human eIF2β for its interaction with other subunits of eIF2 and other proteins. b) the inability to crystallize the protein and c) to understand the functional significance of those unconserved regions of the structure with that of archaeal subunits.

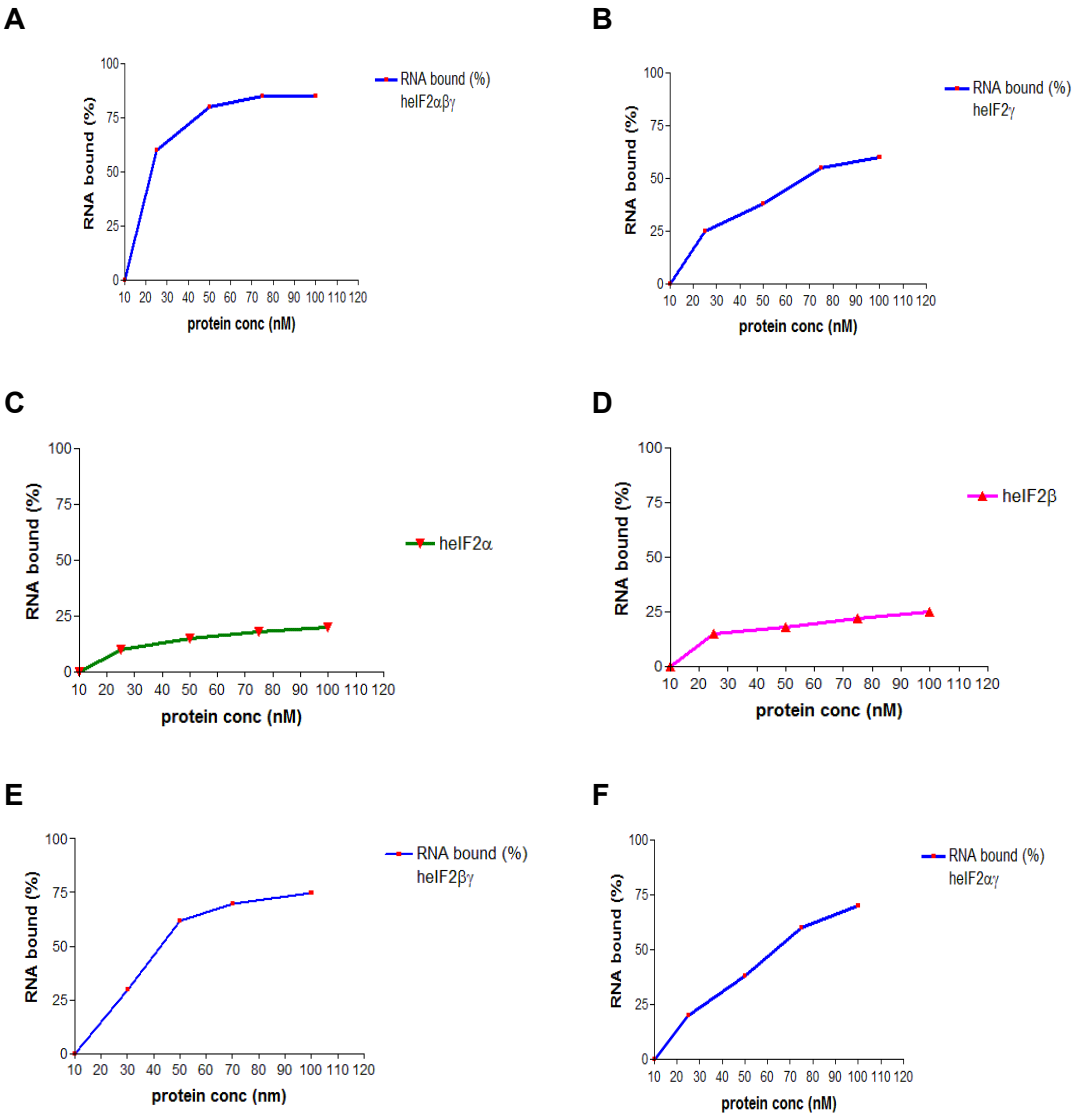

Figure 8.4. Quantification of tRNA binding by eIF2 heterotrimer and its subunits

The binding affinity of the proteins towards Met-tRNAi^{Met} was assessed by filter binding assay and the data were represented in Figs 8.2 and 8.3. The various panels represent the bound percent fraction of tRNA plotted against different protein concentrations. **Panel A** represents percent of tRNA bound to heIF2αβγ; **Panel B**, heIF2γ; **Panel C**, heIF2α; **Panel D**, heIF2β; **Panel E**, heterodimer (heIF2βγ); **Panel F**, heterodimer (heIF2αγ).

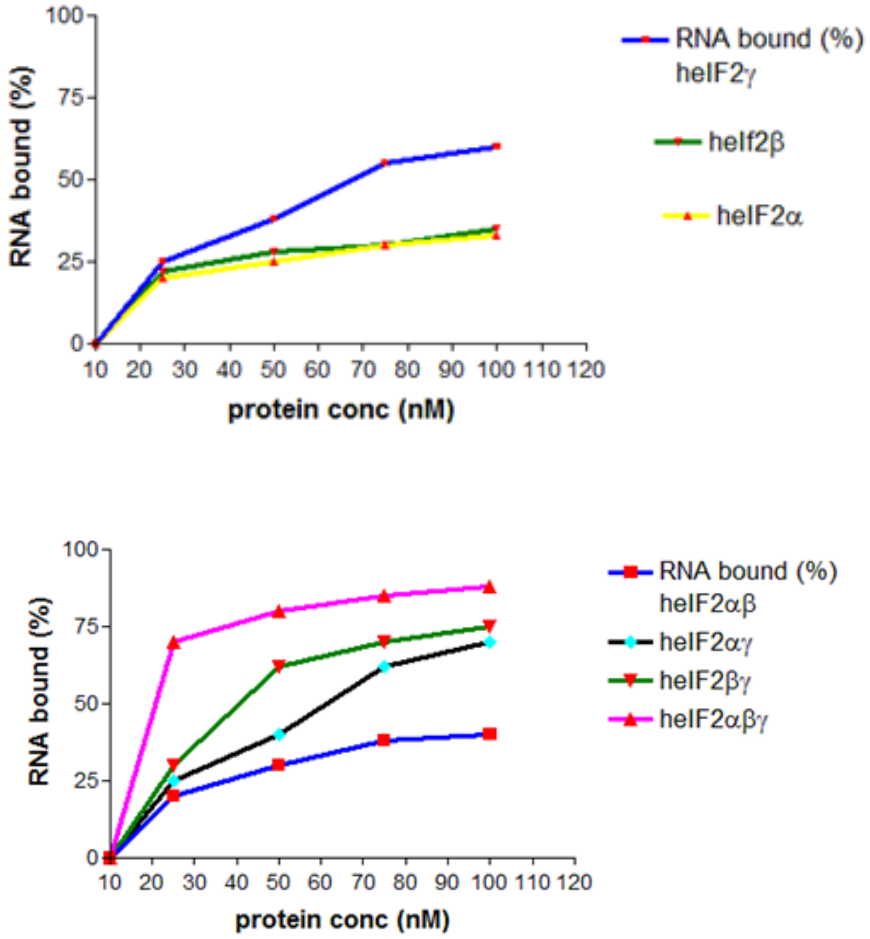

Figure 8.5. Comparative analysis of the subunits for Met-tRNAi^{Met} binding.
The filter- binding data of the proteins to Met-tRNAi^{Met} were quantified and compared from the intensity of the signals on the filters.

S. No.	Enzyme	K_d Value
1	eIF2 γ	1250 nM
2	eIF2 α	1835 nM
3	eIF2 β	1720 nM
4	eIF2 αγ	318 nM
5	eIF2 βγ	107 nM
6	eIF2 αβ	1540 nM
7	eIF2 αβγ	10.8 nM

Table 3.0 Met-tRNAi^{Met} binding constants (K_D) of eIF2 and its subunits.

The K_D values were calculated for tRNA substrates from the graphs shown above in **Fig.8.4.** The values were derived from nonlinear regression analysis of the data using one-site binding hyperbola of GraphPad Prism Software.

Analysis of the sequence information of human eIF2β using NCBI blast P programme against all the protein structures in protein database (PDB) is shown in **Figure 2.1**. Clustal W score indicates that eIF2β has thirty percent identity with archaeal protein (aIF2β). The C-terminal domain of human protein showed maximum similarity to aIF2β. The lysine-rich N-terminal region of eIF2β is found specific to eukaryotes and is variable in different species. PDB analysis reveals that the structure of aIF2β from archaea *Sulpholobus solfataricus* (PDB ID-2NXU) and *Methanobacterium thermoautotrophicum* (PDB ID-1NEE) was solved by NMR studies (Gutierrez et al., 2004 ; Vasile et al., 2003). Neither of eIF2β nor eIF2γ subunits could be crystallized so far. Hence 3D model of human eIF2β was generated using MODELLER (release 9v7) as shown in **Figure 9.0** Panel A. Analysis of the model reveals that amino acids spanning from 170-333 at the C-terminal domain of eIF2β form a proper structure. The C-terminal region of eIF2β consists of residues from 170- 273 folds into a α–β domain. The zinc binding domain, is followed by α–β domain comprises 274-300 amino acid residues. The topological disposition or the homology model of the C-terminal domain of human eIF2β was found similar to full protein of archaeal β-subunit as analyzed by PyMOL programme and shown in **Figure 9.0, Panel B**. A comparison of the archaeal aIF2β sequence with that of human eIF2β also reveals that it has 333 amino acids whereas archaeal subunit has 143 amino acids (**Figure 2.2**). The α–β domain of archaeal protein formed by 1-106 amino acid residues is homologous to the α–β domain of eukaryotic protein formed by 170-273 amino acids. In archaea amino acid residues 108-143 fold into a zinc-binding domain that can be superimposed on the zinc binding domain of eukaryotic protein which is

A

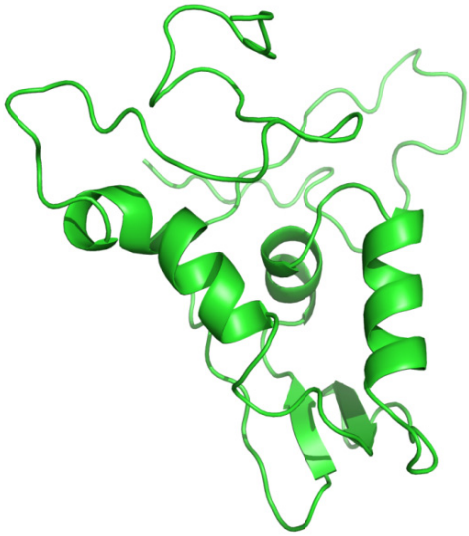

B

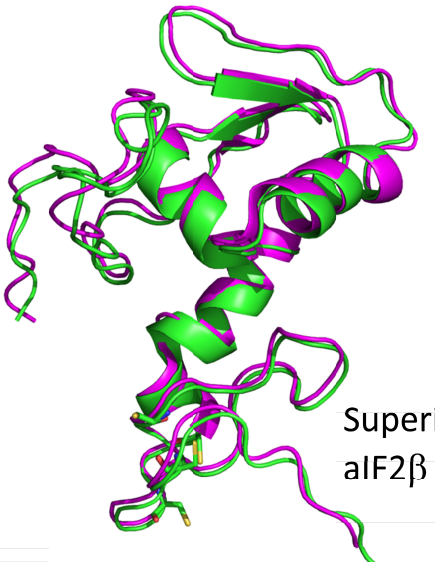

Figure 9.0. Modeled structure of eIF2β generated by MODELLER. The template is aIF2β from *Sulpholobus solfataricus* was downloaded from RCSB; PDB data bank, PDB ID -1NXU. **Panel A** represents the model of C-terminal domain of eIF2β from residues 170-333, which consist of four α–helices and four β–strands. **Panel B** represents the superimposed structure of archaeal (aIF2β) and model eIF2β by PyMOL.

formed by 273-333 amino acids residues (**Figure 9.0, Panel B**). Zinc-binding domain is similar to the structure of ribosomal protein L 36 and this domain is distinguished by a three stranded antiparallel β sheet. It is consists of four conserved cysteine residues (Cys110, 113, 131 and 134) that occur in two CXXC clusters located at the turn between strands α6 and α7 and in the loop just prior to strand α5. The side chains of the four cysteines are located on the same side of the β sheet in such a way that they can bind the zinc ion. N- and C-terminal domains have a linker consisting of 15 amino acid residues i.e. 93-107 in aIF2β and 260-273 in the case eukaryotic protein that connects the α–β domain with zinc-binding domain (**Figure 2.2).** The structural model of eIF2β (170-333) was almost similar to that of the structure of aIF2β with α-carbon positions showing an average rmsd value of about 1.2 Å

The N-terminal region of eIF2β according to the model is not superimposed on aIF2β and it is unstructured. This basic unstructured region appears to be crucial for β-subunit to interact with various proteins and perhaps to the α-subunit in our studies. Interestingly the eukaryotic α-subunit of eIF2 has an acidic C-terminal extension that is absent in archaea. Since α– and β–subunits of eukaryotic eIF2 protein interact with each other, but do not interact in archaea, it is likely that the interaction is mediated by the C-terminal acidic region of the α-subunit and the N-terminal basic region of β-subunit. This can be further substantiated by the fact that phosphorylation of the α-subunit, thereby imparting additional negative charges, enhances the interaction between α– and β–subunits of eIF2B, and it has been demonstrated by this laboratory previously (Rajesh et al., 2008).The homology model structure of

eIF2β on aIF2βγ heterodimer complex shows that the N-terminal helix and the central helix–turn–helix domain of the C-terminal domain of β–subunit bind to the G domain of the γ–subunit as shown in **Figure 9.1.** The residues involved in the interaction between β and γ are conserved in both archaea and eukaryotes suggesting that the C- terminal domain of eIF2β subunit is sufficient for interaction with the γ–subunit. The amino acid sequence and the structural analysis suggest that the basic N-terminal residues of eIF2β interact with the C-terminal domain of eIF2α, whereas the C-terminal domain interacts with the G domain of the γ– subunit.

A

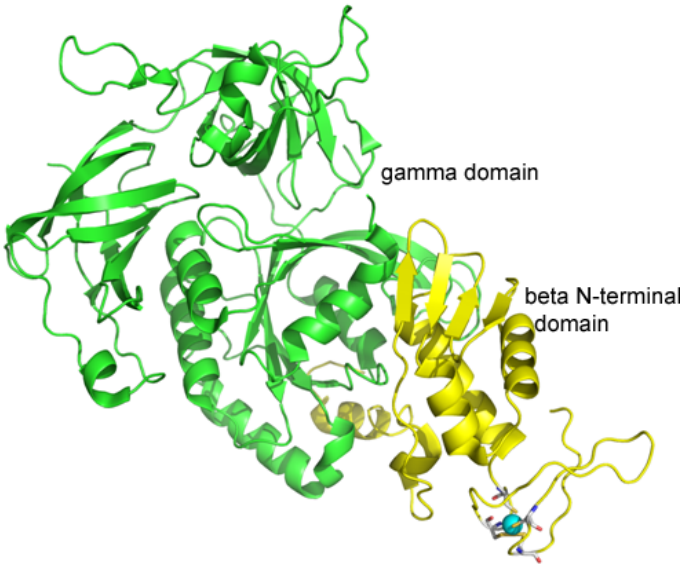

B

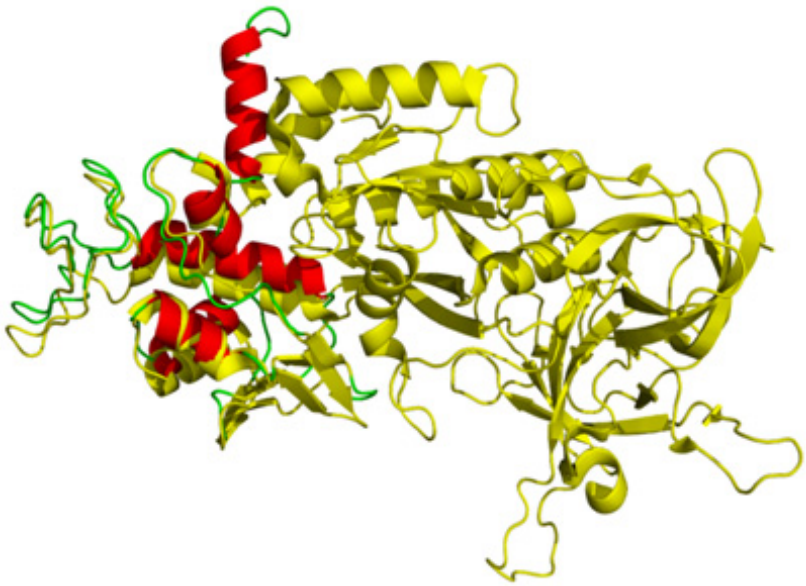

Figure 9.1. The modeled structure of eIF2β generated by MODELLER on archeael βγ heterodimer complex. Panel A indicates the aIF2βγ heterodimer structure downloaded from PDB ID 2D74. **Panel B** represents the superimposed model structure of eIF2β on aIF2βγ heterodimer. The structure indicates the interaction of the C-terminal domain of human eIF2β with γ subunit.

Discussion

CHAPTER 4

DISCUSSION

Eukaryotic Intiation Factor 2 (eIF2) plays a key role in the initiation step of protein biosynthesis and its regulation The native eIF2 is a heterotrimer consisting of α, β and γ subunits in 1:1:1 ratio. It joins methionylated initiator tRNA in the presence of GTP and forms a ternary complex (eIF2.GTP.Met-tRNAi) which is delivered to the small ribosomal subunit (40S subunit). In addition to its role in delivering Met-tRNAi^{Met} to the ribosome, it also plays an important role in the recognition of the initiator AUG codon on mRNA. Previously this laboratory has over expressed all three subunits of eIF2 in the ovarian cells of *Spodoptera frugiperda* (Sf9) using baculovirus expression system to study inter-subunit and inter-protein interactions (Suragani et al., 2005; 2006). These studies have shown that the recombinant subunits of human eIF2 interact with each other to form $\alpha\beta$, $\alpha\gamma$, and $\beta\gamma$ dimers, and $\alpha\beta\gamma$ trimer in ELISA studies. Subsequently bacterially expressed recombinant hexahistidine tagged subunits of eIF2 were also found to interact with each other in the pull down experiments. However, results from other studies indicated that the archaeal and yeast α- and β- subunits of eIF2 do not interact with each other, whereas the $\alpha\gamma$ and $\beta\gamma$ are found to interact with each other (Pedullà et al., 2005; Thompson et al., 2000; reviewed in Schmitt et al., 2010). Based on such studies, Marintchev and Wagner (2004) proposed that γ– subunit of eIF2 in the heterotrimeric complex is the central core and α- and β- subunits interact with the γ– subunit on either side

but there is no direct interaction between α- and β–subunits. To further determine the interactions between α- and β–subunits of eIF2, importance of β–subunit in the initiator tRNA binding, and to understand the possible structure-function relationship of β–subunit, we have constructed and expressed the following forms of α and β- subunits of eIF2 in bacteria. These are the wt, N-terminal domain (comprising 1-183 residues), and C-terminal domain consisting of 186-315 residues of human eIF2α and N-terminal domain (1-170 residues) and C-terminal domain (171-333 residues) of human eIF2β in bacteria (**Figures 2.5 and 2.6**).

The sequence of N- and C- terminal domains in eIF2α were selected based on NMR structure of human eIF2α published by Ito et al., (2004). (**Figures 2.3 and 2.4**). NMR structure of human eIF2α reveals that the N-terminal domain possess two sub domains: S1 sub-domain (residues 15-85) consisting of β barrel followed by α–β helical domain (91-183), and the third domain is the C-terminal domain, which is mobile and flexible and has acidic extension from 275-315 residues (**Figure 2.3**). In our studies here, the recombinant N-terminal of human eIF2α consisting of domains 1 and 2 was found associated with the pellet fraction of the cell extracts but not with the supernatant **(Figure 3.0 Panel B**). Efforts to renature the N-terminal recombinant eIF2α was not successful as the protein was precipitating during refolding. It is likely that the domain may be associated with the membrane proteins. This result is consistent with the earlier reports by Nonato et al., 2002 indicating their inability to refold the N–terminal domain of yeast eIF2α. The C-terminal domain consisting of 185-315 residues, has acidic rich extension was over

expressed and purified as soluble form (**Figure 3.0 Panel C**). The purified wt and C-terminal domain of eIF2α proteins were recognized by a polyclonal anti- eIF2α antibody (**Figure 3.1 Panel B**). In the case of β– subunit, the N-terminal and C-terminal domains were designed based on structure based sequence alignment of archaea (**Figures 2.1 and 2.2)**. The C-terminal domain of β– subunit was found to be in the inclusion bodies where as the N-terminal domain was in the supernatant fraction (**Figure 3.2 Panels A and B**). This may be because of the hydrophobic region in the C-terminal domain of the β-subunit that is shown to interact with the γ-subunit (Sokabe et al., 2006). The exposure of the hydrophobic region in the β-subunit, in the absence of γ-subunit may be cause for the protein to go into the inclusion bodies. Only the wt and the C-terminal domain present in the pellet fraction was recognized by anti-eIF2β antibody (**Figure 3.3 Panel B**). The eIF2β-NTD contains three stretches of lysine boxes, viz., K1, K2, and K3 boxes at position 14, 80 and 128. Interestingly our results of immunoprecipitation analysis suggest that the C-terminal domain of eIF2α interacts with the wt eIF2β subunit (**Figure 4.0 and 4.1**). This is consistent with the suggestion that the negatively charged C-terminus of eIF2α (after pro274) may interact with the positively charged surface consisting of Arg/Lys residues with any of eIFs (Ito et al., 2004). However such an interaction between eIF2α and β-subunits does not occur in yeast eIF2 (Thompson et al., 2006) though the acidic stretches are conserved in C-terminal region of yeast eIF2α. It is not clear whether this is species specific interaction and has any physiological significance. Our observations here indicate that the interaction between human eIF2α and β– subunits are however consistent with the unpublished

observations of Kimball and others mentioning that a) αβ subunits of rat eIF2 interact with each other (unpublished observations of Kimball cited in Kimball et al., 1998) and eIF2β binds either the eIF2B holoprotein, or the isolated δ- or ε-subunits of eIF2B (Kimball et al., 1998). Earlier from this laboratory it has also been suggested that the αβ interaction has a physiological significance because the phosphorylation of eIF2α that inhibits the GDP/GTP exchange activity of eIF2B is relayed to eIF2B through the β-subunit but not by α–subunit of eIF2 (Rajesh et al., 2008). In yeast however, α- and β- subunit interaction was not found, and the phosphorylated eIF2α but not the unphosphorylated α-subunit was found associated tightly with eIF2B, (Krishnamoorthy et al., 2001). In case of archaea, the interaction between α- and β-subunits may not be necessary because archaeal IF2 is not regulated by phosphorylation of the α-subunit or its GDP/GTP exchange is regulated by eIF2B like protein. Based on various mutational studies in yeast, it is suggested that the α– subunit of pentameric eIF2B interacts with the α–subunit of trimeric eIF2 to form eIF2.eIF2B complex. However, while studying the crystal structure of the α subunit of human eIF2B, Hiyama et al., (2009) noted that the affinities of unphosphorylated and phosphorylated eIF2α peptides LLSEL (Sp/S)RRR (46-55 residues) for eIF2Bα as studied by isothermal titration calorimetry, were too low and suggested that perhaps trimeric eIF2, β–subunit or the wt eIF2α may be required for the interaction between eIF2 and eIF2B.

The interaction of αβ was further characterized here by circular dichroism studies (**Figure 5.1 Panel C and Figure 5.2 Panel B**). The results indicate a

rearrangement in the random coil or changes in the secondary structure in the wt β-subunit of eIF2 when it interacts with the wt and the C-terminal domain of α-subunit of eIF2. A recent study, based on circular dichroism studies, has suggested that the N-terminal domain of eIF2β that contains most of the random coils interacts with other proteins like eIF2B and eIF5 (Zuoqi et al., 2012). The N-terminal domain of β- subunit rich in basic amino acids may be involved in the interaction with α–subunit. The affinity of αβ subunit interaction was further characterized by isothermal calorimetry. The dissociation constant of α and β subunit is around 8 μM, (**Figure 6.0**) suggesting that it may not be a very strong association. It could be an ionic interaction because of acidic and basic amino acids on C-terminal and N-terminal domain of eIF2α and eIF2β respectively. Consistent with such a notion, an earlier study from this laboratory observed that phosphorylation of eIF2α increases the net negative charge on eIF2α, enhances the interaction between α- and β- subunits of eIF2 and also between the eIF2 and eIF2B complexes which is mediated by the β-subunit of eIF2.

Conformational characterization of human eukaryotic intiation factor eIF2β

As mentioned in the introduction, structural information on mammalian β-subunit is lacking inspite of the fact that biochemical and mutational studies of yeast eIF2 suggest that it may be important for many functions of eIF2 such as its ability to interact with various proteins and RNA (such as mRNA and tRNA) and in stimulating the GTPase activity of eIF2 (Kapp and Lorch, 2004). Recombinant human eIF2β subunit was purified to homogeneity as assessed

by dynamic light scattering profile as shown in **Figure 6.1** to carry out crystallization studies. Although we attempted crystallization of the β- subunit in the presence of GDP and GTP, we were not successful in our attempts as the protein was unstable and was proteolyzed without yielding diffractable crystals. We do not know if any other ligands or proteins or subunits of eIF2 are required for the crystallization. However, to gain further insights into the structure and stability of β- subunit of eIF2, we characterized the stability of the protein using steady state fluorescence spectroscopy to identify any transition state during unfolding from the native state. The fluorescence of tryptophan is used as a signal to monitor the unfolding of proteins, in particular the intensity of fluorescence and the wave length of its maximum, λmax. Generally the position of the emission maximum of tryptophan fluorescence indicates the relative position of tryptophan residue in the protein. If the tryptophan residue is buried in the protein core surrounded by hydrophobic environment, the λmax of the fluorescence spectra will be around at 332 nm. Our data **(Figure 7.0)** on steady state fluorescence indicate that native eIF2β with a single tryptophan protein (NCBI ID: P20042) shows intrinsic fluorescence spectrum with a λmax at 338 nm indicating tryptophan is not completely in a hydrophobic environment. The Gdn-HCl induced unfolding of heIF2β is monitored on the basis of the intrinsic fluorescence intensity. Unlike the native protein, the Gdn-HCl treated protein showed progressive denaturation with gradual red shift changing the λmax from 338 nm to 357 nm. With increase in the Gdn-HCl, at 6.0 M, the intensity of the fluorescence is also reduced indicating the exposure of tryptophan to the polar environment due to quenching.

The equilibrium unfolding (Gdn-HCl) mediated mechanism of eIF2β suggests that it is a two state process with no intermediates (a native state and an unfolded state) as shown in **Figure 7.1.** The fluorescence studies demonstrate the single trp residue of the β-subunit (located at the juncture of N-terminal and C-terminal domain) present in partially hydrophilic environment. The truncated form of wt β– subunit consisting of C-terminal domain that is predominantly hydrophobic was found in the inclusion bodies, suggesting that the C-terminal domain is probably interacting with the G-domain of the γ–subunit of eIF2. This may be due to the exposure of the hydrophobic region present in the C-terminal domain of the β-subunit. The lack of transition intermediates during unfolding studies suggests that the protein may be behaving like single entity due to lack of proper structure in the N-terminus. Otherwise the unfolding studies would have shown intermediate transition states as has been detected recently with HRI kinase showing three separate domains with multistate unfolding and presence of three stable intermediates. (Sreejith et al., 2011).

Hydrophobic dye binding studies also explain that native eIF2β at physiological pH 7.5 binds ANS and gives an emission of λmax at 458 nm indicating the presence of exposed hydrophobic regions (**Figure 7.2 Panel A**). The hydrophobicity of the β– subunit was observed to be higher compared to the α– subunit under the same conditions (**Figure 7.2 Panel B**). The same β-subunit when incubated at low pH 2.0 exhibits significant binding of ANS and shows an increase in fluorescence intensity suggesting the protein

unfolds at low pH and the hydrophobicity of the protein is completely exposed (**Figure 7.2 Panel A**).

The secondary structure of β–subunit depicts the presence of more unordered structure as shown in **Figure 5.0 Panel B** and in **Table 2.0** as calculated by CD Pro programme, compared to α– subunit which has more of helix content and has less percentage of randomness in the structure. As the temperature is increased from 25°C to 85°C, the negative ellipticity of the protein decreases at 208 nm as measured from CD studies and the T_m of the protein was found to be 45°C (**Figure 7.5)**. The T_m value of the β-subunit estimated here is relatively low compared to the T_m of α–subunit that has been estimated recently. The β-subunit showed retention of 20.5% of α helix content at 85°C based on our studies here. In contrast, α-subunit retains 56% of α-helix structure at 95°C indicating relatively strong forces are involved in the folding of α– subunit (Sreejith et al., 2009). The T_m of the eIF2β protein is only 45°C, suggesting that eIF2β is not very stable due to limited secondary structure compared to α-subunit.

An insight into the secondary structure by far-UV CD spectra studies of eIF2β reveals a loss of α-helix at extreme acidic or alkaline pH suggesting that the protein was denatured due to loss of secondary structure (**Figure 7.4**) and also a major rearrangement of secondary structure at pH10.0. The same protein at physiological pH 7.5 and at low pH 2.0 was also scanned at near UV region from 260-320 nm, to determine the tertiary structure of the protein. The spectra at pH 7.5 and low pH 2.0 was almost similar with a maximum peak at a range of 260- 270 nm suggesting the protein is not properly folded

into distinct tertiary structure and the protein is unstable. Each of the amino acids in a protein tends to have a characteristic wave length profile at near UV. Trp shows a peak close to 290 nm with fine structure between 290 and 305 nm; Tyr gives a peak between 275 and 282 nm, with a shoulder at longer wave lengths often obscured by bands due to Trp; Phe shows weaker but sharper bands with fine structure between 255 and 270 nm (Kelly et al., 2005). Based on such studies, we suspect that much of the tertiary structure in β– subunit may be contributed by phenylalanine because the results of near UV spectra of β- subunit in the presence of pH 7.5 and pH 2.0 (**Figure 7.3**) ranges between 260-270 nm. These findings indicate the instability of the β-subunit is consistent with very early reports that β-subunit is sensitive to proteolysis and that many pure preparation of reticulocyte eIF2 are devoid of the β-subunit (Flynn et al., 1993).

Met-tRNAi^{Met} Binding: In eukaryotes and archaea the heterotrimeric eukaryotic/archaeal translation initiation factor 2 eIF2/aIF2 in its GTP bound form specifically joins Met-tRNAi^{Met} which plays a key role in the selection of the 'start' codon on mRNA, After the 'start' codon recognition, the factor in its GDP bound form has less affinity for Met-tRNAi^{Met}, that eventually dissociates the initiation complex and leaves Met-tRNAi^{Met} in the P-site of the small ribosomal subunit (reviewed in Aitken and Lorsch 2012, reviewed in Hinnebusch 2011). During this process, specific binding of the initiator tRNA by e/aIF2 is crucial for accuracy. Binding of tRNA to intiation factor IF2 was extensively studied in the archaeal system. The γ–subunit of *Pyrococuss abysii*-aIF2 (Pa-aIF2) is able to bind methionylated initiator tRNA, but the measured tRNA binding affinity for the isolated γ– subunit was however highly

reduced with dissociation constant of 5 μM when compared to that of complete heterotrimer Pa-aIF2 with the K_D value of 120 nM as measured by protection-based assays suggesting that the heterotrimer has better affinity than γ–subunit alone. In *Sulpholobus solfataricus* aIF2γ (Ss-aIF2γ) alone had K_D of 100 μM for methionylated initiator tRNA, whereas a K_D value of 1.5 nM was observed with complete trimeric Ss-aIF2. Although these differences between the two archaeal systems may be related to their growth conditions, the archaeal β– subunit does not contribute significantly to the Met-tRNAi binding whereas, the α-subunit provides the heterotrimer with almost its full tRNAi binding affinity. The C-terminal domain (D3) of the archaeal α subunit was responsible for binding to the γ– subunit and it is enough to retrieve the same binding affinity of tRNA as full aIF2 (Yatime et al., 2004; Yatime et al., 2006). Early studies in eukaryotes, had determined the binding of Met-tRNAi^{met} for eIF2.GTP by using nitrocellulose-binding assays and the affinity (K_D) for the tRNAi for eIF2 heterorimer was in the range of 10 nM. (Erickson and Hannig 1996) (Kapp and Lorsch 2004). We studied here the affinity of Met-tRNAi with the reconstituted (1:1:1 ratio) human eIF2 heterotrimer in the presence of 500 μM GTP by filter binding assay. The human tRNAi was *in vitro* transcribed and was acylated using purified *E.coli* methionyl- tRNA synthetase. The in vitro transcribed human tRNAi has an acylation efficiency of 80%, as analyzed by acid-urea PAGE and as shown in **Figure 8.1**. The affinity for the acylated Met-tRNAi for eIF2 heterotrimer was 10.8 nM (**Figure 8.2 panel B**), which was comparable to the earlier reports. The contribution of eIF2α and eIF2β subunits in tRNA binding remained controversial. A number of earlier studies found that there was no difference in Met-tRNAi^{Met}

binding properties of mammalian eIF2 containing or lacking the β– subunit (Mitsui et al., 1981 and Das et al., 1982). On another hand, isolation of βγ heterodimer during purification of rabbit reticulocyte eIF2 lacking α-subunit suggested that α– subunit is not strictly required for Met-tRNAi^{Met} binding (Mouat and Manchester 1998). In our study, filter binding assays were used to measure methionylated tRNAi binding to various forms of eIF2. The K_D value for human eIF2γ subunit alone with Met-tRNAi^{Met} has an affinity of 1250 nM. The other subunits human eIF2α and eIF2β have a K_D of 1835 nM and 1720 nM respectively as shown in **Figure 8.2** and **Table 3.0.** The role of each of the peripheral subunit in tRNA binding was studied in context of heterodimers, we observed that eIF2αγ had K_D of 318 nM and eIF2βγ had K_D of 107 nM respectively as shown in **Figure 8.3**. This explains that human eIF2β is essential for full tRNA binding affinity, and the contribution from eIF2α is comparatively low. This is in contrast to archeal IF2 where the contribution of the α– subunit to the tRNAi binding activity of the heterotrimer is more. Our observations of human heterodimers αγ and βγ to the binding of Met-tRNAi are consistent with a recent study on *E. cuniculi, a* lower eukaryote (Naveau et al., 2010) and also on yeast eIF2 (Nika et al., 2001). In *E. cuniculi,* the γ- subunit of eIF2 is able to bind itself the initiator tRNA and the two peripheral α– and β– subunits contribute equally to tRNA binding affinity. Also studies from the construction of a yeast strain lacking eIF2α, the eIF2βγ heterodimer was purified and was shown to contribute maximally to tRNA binding suggesting that β, but not α–subunit would have an important role in binding (Nika et al., 2001). However, we find the α– subunit promotes modestly to the Met-tRNAi binding to the γ- subunit since the K_D values of

Met-tRNAi binding by αγ was 318 nM, where as for βγ it was 107 nM. The archaeal behavior is consistent with the recently discovered 5- Å crystal structure of archaeal *Sulfolubus solfataricus* IF2 (Ss-aIF2) bound to initiator methionyl-tRNAi (Schmitt et al., 2012, Shin et al., 2011) showing that the tRNA is bound by α- and γ- subunits of aIF2. Further, the ability of α– subunit of archaeal IF2 to binds Met-tRNAi more efficiently than the eukaryotic α-subunit. This is attributed to the absence of acidic C-terminal extension in archeal IF2 and its presence in eukaryotic eIF2α. Progressive deletion of this acidic C-terminal in yeast eIF2α made it to bind to the initiator tRNA (Naveau et al., 2012). The homology model of eIF2β suggests that the C-terminal domain has structural homology with aIF2β protein and the N-terminal domain remained unstructured (**Figure 9.0**). This eIF2β-NTD unstructured may be required for its function which recognizes and binds to different proteins in different stages of translation initiation.

Overall, the present study reiterates that α- and β-subunits of human/mammalian eIF2, unlike archaeal IF2 subunits, interact with each other and the β- subunit together with the γ- subunit confers a higher ability to bind tRNA than the α- and γ- subunits. The biophysical studies suggest that human eIF2β subunit is less ordered and unstable. The unordered structure of β- subunit may be the reason for its interaction with various proteins. These findings together with the ability to bind tRNA and other observations of this laboratory, indicate that β- subunit interacts with eIF5, eIF2B, eIF1A, mRNA, Nck1, and also serves as a substrate for multiple kinases, (Singh et al., 2004; Laurino et al., 1999, Wakula et al., 2006, Kebache et al., 2002, Llorens et al.,

2006) suggest that β- subunit occupies a central role in eIF2 trimer affecting the function and regulation of eIF2.

Summary

CHAPTER 5

SUMMARY

---

1. N-terminal and C-terminal domains of eIF2α and β–subunits were constructed based on the available NMR structure of eIF2α and structure based sequence alignment of archaea aIF2β respectively.
2. The N- and C-terminal domains of α- and β-subunits were cloned in bacterial expression vector, overexpressed and the proteins with hexahistidine tags were purified. The C-terminal domain of eIF2α and N-terminal domain of eIF2β was in soluble form and could be purified, whereas the N-terminal domain of eIF2α and C-terminal domain of eIF2β were found in the inclusion bodies. These mutants and wt proteins were identified by respective antibodies.
3. Using immunoprecipitation assays, we observed that α- and β-subunits interact with each other and it is the C-terminal domain of eIF2α that interacts with eIF2β subunit. The C-terminus of eIF2α consists of an acidic region that might interact with N-terminal region of β–subunit, which has lysine rich region.
4. The interaction was further characterized by biophysical techniques using circular dichroism studies. The secondary structural analysis of the complex eIF2α:eIF2β had shown structural rearrangement of eIF2β subunit that had random coil at its N-terminus. The affinity of eIF2β and eIF2α was characterized by isothermal titration calorimetry studies and the association of α- and β-subunits was found to be weak. This may be because of charge-charge interactions mediated by basic and acidic

amino acids present on N- and C-termini of β- and α-subunits respectively.

5. To understand the conformational transitions and stability, steady state fluorescence studies were carried out with wt recombinant eIF2β. The protein has a single tryptophan residue at 169 position which shows an intrinsic fluorescence spectrum with λ_{max} at 338 nm suggesting that tryptophan is not completely in a hydrophobic environment. The Gdn-HCl treated protein showed progressive denaturation with gradual red shift changing the λ_{max} from 338 nm to 357 nm. With increase in the Gdn-HCl, at 6.0 M, the intensity of the fluorescence is also reduced indicating the exposure of tryptophan to the polar environment due to quenching. The equilibrium unfolding (Gdn-HCl) mediated mechanism of eIF2β suggests that it is a two state process with no intermediates, a native state and an unfolded state. Native eIF2β at physiological pH 7.5 binds ANS and gives an emission of λ_{max} at 458 nm indicating the presence of exposed hydrophobic regions.
6. The structure-based sequence alignment suggests that eIF2β has 30% sequence identify with archael aIF2β. The homology model based on the structure of aIF2β suggests that the N-terminal domain of eIF2β is unstructured and the C-terminal domain is homologous to aIF2β.
7. The CD spectrum of eIF2β exhibits a negative band in the far-UV region at 208 nm that is characteristic for α helix structure. However, the secondary structural analysis indicates that the β-subunit has higher amount of random coil compared to the α-subunit. As the temperature is increased from 25°C to 85°C, the negative ellipticity of

eIF2β decreases at 208 nm as measured from CD studies and the T_m of the protein was found to be 45°C. The loss of secondary structure at high temperature indicates that the protein is not very stable.

8. The analysis of acylated Met-tRNAi binding studies suggests that human βγ hetero dimeric complex of eIF2 binds Met-tRNAi more efficiently than αγ, suggesting that β- subunit rather than α-subunit enhances the Met-tRNAi binding to the γ-subunit.
9. These findings suggests that the interaction between eIF2α and eIF2β subunits. The involvement of β-subunit in Met-tRNAi binding to γ- subunit along with various observations by others indicating that β-subunit is a hub for protein-protein interactions as it interacts with eIF1, eIF1A, eIF3, eIF2B, eIF5, NCK1, interacts with mRNA, serves as a substrate for different kinases and mediates the formation of an inhibitory complex between phosphorylated eIF2α and eIF2B suggests that eIF2β may be central in functioning of eIF2, whereas γ-subunit is central in structure.

References

- Aarti I, Rajesh K, Ramaiah KV (2010), Phosphorylation of eIF2 alpha in Sf9 cells: a stress, survival and suicidal signal. Apoptosis. 2010 Jun;15(6):679-92.
- Aitken CE, Lorsch JR. (2012), A mechanistic overview of translation initiation in eukaryotes.Nat Struct Mol Biol. 2012 Jun 5;19(6):568-76.
- Algire MA, Maag D, Lorsch JR. (2005) Pi release from eIF2 not GTP hydrolysis; is the step controlled by start-site selection during eukaryotic translation initiation. Mol. Cell: 20, 251-262.
- Alone, P.V.; Dever, T.E. (2006) Direct binding of translation initiation factor eIF2gamma-G domain to its GTPase-activating and GDP-GTP exchange factors eIF5 and eIF2B epsilon. J. Biol. Chem., 281, 12636-12644.
- Alone, PV. Cao, C. and Dever, TE. (2008)Translation initiation factor 2gamma mutant alters start codon selection independent of Met-tRNA binding. Mol. Cell. Biol., 28, 6877-6888.
- Andaya A, Jia W, Sokabe M, Fraser CS, Hershey JW, Leary JA. (2011), Phosphorylation of human eukaryotic initiation factor 2γ: novel site identification and targeted PKC involvement. J Proteome Res. 2011 Oct 7;10(10):4613-23.
- Anderson, C. B., Becker, T., Blau, M., Anand, M., Halic, M., Balar, B., Mielke , T., Boesen, T., Pedersen, J. S., Spahn, C. M., et al. (2006) Structure of eEF3 and the mechanism of transfer RNA release from the E-site. Nature, 443:663–668.

- Anthony DD Jr, Kinzy TG, Merrick WC (1990), Affinity labeling of eukaryotic initiation factor 2 and elongation factor 1 alpha beta gamma with GTP analogs. Arch Biochem Biophys. Aug 15;281(1):157-62.
- Asano K, Clayton J, Shalev A, Hinnebusch AG. (2000) A multifactor complex of eukaryotic initiation factors, eIF1, eIF2, eIF3, eIF5, and initiator tRNA (Met) is an important translation initiation intermediate invivo. Genes Dev. 14: 2534-46.
- Asano K, Krishnamoorthy T, Phan L, Pavitt GD, Hinnebusch AG (1999), Conserved bipartite motifs in yeast eIF5 and eIF2Bepsilon, GTPase-activating and GDP-GTP exchange factors in translation initiation, mediate binding to their common substrate eIF2. EMBO J. 1999 Mar 15;18(6):1673-88.
- Baird TD and Wek RC. (2012) Eukaryotic initiation factor 2 phosphorylation and translational control in metabolism, American Society for Nutrition. Adv. Nutr. 3: 307–321.
- Baron-Benhamou J, Fortes P, Inada T, Preiss T, Hentze MW (2003) The interaction of the cap-binding complex (CBC) with eIF4G is dispensable for translation in yeast.RNA. Nat.Struct.Biol. (6):54-62.
- Bommer UA, Lutsch G, Stahl J, Bielka H.(1991), Eukaryotic initiation factors eIF-2 and eIF-3: interactions, structure and localization in ribosomal initiation complexes. Biochimie. 73:1007-19.
- Chapeville F, Lipmann F, Von ehrenstein G, Weisblum B, ray wj Jr, Benzer S. (1962) On the role of soluble ribonucleic acid in coding for amino acids. Proc. Natl. Acad. Sci. U S A. 48:1086-92.

- Choi SK, Olsen DS, Roll-Mecak A, Martung A, Remo KL, Burley SK, Hinnebusch AG, Dever TE. (2000) Physical and functional interaction between the eukaryotic orthologs of prokaryotic translation initiation factors IF1 and IF2. Mol. Cell Biol. 20: 7183-91.
- Das S, Ghosh R, Maitra U. (2001) Eukaryotic translation initiation factor 5 functions as a GTPase-activating protein. J Biol. Chem. 276: 6720-6
- Das S, Maiti T, Das K, Maitra U. (1997) Specific interaction of eukaryotic translation initiation factor 5 (eIF5) with the beta-subunit of eIF2. J Biol. Chem. 272: 31712-8.
- Dhaliwal S, Hoffman DW. (2003) The crystal structure of the N-terminal region of the alpha subunit of translation initiation factor 2 (eIF2alpha) from Saccharomyces cerevisiae provides a view of the loop containing serine 51, the target of the eIF2alpha-specific kinases. J Mol. Biol. 334: 187-95.
- Dholakia JN, Francis BR, Haley BE, Wahba AJ.(1989), Photoaffinity labeling of the rabbit reticulocyte guanine nucleotide exchange factor and eukaryotic initiation factor 2 with 8-azidopurine nucleotides. Identification of GTP- and ATP-binding domains. J Biol Chem. 264 (34):20638-42.
- Donahue TF, Cigan AM, Pabich EK, Valavicius BC. (1988) Mutations at a Zn(II) finger motif in the yeast eIF-2 beta gene alter ribosomal start-site selection during the scanning process. Cell, 54: 621-32
- Dong J, Nanda JS, Rahman H, Pruitt MR, Shin BS, Wong, CM, Lorsch, J.R.; Hinnebusch AG. Genetic identification of yeast 18S rRNA residues required for efficient recruitment of initiator tRNAMet and AUG selection. Genes & Dev 2008, 22, 2242-2255.

- Drabkin H_J, RajBhandary U_L (1998) Initiation of protein synthesis in mammalian cells with codons other than AUG and amino acids other than methionine. Mol Cell Biol. (9):5140-7.
- Erickson FL., Hannig EM. (1996) Ligand interactions with eukaryotic translation initiation factor 2, role of the g-subunit. EMBO J. 15, 6311-6320.
- Ernst H, Duncan RF, Hershey JW. (1987) Cloning and sequencing of complementary DNAs encoding the alpha-subunit of translational initiation factor eIF-2. Characterization of the protein and its messenger RNA. J Biol. Chem. 262: 1206-12.
- Fabian, JR, Kimball, SR, Heinzinger, NK, Jefferson, LS. (1997) Subunit assembly and guanine nucleotide exchange activity of eu-karyotic initiation factor-2B expressed in Sf9 Cells. J. Biol. Chem. 272, 12359-12365.
- Fadden P, Haystead TA, Lawrence JC Jr. (1997) Identification of phosphorylation sites in the translational regulator, PHAS-I, that are controlled by insulin and rapamycin in rat adipocytes. J Biol. Chem. 272: 10240-7
- Farruggio D, Chaudhuri J, Maitra U, Raibhandary UL. (1996) The A1:U72 base pair conserved in eukaryotic initiator tRNAs is important specifically for binding to the eukaryotic translation factor eIF2. Mol Cell Biol 16: 4248-56.
- Flynn A, Oldfield S, Proud CG. (1993) The role of the beta-subunit of initiation factor eIF-2 in initiation complex formation. Biochim. Biophys. Acta. 1174: 117-21.

- Frolova, L.Y., Merkulova, T.I., and Kisselev, L.L. (2000) Translation termination in eukaryotes: polypeptide release factor eRF1 is composed of functionally and structurally distinct domains. RNA, 6, 381-390.
- Frolova, L.Y., Tsivkovskii, R. Y., Sivolobova, G. F., Oparina, N. Y., Serpinsky, O. I., Blinov, V. M., Tatkov, S.I., and Kisselev, L.L. (1999) Mutations in the highly conserved GGQ motif of class 1 polypeptide release factors abolish ability of human eRF1 to trigger peptidyl-tRNA hydrolysis. RNA 5, 1014–1020
- Gaspar NJ, Kinzy TG, Scherer BJ, Hümbelin M, Hershey JW, Merrick WC. (1994) Translation initiation factor eIF-2. Cloning and expression of the human cDNA encoding the gamma-subunit. J Biol. Chem. 269: 3415-22.
- Grunberger D, Weinstein IB, Jacobson KB.(1969), Codon recognition by enzymatically mischarged valine transfer ribonucleic acid. Science. ;166 1635-7.
- Gutiérrez P, Osborne MJ, Siddiqui N, Trempe JF, Arrowsmith C, Gehring K. (2004) Structure of the archaeal translation initiation factor aIF2 beta from *Methanobacterium thermoautotrophicum*: implications for translation initiation. Protein Sci. 13: 659-67.
- Hashimoto NN, Carnevalli LS, Castilho BA. (2002), Translation initiation at non-AUG codons mediated by weakened association of eukaryotic initiation factor (eIF) 2 subunits. Biochem J. 2002 Oct 15;367(Pt 2):359-68.
- Jackson, R.J., Hellen, C.U.T. & Pestova, T.V. (2010) The mechanism of eukaryotic translation initiation and principles of its regulation. Nat. Rev. Mol. Cell Biol. 11, 113–127.

- Hinnebusch AG (2011) Molecular Mechanism of Scanning and Start Codon Selection in Eukaryotes, 75: 434–467.
- Hinnebusch AG. (2005) Translational regulation of GCN4 and the general amino acid control of yeast. Annu. Rev. Microbiol. 59: 407-50.
- Hinnebusch G, Mechanism and regulation of initiator methionyl tRNA binding to ribosomes, in: N. Sonenberg, J.W.B. Hershey, M.B. Mathews (Eds.), Translational Control of Gene Expression, Cold Spring Harbor Laboratory Press, Cold Spring Harbor, New York, 2000, pp. 185–243.
- Hinnebusch, A.G. and Natarajan, K. (2002). Gcn4p, a master regulator of gene expression, is controlled at multiple levels by diverse signals of starvation and stress. Eukaryotic Cell 1:22-32
- Hinnebusch, A.G.; Dever, T.E.; Asano, K.A.; Mechanism of trans-lation initiation in the yeast Saccharomyces cerevisiae. In, Sonen-berg N, Mathews M, Hershey JWB, editors. Translational Control in biology and medicine. Cold Spring Harbor, NY., Cold Spring Harbor Laboratory Press, 2007, pp. 225-268.
- Hiyama TB, Ito T, Imataka H, Yokoyama S Crystal structure of the alpha subunit of human translation initiation factor 2B. (2009) J Mol Biol. 392(4):937-51.
- Imataka H, Gradi A, Sonenberg N. (1998) A newly identified N-terminal amino acid sequence of human eIF4G binds poly(A)-binding protein and functions in poly(A)-dependent translation. EMBO J. 17: 7480-9.
- Imataka H, Sonenberg N. (1997) Human eukaryotic translation initiation factor 4G (eIF4G) possesses two separate and independent binding sites for eIF4A. Mol. Cell Biol. 17: 6940-7.

- Ito T, Marintchev A, Wagner G. (2004) Solution structure of human initiation factor eIF2alpha reveals homology to the elongation factor eEF1B. Structure, 12: 1693-704.
- Ito, K., Uno, M., and Nakamura, Y. (2000). A tripeptide anticodon deciphers stop codon in messenger RNA. Nature, 403, 680-684.
- Kainuma M, Hershey JW. (2001) Depletion and deletion analyses of eucaryotic translation initiation factor 1A in Saccharomyces cerevisiae. Biochimie. 83: 505-14.
- Kamindla R, Iyer A, Suragani RN, Ramaiah KV. (2008) Intersubunit and interprotein interactions of α - and β -subunits of human eIF2: Effect of phosphorylation Biochem. Biophys. Res. Commun. 374: 336–340.
- Kapp LD, Lorsch JR. (2004) GTP-dependent recognition of the methionine moiety on initiator tRNA by translation factor eIF2. J. Mol. Biol., , 335, 923-936
- Kapp LD, Lorsch JR. (2004) The molecular mechanics of eukaryotic translation. Annu Rev Biochem; 73: 657–704.
- Kebache S, Zuo D, Chevet E, Larose L, (2002) Modulation of protein translation by Nck-1, Proc. Natl. Acad. Sci. USA: 99 5406–5411..
- Kelly SM, Jess TJ, Price NC (2005), How to study proteins by circular dichroism BBA, Vol. 1751, 119-139.
- Kimball SR, Heinzinger NK, Horetsky RL, Jefferson LS. (1998) Identification of interprotein interactions between the subunits of eukaryotic initiation factors eIF2 and eIF2B. J Biol. Chem. 273: 3039-44.

- Kisselev, L., Ehrenberg, M., and Frolova, L. (2003) Termination of translation: interplay of mRNA, rRNAs and release factors? EMBO J., 22(2):175-82.
- Kleijn M, Scheper GC, Voorma HO, Thomas AA. (1998) Regulation of translation initiation factors by signal transduction. Eur. J Biochem. 253: 531-44.
- Kozak M. (1989), The scanning model for translation: an update. J Cell Biol. 108: 229-41.
- Krishnamoorthy T, Pavitt GD, Zhang F, Dever TE, Hinnebusch AG. (2001) Tight binding of the phosphorylated alpha subunit of initiation factor 2 (eIF2alpha) to the regulatory subunits of guanine nucleotide exchange factor eIF2B is required for inhibition of translation initiation. Mol. Cell Biol. 21: 5018-30.
- Lamphear BJ, Kirchweger R, Skern T, Rhoads RE. (1995) Mapping of functional domains in eukaryotic protein synthesis initiation factor 4G (eIF4G) with picornaviral proteases. Implications for cap-dependent and cap-independent translational initiation. J Biol. Chem. 270: 21975-83.
- Laurino JP, Thompson GM, Pacheco E, Castilho BA.(1999) The beta subunit of eukaryotic translation initiation factor 2 binds mRNA through the lysine repeats and a region comprising the C2-C2 motif. Mol. Cell Biol. 19: 3224.
- Leibundgut M, Frick C, Thanbichiler M, Bock A, Ban N (2005). Selenocysteine tRNA-specific elongation factor SelB is a structural chimaera of elongation and initiation factors. EMBO 24, 11–22.

- Lin PJ, Chang CH, Yao PC, Hsieh HC, Hsieh MJ, Kao CL, Tsai KT. (1994) Enhancement of endothelium-dependent contraction of the canine coronary artery by UW solution. Transplantation, 58: 1323-8.
- Llorens F, Duarri A, Sarró E, Roher N, Plana M, Itarte E. (2006) The N-terminal domain of the human eIF2beta subunit and the CK2 phosphorylation sites are required for its function. Biochem. J. 394: 227-36.
- Ledoux, S., and Uhlenbeck, O.C. (2008). [3'-32P]-labeling tRNA with nucleotidyltransferase for assaying aminoacylation and peptide bond formation. Methods *44*, 74-80.
- Mader S, Lee H, Pause A, Sonenberg N. (1995) The translation initiation factor eIF-4E binds to a common motif shared by the translation factor eIF-4 gamma and the translational repressors 4E-binding proteins. Mol. Cell Biol. 15: 4990-7.
- Marintchev A, Edmonds KA, Marintcheva B, Hendrickson E, Oberer M, Suzuki C, Herdy B, Sonenberg N, Wagner G. (2009) Topology and regulation of the human eIF4A/4G/4H Helicase complex in translation initiation. Cell, 136:447-460.
- Marintchev A, Wagner G. (2004) Translation initiation: structures, mechanisms and evolution. Q Rev. Biophys. 37: 197-284.
- Marton, M. J., Vazquez de Aldana, C. R., Qiu, H., Chakraburtty, K., Hinnebusch, A. G. (1997), Evidence that GCN1 and GCN20, translational regulators of GCN4, function on elongating ribosomes in activation of eIF2alpha kinase GCN2. Mol Cell Biol 17:4474–4489.

- Merrick WC (2010), Eukaryotic protein synthesis: still a mystery. J Bio. Chem. Jul 9;285(28):21197-201.
- Minich WB, Balasta ML, Goss DJ, Rhoads RE. (1994) Chromatographic resolution of in vivo phosphorylated and nonphosphorylated eukaryotic translation initiation factor eIF-4E: increased cap affinity of the phosphorylated form. Proc. Natl. Acad. Sci. USA. 91: 7668-72
- Mouat MF, and Manchester K. (1998) An alpha subunit-deficient form of eukaryotic protein synthesis initiation factor eIF-2 from rabbit reticulocyte lysate and its activity in ternary complex formation. Mol. Cell. Biochem. 183, 69–78.
- Naranda T, Sirangelo I, Fabbri BJ, Hershey JW. (1995) Mutations in the NKXD consensus element indicate that GTP binds to the gamma-subunit of translation initiation factor eIF2. FEBS Lett. 372: 249-52.
- Naveau M, Lazennec-Schurdevin C, Panvert M, Dubiez E, Mechulam Y and Schmitt E (2012) Roles of yeast eIF2α and eIF2β subunits in the binding of the initiator methionyl-tRNA.
- Naveau M, Lazennec-Schurdevin C, Panvert M, Mechulam Y, and Schmittt E RNA binding properties of eukaryotic translation initiation factor 2 from *Encephalitozoon cuniculi* (2010) Biochemistry, 49, 8680–8688.
- Nika J, Rippel S, Hannig EM. (2001) Biochemical analysis of the eIF2β gamma complex reveals a structural function for eIF2α in catalyzed nucleotide exchange. J Biol. Chem. 276: 1051-6.

- Nonato M.C, Widom J, Clardy J (2002) Crystal structure of the N-terminal segment of human eukaryotic translation initiation factor 2α J. Biol. Chem., 277 pp. 17057–17061.
- Nurenberg E, Tampe R, (2013) Tying up loose ends: ribosome recycling in eukaryotes and archaea, Trends in Biochi. Sci.Vol.38, 64-74.
- Olsen DS, Savner EM, Mathew A, Zhang F, Krishnamoorthy T, Phan L, Hinnebusch AG. (2003) Domains of eIF1A that mediate binding to eIF2, eIF3 and eIF5B and promote ternary complex recruitment in vivo. EMBO J. 22: 193-204.
- Pathak VK, Nielsen PJ, Trachsel H, Hershey JW. (1988) Structure of the beta subunit of translational initiation factor eIF2. Cell, 54: 633-9.
- Pause A, Belsham GJ, Gingras AC, Donzé O, Lin TA, Lawrence JC Jr, Sonenberg N. (1994) Insulin-dependent stimulation of protein synthesis by phosphorylation of a regulator of 5'-cap function. Nature, 371: 762-7.
- Pavitt GD, Ramaiah KV, Kimball SR, Hinnebusch AG. (1998) eIF2 independently binds two distinct eIF2 β subcomplexes that catalyze and regulate guanine-nucleotide exchange. Genes Dev.12: 514-26.
- Pavitt GD. (2005) eIF2β, a mediator of general and gene-specific translational control. Biochem. Soc. Trans. 33: 1487-92.
- Paytubi, S., Wang, X., Lam, Y. W., Izquierdo, L., Hunter, M. J., Jan, E., Hundal, H. S., Proud, C. G., (2009) ABC50 promotes translation initiation in mammalian cells. J Biol Chem., 284(36):24061-24073.

- Pedullà N, Palermo R, Hasenöhrl D, Bläsi U, Cammarano P, Londei P. (2005) The archaeal eIF2 homologue: functional properties of an ancient translation initiation factor Nucleic Acids Res. **2005** Mar 23;33(6):1804-12.
- Pestova TV, Hellen CU. (2001) Preparation and activity of synthetic unmodify mammalian tRNAI(Met) in initiation of translation invitro. RNA Vol.7. 1496-1505.
- Pestova TV, Lorsch JR, Hellen CU. (2007) The Mechanism of Translation Initiation in Eukaryotes. In: Mathews, MB.; Sonenberg, N.; Hershey, JWB., editors. Translational Control in Biology and Medicine. Cold Spring Harbor Laboratory Press; Cold Spring Harbor, NY: 2007. p. 87-128.
- Pestova TV, Shatsky IN, Hellen CU. (1996) Functional dissection of eukaryotic initiation factor 4F: the 4A subunit and the central domain of the 4G subunit are sufficient to mediate internal entry of 43S preinitiation complexes. Mol. Cell Biol. 16: 6870-8
- Pisarev, A. V., Skabkin, M.A., Pisareva, P. V., 1, Skabkina, O. V., Aurélie M. Rakotondrafara, A. M., Hentze, M.W., 2, Christopher U. T. Hellen, C U T., and Pestova, T. V., (2010) The role of ABCE1 in eukaryotic post-termination ribosomal recycling *(2010) Mol Cell*., 37(2): 196–210.
- Pisarev, AV, Kolupaeva, VG, Pisareva,VP, Merrick, WC, Hellen CU, Pestova, TV (2006) Specific functional interactions of nucleo-tides at key -3 and +4 positions flanking the initiation codon with components of the mammalian 48S translation initiation complex. Genes. Dev. 20, 624-636.
- Presis T, Hentze HW, (2003), Starting the protein synthesis machine; eukaryotic translation initiation. Bioessays 25; 1201-11

- Ramaiah KV, Davies MV, Chen JJ, Kaufman RJ. (1994) Expression of mutant eukaryotic initiation factor 2 alpha subunit (eIF2α) reduces inhibition of guanine nucleotide exchange activity of eIF-2B mediated by eIF2 α phosphorylation. Mol. Cell Biol. 14: 4546-53.
- Rao, A. R. & Varshney, U. (2002). Characterization of Mycobacterium tuberculosis ribosome recycling factor (RRF) and a mutant lacking six amino acids from the C-terminal end reveals that the C-terminal residues are important for its occupancy on the ribosome. Microbiology,148 , 3913 –3920.
- Raychaudhuri P, Stringer EA, Valenzuela DM, Maitra U. (1984) Ribosomal subunit antiassociation activity in rabbit reticulocyte lysates. Evidence for a low molecular weight ribosomal subunit antiassociation protein. J Biol. Chem. 259: 11930-5.
- Roll-Mecak A, Alone P, Cao C, Dever T E, Burley SK (2004). X-ray structure of translation factor eIF2γ. J. Biol. Chem 11: 10634-10642.
- Russell DW, Spremulli LL. (1979) Purification and characterization of a ribosome dissociation factor (eukaryotic initiation factor 6) from wheat germ. J Biol. Chem. 254: 8796-800.
- Sachs AB, Varani G (2000), Eukaryotic translation initiation: there are (at least) two sides to every story. Nat Struct Biol. 2000 May;7(5):356-61.
- Scheper GC, van Kollenburg B, Hu J, Luo Y, Goss DJ, Proud CG. (2002) Phosphorylation of eukaryotic initiation factor 4E markedly reduces its affinity for capped mRNA. J Biol. Chem. 277: 3303-9.

- Scheuner D, Song B, McEwen E, Liu C, Laybutt R, Gillespie P, Saunders T, Bonner-Weir S, Kaufman RJ, (2001) Translational control is required for the unfolded protein response and in vivo glucose homeostasis, Mol. Cell 7 1165–1176.
- Scheuner D, Kaufman RJ. (2008) The unfolded protein response: a pathway that links insulin demand with beta-cell failure and diabetes. Endocr Rev.29: 317–33.
- Schmitt E, Blanquet S, Mechulam Y. (2002) The large subunit of initiation factor aIF2 is a close structural homologue of elongation factors. EMBO J. 21: 1821-32.
- Schmitt E, Naveau M, MechulamY (2010) Eukaryotic and archaeal translation initiation factor 2: A heterotrimeric tRNA carrier. FEBS Letters, 584: 405–412
- Schmitt E, Panvert M Lazennec-Schurdevin C, Coureux PD, Perez J, Thompson A Mechulam Y (2012) Structure of the ternary initiation complex aIF2–GDPNP–methionylated initiator tRNA Nat. Struc. Mol. Biol. 19: 450-455.
- Schmeing T M & Ramakrishnan V (2009) **What recent ribosome structures have revealed about the mechanism of translation** *Nature* **461**, 1234-1242.
- Seshadri, A., Sadananda Singh, N., and Varshney, U. (2010) Recycling of the post- termination complexes of Mycobacterium smegmatis and Escherichia coli ribosomes using heterologous factors, J. Mol. Biol., 401, 854-865

- Shin BS, Kim JR, Walker SE, Dong J, Lorsch JR Dever TE (2004) Initiation factor ZeIF2g promotes eIF2-GTP-Met-tRNAiMet ternary complex binding to the 40S ribosome. Nat. Struct. Mol. Biol. 18: 1227-1234.
- Shin BS, Kim JR, Walker SE, Dong J, Lorsch JR, Dever TE(2011), Initiation factor eIF2γ promotes eIF2-GTP-Met-tRNAi(Met) ternary complex binding to the 40S ribosome. Nat Struct Mol Biol. 16;18(11):1227-34.
- Singh CR, Yamamoto Y, Asano K, (2004) Physical association of eukaryotic initiation factor (eIF5) carboxyl-terminal domain with the lysine-rich eIF2beta segment strongly enhances its binding to eIF3, J. Biol. Chem. 279 49644–49655.
- Singh, N.S., Das, G., Seshadri, A., Sangeetha, R., Varshney, U (2005) Evidence for a role of initiation factor 3 in recycling of ribosomal complexes stalled on mRNAs in *Escherichia coli***.** Nucleic Acids Res., 30, 5591-5601
- Sokabe M, Yao M, Sakai N, Toya S, Tanaka I. (2006), Structure of archaeal translational initiation factor 2 betagamma-GDP reveals significant conformational change of the beta-subunit and switch 1 region. Proc Natl Acad Sci U S A. 103:13016-21.
- Sonenberg N, Hinnebusch AG. (2009) Regulation of translation initiation in eukaryotes: mechanisms and biological targets. Cell, 136: 731–45.
- Song, H., Mugnier, P., Das, A.K., Webb, H. M., Evans, D.R., Tuite, M.F., Hemmings, B. A., and Barford, D. (2000) The crystal structure of human eukaryotic release factor eRF1-mechanism of stop codon recognition and peptidyltRNA hydrolysis. Cell, 100, 311-321.
- Sreejith RK, Suresh CG, Bhosale SH, Bhavani V, Kumar A, Gaikwad SM and Pal JK (2011) Conformational transitions of the catalytic domain of

heme-regulated eukaryotic initiation factor2α kinase, a key translational regulatory molecule

- Sreejith RK, Yadav VN, Varshney NK, Berwal SK, Suresh CG, Gaikwad SM, Pal JK. (2009), Conformational characterization of human eukaryotic initiation factor 2alpha: a single tryptophan protein.Biochem Biophys Res Commun. 390(2) :273-9.
- Stringer EA, Chaudhuri A, Valenzuela D, Maitra U. (1980), Rabbit reticulocyte initiation factor 2 contains two polypeptide chains of molecular weights 48,000 and 38,000. Proc Natl Acad Sci U S A. (6):3356-9.
- Sudhakar A, Ramachandran A, Ghosh S, Hasnain SE, Kaufman RJ, Ramaiah KV. (2000) Phosphorylation of serine 51 in initiation factor 2 alpha (eIF2 alpha) promotes complex formation between eIF2 alpha(P) and eIF2B and causes inhibition in the guanine nucleotide exchange activity of eIF2B. Biochemistry, 39: 12929-38
- Suragani RN, Ghosh S, Ehtesham NZ, Ramaiah KV. (2006) Expression and purification of the subunits of human translational initiation factor 2 (eIF2): phosphorylation of eIF2 alpha and beta. Protein Expr. Purif. 47: 225-33.
- Suragani RN, Kamindla R, Ehtesham NZ, Ramaiah KV. (2005) Interaction of recombinant human eIF2 subunits with eIF2B and eIF2alpha kinases. Biochem. Biophys. Res. Commun. 338: 1766-72.
- Schrodinger, LLC (2010). The PyMOL molecular graphics system. version 1.3r1. http://www.pymol.org
- Thompson GM, Pacheco E, Melo EO, Castilho BA. (2000) Conserved sequences in the beta subunit of archaeal and eukaryal translation

initiation factor 2 (eIF2), absent from eIF5, mediate interaction with eIF2gamma. Biochem J. 347 3:703-9.

- Ting NS, Kao PN, Chan DW, Lintott LG, Lees-Miller SP. (1998) DNA-dependent protein kinase interacts with antigen receptor response element binding proteins NF90 and NF45. J Biol. Chem. 273: 2136-45.
- Trachsel H, Erni B, Schreier MH, Staehelin T. (1977) Initiation of mammalian protein synthesis. II. The assembly of the initiation complex with purified initiation factors. J Mol. Biol. 116: 755-67.
- Valásek LS (2012) 'Ribozoomin'–Translation initiation from the perspective of the ribosome-bound eukaryotic initiation factors (eIFs). Curr. Pro. Pep. Sci. 13: 305-330.
- Varshney U, Lee CP, RajBhandary UL (1991) Direct analysis of aminoacylation levels of tRNAs in vivo. Application to studying recognition of Escherichia coli initiator tRNA mutants by glutaminyl-tRNA synthetase. J Biol Chem 25: 266-268.
- Vasile F, Pechkova E, Nicolini C (2006) Solution structure of the beta-subunit of the translation initiation factor aIF2 from archaeabacteria Sulfolobus solfataricus Proteins, 70: 1112-2006.
- Vattem KM, Wek RC (2004), Reinitiation involving upstream ORFs regulates ATF4 mRNA translation in mammalian cells. Proc Natl Acad Sci U S A. 2004 Aug 3;101(31):11269-74.
- Wakula P, Beullens M, van Eynde A, Ceulemans H, Stalmans W, Bollen M. (2006) The translation initiation factor eIF2β is an interactor of protein phosphatase-1. Biochem. J. 400: 377-83.

- Webb BL, Proud CG. (1997), Eukaryotic initiation factor 2B (eIF2B). Int J Biochem Cell Biol. 29(10):1127-31.
- Wei CL, Kainuma M, Hershey JW. (1995) Characterization of yeast translation initiation factor 1A and cloning of its essential gene. J Biol. Chem. 270: 22788-94.
- Welsh GI, Price NT, Bladergroen BA, Bloomberg G, Proud CG. (1994) Identification of novel phosphorylation sites in the beta-subunit of translation initiation factor eIF-2. Biochem. Biophys. Res. Commun. 201: 1279-88.
- Yatime L, Mechulam Y, Blanquet S, and Schmitt E (2007) Structure of an archaeal heterotrimeric initiation factor 2 reveals a nucleotide state between the GTP and the GDP states. Proc. Natl. Acad. Sci. U.S.A. 104: 18445–1845.
- Yatime L, Schmit E, Blanquet S, Mechulam Y (2004) Functional molecular mapping of archaeal translation initiation factor 2. J. Biol. Chem., 2004, 279, 15984-15993.
- Yatime, L., Mechulam, Y., Blanquet, S. and Schmitt, E. (2006) Structural switch of the gamma subunit in an archaeal aIF2$\alpha\gamma$ heterodimer. Structure 14, 119–128.
- Ye X, Cavener DR. (1994) Isolation and characterization of the Drosophila melanogaster gene encoding translation-initiation factor eIF2β .Gene,142: 271-4.

- Zuoqi G, Kitagawa Y, Yoshikazu T, Nobutaka S, Keisuke K, Isao T, Min Y, (2012). The Binding mechanism of eIF2β with its partner proteins, eIF5 and eIF2Bε, Biochem. Biophys. Res. Commun. 423: 515-519.